The Converging Roles of Cholesterol and C-Terminal Src Kinase in the Regulation of Extracellular Matrix Degradation at Invadopodia

Thesis

The Converging Roles of Cholesterol and C-Terminal Src Kinase in the Regulation of Extracellular Matrix Degradation at Invadopodia

Kristyna Bicanova

Discipline: Life Sciences

Affiliated Research Centre: Fondazione Mario Negri Sud

Thesis submitted in accordance with the requirements of the Open University for the degree of Doctor of Philosophy

January 2014

DATE OF SUBMISSION: 30 JANUARY 2014

DATE OF AWARD: 14 JULY 2014

ProQuest LLC.
789 East Eisenhower Parkway
P.O. Box 1346
Ann Arbor, MI 48106 – 1346

To my grandmother Eva

Abstract

Metastasis, the leading cause of mortality in cancer patients, is the dissemination of cancer cells from the primary tumour and spread to the distant sites of the body. This is a complex process during which tumour cells need to overcome several natural barriers to gain entry into the bloodstream and thus allow formation of secondary tumour in distant location. In the last two decades, much effort has been focused on showing that tumour cells use specialized actin-based membrane protrusions termed invadopodia to perform matrix degradation. Invadopodia gain their protrusive capacity combining the mechanical force of actin polymerization with the chemical activity of matrix degradation. As such, invadopodia are F-actin-rich structures enriched in integrins, tyrosine kinases signalling machinery, soluble and membrane proteases, including matrix metalloproteases (MMPs), and actin-associated proteins. How all these components are specifically recruited to the ECM degradation sites has not been fully clarified yet.

An emerging model describes invadopodia as dynamic cellular platforms where the signalling, membrane trafficking and cytoskeleton remodelling converge upstream of ECM degradation at spatially confined cholesterol-rich membrane compartments. Despite the field of invadopodia biogenesis and function is still a very recent, it is witnessing an increasing interest and an increasing number of molecular players have been identified in the last two decades. Although the existence of the invadopodia-like structures *in vivo* settings still needs to be determined, invadopodia represent powerful experimental paradigm to study the tight integration between the signalling, the

membrane trafficking and cytoskeleton remodelling upstream of ECM degradation, the rate-limiting step in cell invasion, and might provide better understanding of cancer cell invasion and metastasis.

In order to investigate the cholesterol-rich lipid raft feature of invadopodia, I followed three lines. First, I showed that inhibition of cholesterol formation at penultimate step of its biosynthesis, and subsequent accumulation of desmosterol, blocks formation and function of invadopodia, thus demonstrating that the central role of cholesterol is connected to its presence in functional lipid rafts. In the second approach, I found that the SFKs inhibitory kinase Csk is a negative regulator of invadopodia-mediated ECM degradation and its role depends on the localization in the cholesterol-rich lipid rafts. Finally, I demonstrated that free cholesterol-dependent ARF6-associated recycling pathway might be involved in the trafficking to invadopodia, while the ARF6-pathway constituents are localized at ECM degradation sites and ARF6-specific cargo CD147 is recycled to invadopodia.

Taken together, my findings provide novel insight towards the elucidation of invadopodia as specialized cholesterol-dependent membrane domains where signal transduction and membrane trafficking events might be temporally and spatially confined.

Table of Contents

List of Figures

List of Tables

Abbreviations

2D	two-dimensional
3D	three-dimensional
ABC	ATP-binding cassette
ABD	actin-binding domain
Abl	Ableson kinase
ACAT	acetyl-coenzyme A acetyltransferase
ADAM	a disintegrin and metalloproteinase
ADF	actin depolymerizing factor
AMAP1	AMY-1-binding protein 1
apoA-I	apoliprotein A-I
ARF	ADP-ribosylation factor
Arg	Abl-related gene
Arp	actin-related protein
ArpC	actin-related protein complex
ASAP	ASter-Associated Protein
ASPP	apoptosis-stimulating protein of p53
ATP	adenosine triphosphate
BAR	Bin-Amphiphysin-Rsv domain
BB94	batimastat
bHLH	basic helix-loop-helix motif
BSA	bovine serum albumin
Cas	Crk-associated substrate

CDE	clathrin-dependent endocytosis
CFP	cyan fluorescent protein
CIE	clathrin-independent endocytosis
CIP	Cdc42-interacting protein
Chk	C-terminal homologue kinase
CLEM	confocal light electron microscopy
CSD	caveolin scaffolding domain
CSC	cancer stem cells
Csk	C-terminal Src kinase
dFCS	delipidized foetal calf serum
DMEM	Dulbecco modified Eagle's medium
DNA	deoxyribonucleic acid
DOC	sodium deoxycholate
DRF	Diaphanous-related formin
EEA1	early endosomal autoantigen 1
ECL	enhanced chemoluminiscence
ECM	extracellular matrix
EGF	epidermal growth factor
EGFR	epidermal growth factor receptor
EMT	epithelial-mesenchymal transition
ER	endoplasmic reticulum
ERC	endocytic recycling compartment
Epo	erythropoietin

Erk	extracellular signal regulated protein kinase
F-actin	filamentous actin
FAK	focal adhesion kinase
Fgd	faciogenital dysplasia protein
FIPI	5-fluoro-2-indolyl des-chlorohalopemide
FRET	Förster resonance energy transfer
g	acceleration of gravity
G-actin	globular actin
GAP	GTPase activating protein
GDI	guanine nucleotide dissociation inhibitor
GEF	guanine nucleotide exchange factor
GFP	green fluorescent protein
GLUT	glucose transporter
GTP	guanosine triphosphate
HDL	high-density lipoprotein
Hic5	Hydrogen peroxide-inducible clone 5 protein
HIF	hypoxia inducible factor
HNSCC	head and neck squamous cell carcinoma
IF	immunofluorescence
ILK	integrin-linked kinase
Insig1	Insulin-induced gene 1
IQGAP	IQ motif containing GTPase activating protein
LDL	low density lipoprotein

LDL-R	low density lipoprotein receptor
LTP	lipid transfer protein
LXR	liver X receptor
MAP	mitogen activated protein kinase
MHC I	major histocompatibility complex class I
MMP	matrix metalloprotease
mRNA	messenger RNA
MT1-MMP	membrane bound matrix metalloprotease 1
Nck	non-catalytic region of tyrosine kinase adaptor protein
NHE1	sodium-hydrogen (Na^+/H^+) exchanger type 1
Nox	NADPH oxidase
NPC	Niemann Pick type C protein
NPF	nucleation promoter factor
NTA	N-terminal acidic domain
ORP	oxysterol binding related protein
P_2	bis-phosphate
P_3	trisphosphate
PAK	p21-activated serine/threonine kinase
PBS	phosphate buffered saline
PDGF	platelet-derived growth factor
PDGFR	platelet-derived growth factor receptor
PH	pleckstrin homology domain
PLD2	phospholipase D2

PX	Phox domain
PI3K	phosphoinositide 3-kinase
PIP5KIα	phosphatidylinositol 4-phosphate 5-kinase type Iα
PKA	protein kinase A
PKC	protein kinase C
PKD	protein kinase D
PRD	proline-rich domain
PtdIns	phosphatidylinositol
RNA	ribonucleic acid
RNAi	RNA interference
ROS	reactive oxygen species
RT	room temperature
RTK	receptor tyrosine kinase
SCAP	SREBP cleavage activating protein
SCAR	suppressor of cyclic AMP repressor
SFK	Src family kinase
SH	Src homology
SHG	second harmonic generation
siRNA	small interfering RNA
SNARE	soluble N-ethylmaleimide-sensitive factor attachment protein receptor
SOCS1	Suppressor of cytokine signalling 1
SRB1	scavenger receptor B1
SREBP	sterol regulatory element binding protein

TGB-β	transforming growth factor beta
THG	third harmonic generation
TIC	tumour initiating cells
TIRF	total internal reflection fluorescence
Tks	tyrosine-kinase substrate
Toca	transducer of Cdc42-dependent actin assembly 1
uPAR	urokinase-type plasminogen activator receptor
VCA	verprolin homology, cofilin homology (or central) and acidic domain
VLDL	very low density lipoprotein
WASP	Wiscott-Aldrich syndrome protein
WAVE	WASP family verprolin-homologous protein
WBD	WASP-binding domain
WD	tryptophan-aspartic acid repeat
WIP	WASP interacting protein
WT	wild type

CHAPTER 1: Introduction

1.1 Tumour cell invasion

Cancer is not one but many diseases that arise from a host of different genetic causes. Generally speaking, the neoplastic progression requires the acquisition of genetic mutations that lead either to loss of tumour suppressors or activation of oncogenes. Broadly, tumours are classified based on the tissue of origin and subsequently by the molecular markers or genetic abnormalities they possess. Notwithstanding their heterogeneity, it is accepted that cells must gain several properties to become malignant. Hanahan and Weinberg (2011) provided in their updated influential review a logical framework to analyze the complexity of malignant transformation. The seminal distinctive capabilities of cancer cells that lead to tumourigenesis is primarily characterized by genomic instability leading to aberrant proliferation signalling, insensitivity to growth suppressors, resistance to apoptosis, neoangiogenesis, limitless replication potential, reprogramming of cell energy metabolism, evasion of the immune system response, and tissue invasion and metastasis (Hanahan and Weinberg, 2011).

Metastasis, a leading cause of mortality in cancer patients, is a common phenomenon of malignant tumours, which makes it an excellent target for therapeutic intervention. The metastatic process is a multistage one whereby cancer cells escape from the primary tumour and break through basement membrane to invade local tissue and vessels to eventually colonize distant sites to form a secondary tumour. It is

believed that the ability of tumour cells to cross the tissue barriers is facilitated by forming specific F-actin rich invasive structures that, *in vitro*, are visualised and studied as invadopodia ("invasive feet"), that focalize the degradation of the surrounding matrix and serves as platforms where the cytoskeletal, cell signalling, membrane trafficking and proteolytic pathways are integrated towards a defined biological function.

1.2 Invadopodia: The invasion machinery of cancer cells

As aforementioned, breaking through the ECM barrier is essential for the invasion of tumour cells and proteolytic degradation associated with migratory phenotype is a common feature of tumour cells. Hence, understanding this process is of a particular importance for targeting the therapeutic intervention. Invadopodia, the F-actin rich structures that localize the degradative capability of tumour cells, provide an excellent platform to understand the mechanism and biology of cancer cell invasion. In the last two decades, invadopodia witnessed an increasing interest and the accumulating data have shed light on the molecular complement and on the molecular mechanism governing the formation and function of invadopodia, as it is discussed in a number of recent reviews focusing on diverse aspects of invadopodia biology, such as signalling to invadopodia (Boateng and Huttenlocher, 2012; Destaing et al., 2011; Hoshino et al., 2013; Sibony-Benyamini and Gill-Hen, 2012), pathological role of invadopodia (Eckert and Yan, 2011; Stylli et al., 2008; Yamaguchi, 2012), actin polymerization and remodelling (Albiges-Rizo et al., 2009), and trafficking to invadopodia (Caldieri and Buccione, 2009; Frittoli et al., 2010).

1.2.1 Definition of invadopodia

Invadopodia are plasma membrane structures with the ability to degrade extracellular matrix, first described in the Chen's laboratory as rosette-shaped adhesion

sites formed by Rous sarcoma virus-transformed chicken embryonic fibroblasts (Chen, 1989). They are stable actin-rich protrusions emanating from the ventral surface of invasive tumour or transformed cells. Importantly, these structures can degrade extracellular matrix (ECM) by modulating the focused release and activation of proteases, when plated on ECM substrate, such as gelatine, collagen I, collagen IV, fibronectin or laminin (Kelly et al., 1994).

Invadopodia are mainly visualized on a thin layer of ECM covered coverglasses, on which can be seen as roundish actin-rich structures that are associated with sites of matrix degradation, are not confined to the cell periphery and contain actin-related proteins, such as cortactin, and/or phosphotyrosines (Baldassarre et al., 2006; Bowden et al., 2006).

In point of fact, the ability of tumour cells to form invadopodia often correlates with their metastatic and invasive potential. For instance, invadopodia formation has been confirmed in primary tumour cells obtained from the patients with invasive head and neck squamous cell carcinoma (HNSCC) (Clark et al., 2007), glioblastoma (Stylli et al., 2008) and bladder cancer (Yamamoto et al., 2011).

1.2.2 Podosomes or invadopodia?

Due to the functional and structural similarities, the terms podosomes and invadopodia have been initially used interchangeably. A defining feature of both invadopodia and podosomes is indeed the coordination between the attachment to ECM and pericellular proteolysis activity, supported by the presence of a range of proteases in

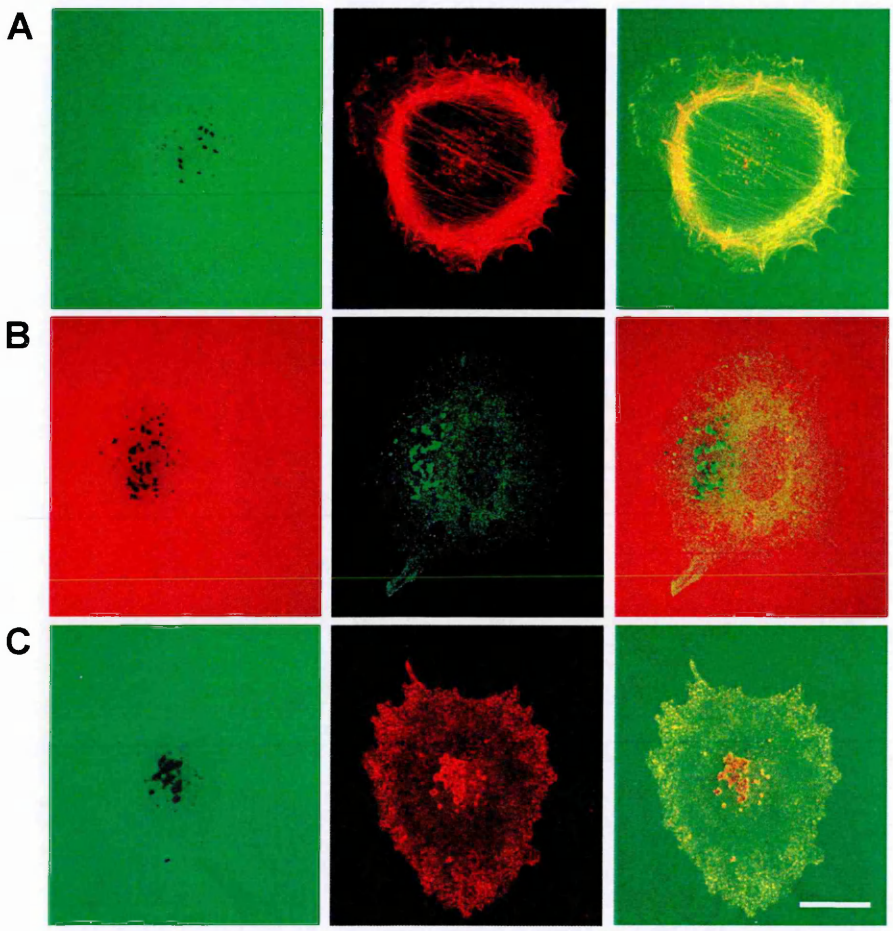

Fig. 1.1. Identification of invadopodia. Double staining of A375MM melanoma cells grown on FITC (green) or rhodamine (red)-conjugated gelatin and then fixed and stained for: (a) actin; (b) cortactin; (c) dynamin. Invadopodia match underlying areas of degradation (black patches). A merged image is also shown. Scale bar 10 μm.

both structures. Consequently, they share many common molecular constituent and activating pathways. Despite the numerous similarities between the structures, there are some notable differences and clear distinctions have been made based on the cell origin, lifetime and morphological classification. Podosomes are generally considered as more typical of differentiated cell lines, such as osteoclasts, macrophages, vascular endothelial and smooth muscle cells, whereas invadopodia are formed by transformed or tumour cells as a result of neoplastic aberrations. Podosomes consist of a densely packed actin core surrounded by a ring of components commonly found in focal adhesion structures (Gimona et al., 2008; Linder, 2009; Linder, 2007). Podosomes are dynamic, rapidly turning-over (2-12 minutes), relatively small (1 μm in diameter and x 0.4 μm in height), dot-like structures organised in rings and/or distributed at the leading edge, typically present in large numbers (20-100). At variance, invadopodia are persistent (up to 3 hours), large (up to 8x5 μm), irregularly shaped actin-rich formations, which tend to be confined to the central area of cells, and are less numerous than podosomes (1-10/cell). As a consequence of invadopodia persistence, the pattern of degradation mediated by invadopodia is deeper and more focused compared to the shallow, widespread degradation by podosomes.

Interestingly however, observation by live-cell total internal reflection fluorescence (TIRF) microscopy revealed fundamental differences in membrane dynamics of both structures. This study suggests a highly dynamic nature of the invadopodial structure where the ruffling and undulation of the invadopodial membrane is accompanied by formation of filament-like invadopodia. On the contrary, parallel TIRF microscopy studies of macrophage podosomes compared to invadopodia

established that the podosome membrane does not form any filament-like membrane extensions or protrusions in cells on the two-dimensional (2D) ECM (Artym et al., 2010).

In addition, comparison of the podosome consensus list of proteins with published invadopodia proteome revealed extensive overlap, which seems to consist mainly of metabolic proteins (Attanasio et al., 2011; Cervero et al., 2012).

1.2.3 Invadopodial structure

Early electron microscopy studies of transformed fibroblast invading thin 2D matrices suggested that invadopodia are regions of ventral plasma membrane extending into the underlying ECM, with a central electron dense cytoplasmic core or with the central core extending into long filaments (Chen, 1989). Later observation on a breast cancer-derived cell line grown on gelatine cross-linked beads confirmed this concept of invadopodia (Bowden et al., 1999). Further detailed ultra-structural analysis of melanoma cells using a correlative confocal light electron microscopy (CLEM) approach shows multiple filament-like invadopodia to be a part of an invasion superstructure of profound ventral cell membrane invaginations that measured in average 8 μm in width and 2 μm in depth. From within, many surface protrusions originated, with diameters ranging from hundreds of nanometres to a few micrometres, and 500 nm in length, which sometimes penetrated into the matrix (Baldassarre et al., 2006). In addition, by the same approach, CLEM, invadopodial invaginations were found to be in close relationship with Golgi complex (Baldassarre et al., 2003).

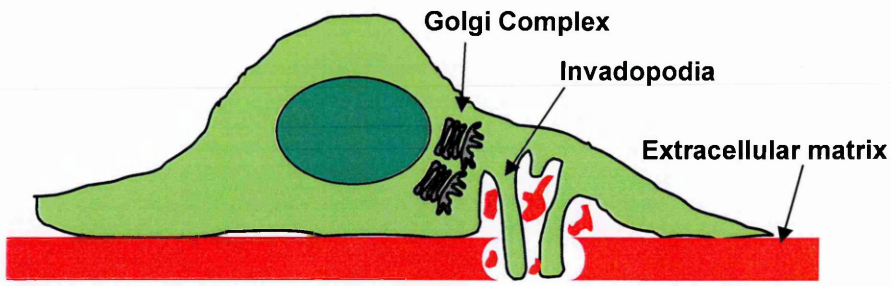

Fig. 1.2. Schematic diagram of invadopodia organisation. This drawing is based on correlative light-electron microscopy reconstructions from serial sections of A375MM melanoma cells (Baldassarre et al., 2003). Invadopodial protrusions originate from profound invaginations of the ventral surface of the plasma membrane; within the area delimited by the large invagination, large fragments of gelatin can often be seen. Also shown are the spatial relationships with the nucleus and the Golgi complex.

More recently, transmission electron microscopy has been employed to analyze the ultra-structural organization of invadopodia formed in the chemo-invasion assay, where invadopodia are allowed to grow through membrane pores, thus forming longer protrusions (Schoumacher et al., 2010). In transmission electrographs, the randomly arranged actin bundles have been identified at the very tip or at the sides of invadopodia. Unexpectedly, the presence of intermediate filaments and microtubules has been confirmed in this long mature invadopodia. This is a first evidence of the presence of such cytoskeletal elements at invadopodia. Neither intermediate filaments nor microtubules are required for invadopodial formation, but they appear to be essential for the elongation of invadopodia. Typically, one to two microtubules were embedded in the meshwork of intermediate filaments at the core of long mature invadopodia. Finally, many vesicles were found within protrusions, implying active traffic at mature invadopodia (Schoumacher et al., 2010).

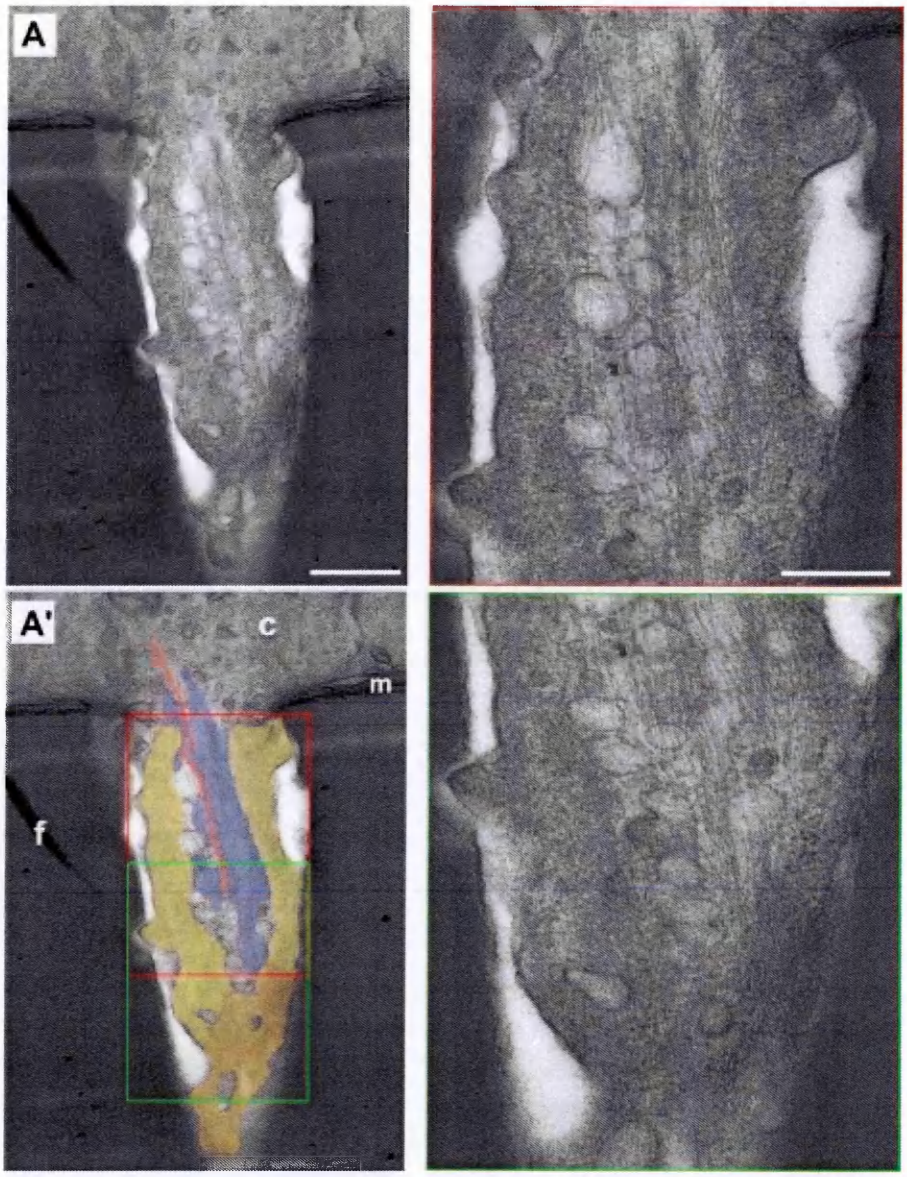

Fig. 1.3. Electron micrographs of mature invadopodia. Image A shows mature invadopodia in MDA-MB-231 on Matrigel-coated transwell. The same image (A') is color coded to distinguish cytoskeleton network: orange-microtubules, blue-intermediate filaments, and actin in yellow.. Images on the right are a higher magnification of the corresponding boxed regions in A (red-base; green-tip of invadopodia.) c, cell; f, filter; m, Matrigel. Bars: (A and A [left]) 0.5 μm; (A, right) 0.25 μm. Image taken from Schoumacher et al., (2010).

1.2.4 Invadopodial components

A majority of studies has used immunofluorescence and fluorescent protein-tagged proteins to image the localization of specific proteins at invadopodia. This approach together with siRNA-mediated interference of definite proteins has led to identification of an expanding list of proteins involved in invadopodia biogenesis, including integrins, proteins of canonical signalling pathways, soluble and membrane bound proteases, actin and actin-associated proteins.

More recently, a proteomic study conducted on invadopodia-enriched cell fractions came up with a significant number of new invadopodia-associated proteins, provided a quantitative analysis of protein levels by Difference Gel Electrophoresis (DIGE) on invasive human melanoma cell line A375MM. Almost 60 new proteins were identified that could be divided into different functional classes: a) protein synthesis, degradation and folding; b) glycolytic and associated metabolic proteins; c) cytoskeletal components and membrane associated proteins (Attanasio et al., 2011).

1.2.5 Regulation of invadopodia formation

Beside the description of molecular components of invadopodia, much attention is centered to the comprehension of the regulation of invadopodia formation and their initiation, which might ultimately aid comprehension of factors that lead to metastatic behaviour. In addition to the adhesion, the regulation of invadopodia formation has been connected to other stimulants, including growth factors, and substrate stiffness and

membrane curvature may also play an important role in the invadopodia induction, as discussed briefly hereafter.

1.2.5.1 Role of ECM and adhesion protein signalling

Adhesion signalling, especially by integrins, is likely to be a critical regulatory event in the formation and function of invadopodia. Integrins belong to the family of heterodimeric transmembrane adhesion proteins consisting of 18 α and 8 β subunits that can make up 24 distinct non-covalently linked heterodimers with specific tissue distribution. Various combinations of α and β subunits endow integrins with specific ligand binding characteristics. Due to their ability to switch from low to high affinity conformation, they are likely to sense physicochemical properties of the substrate. Though their primary function is to mediate cell-cell and cell-ECM adhesion, respectively, integrins play also an important role in signal transduction and cytoskeletal reorganization. Integrins directly interact with ECM components and transmit the extracellular information in the cell (outside-in signalling) as well as other way round (inside-out signalling).

The role of integrins at invadopodia is incompletely understood. The engagement of cell surface integrins by substrate components is the thought to be the trigger of invadopodia formation (Mueller et al., 1999; Nakahara et al., 1998; Nakahara et al., 1996). To date, which integrin(s) subunit(s) is responsible for invadopodia regulation remains unclear. The specific integrin combinations that, when engaged, lead to invadopodia formation, might be cell-type dependent. For example, invadopodia still

form in the absence of β3 integrin but they are inhibited in case of loss of β1 integrin (Beaty et al., 2013).

Another line of evidence accounts for β1 involvement in the invadopodia-dependent degradation process. Deregulation of β1 has been associated with tumour aggressiveness in number of models, such as pancreatic, skin, breast and ovarian cancer. In melanoma cells, activation of α6β1 promoted SFK-dependent phosphorylation of p190RhoGAP, which resulted in Rho family GTPases-dependent rearrangements of actin cytoskeleton and eventually, invadopodia formation (Nakahara et al., 1998). Beaty et al. (2013) showed that β1 is not required for invadopodia precursor formation upon epidermal growth factor (EGF) stimulation; however, it is indispensable for formation of mature, fully active invadopodia (Beaty et al., 2013).

Involvement of integrins in the degradation process might imply a direct effect on the protease secretion. For instance, collagen-induced α3β1 association with the serine protease seprase was shown to drive the degradative activity of this gelatinolytic enzyme specifically at the tip of invadopodia (Artym et al., 2002). An inhibitory anti-β1 integrin antibody prevented the association between urokinase-type plasminogen activator receptor (uPAR) and seprase at invadopodia, suggesting a fundamental role for β1 in the organisation and targeting of proteases at sites of ECM degradation (Artym et al., 2002). Moreover, integrins cooperated with membrane-type 1 matrix metalloprotease (MT1-MMP) to localize and enhance proteolysis through the activation of matrix metalloproteinase-2 (MMP2) (Deryugina et al., 2002). Recently, a formation of integrin and integrin linked kinase (ILK)-dependent adhesion rings has been described. The adhesion rings formed around invadopodia shortly after their formation

and correlated positively with invadopodia activity. Strikingly, prevention of formation of the adhesion rings reduced both recruitment of IQ motif containing GTPase activating protein (IQGAP) and MT1-MMP accumulation at invadopodia site, probably through the impaired capture of MT1-MMP-containing vesicles (Branch et al., 2012). Similarly, it had been shown in another study that actin core assembled before the integrin-containing adhesion ring, and actin disruption was a prerequisite for invadopodia disassembly (Badowski et al., 2008).

In conclusion, it has not been fully elucidated how integrins regulate invadopodia biogenesis. The latest evidence suggest that rather than inducing invadopodia formation, integrins act lately during invadopodia maturation by activating downstream signalling events and serving as docking sites for proteases.

1.2.5.2 Role of growth factors

Many growth factors have been shown to promote the formation of both invadopodia and podosomes (Hoshino et al., 2013). Here, I will simply mention those known to induce the formation of invadopodia in cancer cells. A well-characterized and studied inducer of invadopodia is epidermal growth factor (EGF) (Yamaguchi et al., 2005). Subsequent studies showed that the basic helix-loop-helix (bHLH) transcription factor TWIST, an inducer of epithelial-mesenchymal transition (EMT), promoted invadopodia formation by upregulation of platelet-derived factor receptor α (PDGFRα) (Eckert et al., 2011). Moreover, knockdown of TWIST1 blocked the ability of TGFβ to induce invadopodia formation via PDGFRα. The implicated role of TGFβ is also

supported by a study showing that stimulation by TGFβ led to phosphorylation of hydrogen peroxide-inducible clone 5 protein (Hic5), required for invadopodia formation and invasion (Pignatelli et al., 2012).

1.2.5.3 Role of matrix stiffness

Matrix stiffness due to collagen deposition is known to play a role in the propensity of metastatic behaviour of tumour cells (reviewed in Boyd et al., 2005). Still, both the occurrence and relevance of mechanosensing at invadopodia remain to be fully understood. In a first report addressing this issue, Alexander et al. (2008) showed that breast cancer cells increased both the number and activity of invadopodia when plated on increasing concentrations of gelatine without altering the protein composition of the substrate. This study suggested that regulation of invadopodia formation by substrate rigidity might occur via a myosin II-focal adhesion kinase (FAK)/Crk-associated substrate (Cas) axis, which acts as a mechanosensing machine (Alexander et al., 2008).

1.2.5.4 Role of membrane curvature

Invadopodia are protrusive structures formed through mechanism a coupling actin polymerization with membrane curvature (Albiges-Rizo et al., 2009), therefore continuous membrane remodelling is required to allow the growth of invadopodia. The Bin-Amphiphysin-Rsv domain (BAR) and F-BAR proteins are involved in the formation of positive curvature of the membrane, i.e. inward bending of the membrane.

Recently, the F-BAR protein, Cdc42 interacting protein 4 (CIP4), has been show to play a role at invadopodia both as means to promote membrane curvature and as a scaffold protein to promote actin polymerization (Hu et al., 2011; Pichot et al., 2010).

Expression of CIP4 is elevated in aggressive breast cancer and appears to confer an invasive phenotype by promoting cell migration and invadopodia formation and function. It has been demonstrated that the action of CIP4 is based on Src-dependent phosphorylation of N-WASP that initiates actin polymerization. Since CIP4 serves as a scaffold for Cdc42, Src and N-WASP, to target actin polymerization to the sites of membrane curvature, which could be the very case of invadopodia protrusions (Pichot et al., 2010). Shortly thereafter, another study on CIP4 was published, describing its role in the contrast as a negative regulator of invadopodia formation by promoting MT1-MMP internalization (Hu et al., 2011). Although both studies were executed in the same cell line, breast cancer-derived MDA-MB-231 cell line, methodological differences might account for the varied results. The main difference was in the use of acute, siRNA-mediated knock-down of CIP4 (Pichot et al., 2010) or stable, shRNA-mediated knock-down of CIP4 (Hu et al., 2011).

Similarly, expression of F-BAR domain containing adaptor protein transducer of Cdc42-dependent actin assembly-1 (Toca 1) correlates with malignant phenotype of breast cancer cells, and Toca 1 associates with a number of actin regulatory proteins present at invadopodia. Toca 1 colocalized with actin-rich cortactin core of invadopodial protrusion and promoted invadopodia formation, most likely due to promotion of actin branching (Chander et al., 2013).

1.2.6 Signalling to invadopodia

Following the detection of signal inputs such as cross-linked integrins or growth factors, series of signalling pathways are activated that induce the actin polymerization and other events required for invadopodia initiation and formation. Recent research has highlighted the importance of a number of signalling elements, including Src family kinases (SFKs), Abelson kinases (Abl), protein kinase C (PKC) and some members of Ras superfamily of small GTPases, as I will discuss in this section.

1.2.6.1 Tyrosine phosphorylation at invadopodia

Tyrosine phosphorylation is a convenient, reversible switch to regulate cellular processes by the addition of negatively charged phosphate groups to the specific tyrosine residues. As a result, the chemical and functional properties of proteins are altered substantially, which includes allosteric modification, formation of a new protein complex, activation or deactivation, or a release from an inhibitory complex.

Invadopodia were historically described as a major cytoskeleton reorganization induced by the expression of oncogene v-Src (Chen, 1989); high levels of tyrosine phosphorylation and dependence on Src activity were subsequently and specifically associated with such structures (Mueller et al., 1992). The non-receptor Src family of tyrosine kinases (SFK) comprises nine closely related members that share three important structural domains, designated as Src Homology (SH) domains: a catalytic domain SH1 preceded by non-catalytic SH2 and SH3 domains. The SH2 domain is

responsible for binding to phosphotyrosine rich protein regions, whereas SH3 domain binds polyproline sequences. Localization to specific cell membranes is regulated by N-terminal "unique" domain, highly diverse among family members. Additionally, SFK activity is controlled through activatory phosphorylation in the A-loop and the C-terminal autoinhibitory phosphorylation site (Y527 in Src) (Ingley, 2008; Thomas and Brugge, 1997). Src is indispensable for invadopodia formation and function, and the degree of tyrosine phosphorylation positively correlates with invadopodia activity, as has been demonstrated through several different approaches. Initially, Bowden et al. (2006) showed that the majority of the tyrosine phosphorylated proteins resides in the invadopodia-enriched fraction and the cell treatment with phosphatase inhibitor orthovanadate to prevent dephosphorylation resulted in a higher degree of matrix degradation (Bowden et al., 2006). Several studies have confirmed that cell treatment with SFK inhibitors blocks the formation of invadopodia and consequently of matrix degradation; also, transfection with kinase-active or kinase- inactive Src mutants, increased or decreased the levels of ECM degradation, respectively, as compared to the wild type Src-expressing cells (Bowden et al., 2006; Hauck et al., 2002).

Another non-receptor tyrosine kinase of the Abelson (Abl) family of tyrosine kinases has recently been brought into the picture. Abl family includes Abl and Abl-related gene (Arg) kinases, both of which are the only known tyrosine kinases to interact with the cytoskeleton (reviewed in Colicelli, 2010). Src phosphorylates and activates Abl and Arg upon the signalling input of growth factors such as EGF and PDGF. The subsequent activation led to direct phosphorylation of cortactin, responsible for maturation of invadopodia in melanoma and breast cancer cell lines (Mader et al.,

2011; Smith-Pearson et al., 2010). However, the effect of Abl kinases might be more complex, as was reported in a comparative study of MDA-MB-231 (a breast cancer-derived cell line widely used for studying of invadopodia biology) and HNSSC (a head and neck squamous carcinoma-derived cell line). While in MDA-MB-231 cells silencing of Abl kinases prevented invadopodia formation, in HNSSC cells ablation of Abl led to promotion of invadopodia formation and associated matrix degradation (Hayes et al., 2012). On the contrary, in a study focusing on the role of cortactin, Abl was shown not to play a role in the invadopodia formation in another widely used cell model A375MM melanoma cells (Ayala et al., 2008). Thus, further research is needed to gain insight into the mechanistic of Abl role at invadopodia and cancer cell invasion in general.

A central role of SFK in invadopodia regulation is further inferred by the relevance of a number of direct SFK substrates involved in invadopodia function. Among the most relevant is cortactin, which I will be discussing in section 1.2.7.3.

Paxillin is a multi-domain adaptor protein that localizes to the extracellular matrix contacts. It consists of multiple protein-binding modules, many of which are under the control of phosphorylation, and thus interacts with numerous regulatory and structural proteins to control cell adhesion, cytoskeletal remodelling and gene expression in cell migration, invasion and survival. In particular, paxillin emerged as an important regulator of the spatiotemporal action of Rho GTPases, by recruiting a number of their accessory proteins (reviewed in Deakin and Turner, 2008). Phosphorylation of paxillin at tyrosines 31 and 118 aids a formation of a complex with PKC and cortactin to increase invasiveness of the cell lines tested (Bowden et al., 1999).

Moreover, expression of phosphorylation deficient mutants resulted in impaired disassembly of invadopodia actin core and consequent formation of thick, less degrading invadopodia with small lumens (Badowski et al., 2008).

The Src substrate tyrosine-kinase substrate (Tks) 5, formerly known as FISH, is required for invadopodia formation and invasive behaviour of a number of cancer cell lines (Abram et al., 2003; Seals et al., 2005). Of particular interest is observation that Tks5 is expressed exclusively in invasive cancer cells, but not in their non-invasive counterparts (reviewed in Courtneidge, 2012). Tks5 is a scaffolding protein featuring lipid-binding Phox (PX) domain followed by five SH3 domains. Recently discovered Tks5-related protein Tks4, that shares the similar domain architecture with Tks5 but missing one SH3 domain, has been found to be tyrosine phosphorylated and predominantly localized at invadopodia-like structures in Src-transformed fibroblasts; in addition, Tks4 knockdown inhibited ECM degradation. Interestingly, Tks 4 and 5 do not appear to have overlapping functions as ECM degradation was not rescued by over-expression of Tks5, probably due to non-redundant role of Tks4 in the MT1-MMP recruitment to invadopodia (Buschman et al., 2009). The involvement of Tks proteins at invadopodia is not fully elucidated but the emerging knowledge is pointing to many aspects of invadopodia biology. Invadopodia formation is initiated at membranes sites rich in PtdIns(3,4)P_2 (Oikawa et al., 2008). Indeed, the lipid binding PX domain is essential for Tks5 function at invadopodia. Moreover, Tks5 binds and modulates the actin polymerization regulators N-WASP (Oikawa et al., 2008) and Nck1 (Stylli et al., 2009). Both Tks5 and Tks4 protein associates with members of the A Disintegrin And Metalloproteinase (ADAM) family of proteases, namely ADAMs 12,15 and 19,

involved in processes such as cell adhesion and motility (Abram et al., 2003; Buschman et al., 2009). More recently, it has been shown that Tks proteins act as organizers of reactive oxygen species (ROS) signalling mediated by NADPH oxidases (Nox) (Diaz et al., 2009). In non-phagocytic cells, ROS prove to be mediator of various cellular responses and their role at invadopodia formation has been approved (Diaz et al., 2009). The effect of ROS on invadopodia has not been elucidated yet, but might involve the ROS effect on modulation of activity of SFKs, PKC and small GTPases, combined with inhibition of phosphatases and increased secretion of MMPs (reviewed in Giannoni et al., 2010).

The protein caveolin is a major regulator of cholesterol homeostasis at the plasma membrane and has been directly implicated in invadopodia biogenesis (Caldieri et al., 2009; Yamaguchi et al., 2009). Caveolin is also the major component of lipid-raft enriched caveolae, flask-shaped invaginations of the plasma membrane implicated in endocytosis (Parton et al., 2006; Williams, 2004). The caveolin family consists of three members. Caveolin 1 is a ubiquitous isoform, caveolin 2 is tightly co-expressed with caveolin 1 and caveolin 3 replaces caveolin 1 in striated muscle. Caveolin 3 shares 85% similarity with caveolin 1 and these two isoforms are mutually interchangeable. The caveolins are small proteins (18/24 kDa) with cytosolic C- and N-termini and a central domain consisting of 33 hydrophobic amino acids that spans the plasma membrane to exhibit an unusual hairpin-like configuration. Caveolins have been approved in numerous cell functions, ranging from the regulation of cholesterol homeostasis, vesicular transport and regulation of signal transduction (reviewed in Williams and Lisanti, 2004). Caveolin has also been directly implicated in tumorigenesis, although,

depending on cell type and/or tumour stage, it appears to act as a tumour suppressor or as an oncogene. This discrepancy might be explained by fact that caveolin has several domains with opposing functions (Mercier et al., 2009; Williams, 2004). The caveolin scaffolding domain (CSD) between residues 82 and 101 inhibits growth stimulatory activity of several signalling proteins, e.g. receptor tyrosine kinases (RTKs) and Src-family kinases (SFK), thus acting inhibitory towards growth. Phosphorylation of caveolin 1 on tyrosine 14 activates a binding site for SH2-domain containing proteins, such as Grb-7 to enhance anchorage-independent growth and EGF-stimulated cell migration (Lee et al., 2000), or C-terminal kinase (Csk) to inhibit Src-family kinases (SFK). Caveolin 1 phosphorylated on Y14 (pY14-Cav1) also promotes focal adhesion disassembly and turnover via the stabilization of focal adhesion kinase (FAK) exchange to stimulate migration in breast cancer cells (Goetz et al., 2008). Strikingly, the phosphorylation of caveolin 1 on Y14 is an important event in ECM degradation, inversely correlating with invadopodia formation (Caldieri et al., 2009).

1.2.6.2 Serine/threonine phosphorylation at invadopodia

Phosphorylation of serine or threonine in specific consensus sites by specific kinases is another cellular mechanism to control the activity of proteins. Recently, serine/threonine kinases have also been associated with invadopodia biogenesis. Extracellular signal regulated protein kinase 1/2 (Erk1/2) is a part of a large signalling network of mitogen activated protein (MAP) kinases, which regulate a number of processes. The Erks are activated by plethora of stimuli, including growth factors acting

through receptor tyrosine kinases, cytokine binding to receptors that consequently activate tyrosine kinases or agonists of G protein-coupled receptors (reviewed in Kolch, 2005). Erk1/2 has been shown to be involved in invadopodia-mediated ECM degradation, most likely by phosphorylating cortactin (Ayala et al., 2008) and by being activated by the small GTPase ARF6 (Tague et al., 2004) or paxillin (Badowski et al., 2008).

The family of p21-activated kinases (PAK) comprises six isoforms - group A (PAK 1-3) and B (PAK 4-6) with partly overlapping but also clearly distinct roles. Generally, the substrates of conventional group A PAKs are involved in the regulation of adhesion and cytoskeletal events and are targets of small GTPases Rac1 and Cdc42 (Lim et al., 1996). Interestingly, the PAK 1 gene maps to the 11q13 amplicon, the very same region that encodes cortactin (Bekri et al., 1997). Consequently, PAK 1 over-expression has been documented in a number of carcinomas (Kamai et al., 2010; Li et al., 2008; Lu et al., 2013). Specifically, PAK 1 phosphorylated cortactin on S113, causing its reduced binding to F-actin (Webb et al., 2006). The non-phosphorylatable S113A cortactin reduced invadopodia-dependent matrix degradation (Ayala et al., 2008). Nevertheless, the role of PAK and possible involvement of its other substrates invadopodia is not widely studied and remains to be defined.

1.2.6.3 Phospholipases and regulation of invadopodia by phosphatidylinositols

The role of the class I phosphoinositide 3-kinases (PI3Ks) in invadopodia organisation has been repeatedly demonstrated by the use of PI3K inhibitors and

siRNA-mediated silencing, which both led to reduced number and activity of invadopodia (Hoshino et al., 2012; Yamaguchi et al., 2011). Furthermore, expression of PI3K catalytic subunit p110α stimulated the degradation capability of breast cancer cells (Yamaguchi et al., 2011).

All class I PI3Ks phosphorylate phosphatidylinositol 4,5-bisphosphate [PtdIns(4,5)P_2] at the D3 position to generate phosphatidylinositol 3,4,5-trisphosphate [PtdIns(3,4,5)P_3]. PtdIns(3,4,5)P_3 then either activates the classical, PDK-Akt dependent PI3K signalling pathway, or, alternatively, serves as a precursor lipid for PtdIns(3,4)P_2. Altogether, all three types of phosphatidylinositols have been implicated in invadopodia formation (reviewed in Hoshino et al., 2013). PtdIns(4,5)P_2 is primarily generated by type I phosphatidylinositol 4-phosphate 5-kinases (PIP5KI). Three isoforms of PIP5KI exist in the mammalian cells, whereof subcellular location is unique. At invadopodia, the α-isoform of PIP5KI (PIP5KIα) might locally produce PtdIns(4,5)P_2 and cause its accumulation in the proximity of invadopodial protrusion (Yamaguchi et al., 2010). Consequently, both PIP5KIα and its product PtdIns(4,5)P_2 are necessary for ECM degradation by breast cancer cells (Yamaguchi et al., 2010). As PtdIns(4,5)P_2 regulates some actin-related proteins, such as N-WASP (Rohatgi et al., 1999; Rohatgi et al., 2000) and cofilin (van Rheenen et al., 2007), it might directly control actin polymerization at invadopodia sites (reviewed in Hoshino et al., 2013).

PtdIns(4,5)P_2-derived PtdIns(3,4,5)P_3 could be dephosphorylated by specific phosphatase, possibly synaptojanin (Chuang et al., 2004), to form PtdIns(3,4)P_2. Local accumulation of PtdIns(3,4)P_2 is an early event in invadopodia formation that precedes

the accumulation of Tks5 (Oikawa et al., 2008). Subsequently, Tks5 binding to PtdIns(3,4)P_2 by its PX domain to commence invadopodia formation.

The remaining question is how phosphoinositide turnover is spatiotemporally regulated at invadopodia, as it seems that different phosphoinositides are involved in different stages of invadopodia formation.

1.2.6.4 Ras-superfamily of small GTPases

First identified as proto-oncogenes, the members of the Ras superfamily of small GTPases control a staggering variety of biological processes, including regulation of gene transcription, proliferation, motility, invasion, intracellular trafficking and actin cytoskeleton modification. Typically, these proteins function as molecular switches that cycle between an inactive GDP-bound and an active GTP-bound form. The exchange of GDP for GTP induces a conformational change that allows interaction with downstream effectors; this active state is terminated by hydrolysis of bound GTP to GDP. The activity of the hydrolytic cycle is primarily controlled by three sets of the accessory proteins: guanine nucleotide exchange factors (GEF), GTPase activating proteins (GAP) and guanine nucleotide dissociation inhibitors (GDI). The members of Ras superfamily fall into five subfamilies, named Ras, Rho, Rab, Ran and ARF, with distinct functions. In the following text, I will discuss only the small Ras GTPases, whose role at invadopodia has been demonstrated.

The strongest evidence to date points to Cdc42 as a central small GTPase at invadopodia thanks to its induction of actin polymerization, probably owing to its ability to directly activate N-WASP and thereby promote Arp2/3 complex dependent actin polymerization (Rohatgi et al., 1999). When Cdc42 is down-regulated by RNA interference, or when a constitutively inactive mutant is transfected, invadopodia formation is inhibited in the metastatic MTLn3 (Yamaguchi et al., 2005), whereas dominant-active mutant of Cdc42 enhanced dot-like and diffused fibronectin degradation, respectively, in RPMI17951 melanoma cells (Nakahara et al., 2003) and GFP-tagged Cdc42 was localized at invadopodia in A375MM melanoma cells (Baldassarre et al., 2006). Similarly, Cdc42 ablation blocks invadopodia formation, while preventing the efficient targeting of MT1-MMP to the invadopodia (Sakurai-Yageta et al., 2008).

The involvement of other RhoGTPases has been also implicated in invadopodia biogenesis, with variable effects, though, probably because of their indirect role in the actin polymerization. Similarly to Cdc42, active RhoA triggered the association of exocyst complex subunit Sec8 with the polarity protein IQGAP (discussed in the section 1.2.9) for the efficient targeting of MT1-MMP at sites of matrix degradation (Sakurai-Yageta et al., 2008) and accordingly the ablation of RhoA resulted in dramatic decrease of matrix degradation (Bravo-Cordero et al., 2011; Lizarraga et al., 2009; Roh-Johnson et al., 2013; Sakurai-Yageta et al., 2008), possibly also by affecting the actin-elongation factors formins (DRF1-3) (Lizarraga et al., 2009).

RhoC GTPase has been shown to affect invadopodia morphology and function without affecting their formation. After RhoC knock-down, melanoma cells rather that

forming straight, long invadopodia, formed invadopodia that are wider and shorter. Against all the expectations, RhoC depleted cells degraded the matrix more efficiently, but failed in invasive migration. Therefore, it seems that invadopodial protrusions must be strictly focused for the efficient migration. Using Förster resonance energy transfer (FRET) RhoC biosensor, it was shown that active RhoC formed a ring around invadopodial core, thus confining the invadopodia-associated molecules to restrict the size and directionality of invadopodia. The intriguing hypothesis of zonal activation of RhoC is that it occurs through selective localization of the accessory proteins. In the same study, Bravo-Cordero et al. (2011) showed that inhibitory p190GAP localized to the invadopodial core to block RhoC activity. Conversely, activatory p190GEF was excluded from the core and was instead found in the ring of active RhoC. Further, the localized activity of RhoC led to zonal activation of cofilin. Unphosphorylated active cofilin was abundant within the invadopodial core, whereas inactive serine phosphorylated cofilin was present in the surrounding area to compartmentalize the actin-free barbed end formation (Bravo-Cordero et al., 2011). The importance of Rho activity at invadopodia is further supported by previous observations that phosphorylation of p190RhoGAP was found to activate the membrane-protrusive activity required for invadopodia formation and cell invasion (Nakahara et al., 1998).

As mentioned above, accessory proteins modulate the activity of small GTPases through the regulation of the hydrolytic cycle of GTP. Among them, the known GEFs outnumber Rho family GTPases themselves (Schmidt and Hall, 2002); thus, it is likely that GEFs are the key in regulating the specificity of downstream signalling from Rho GTPases and their interaction with different effectors (Zhou et al., 1998).

The functional consequence of GEF over-expression is to elevate cellular levels of activated Rho GTPases, hence deregulated GEF expression might lead to aberrant growth, invasiveness and/or increased metastatic potential. Although how GEFs are regulated is still unknown, they clearly represent powerful candidates as spatial and temporal Rho-GTPase regulators.

A first GEF be shown to have a role in invadopodia biology was Cdc42-specific GEF faciogenital dysplasia protein 1 (Fgd1), in a study showing that the Cdc42 GEF Fgd1 is required for invadopodia biogenesis in melanoma, breast and prostate carcinoma cells. In addition, its expression levels correlated with the level of aggressiveness of the human prostate and breast cancer tumours. Fgd1 appeared to be a transient component of invadopodia, in accordance with the stepwise formation and maturation of invadopodia. In detail, shortly after invadopodia initiation Fgd1 locally accumulated at puncta with no underlying matrix degradation, which might be nascent invadopodia where Fgd1 appears ahead of actin. Later on, structures where Fgd1 co-localized with F-actin and underlying degradation are described to be fully active "early" invadopodia. On contrary, mature fully active invadopodia are Fgd1 negative (Ayala et al., 2009).

ADP-ribosylation factor 6 (ARF6) is a member of Ras superfamily of small GTPases and, like most GTPases, alternates between inactive GDP-bound active GTP-bound form. ARF6 has been intensely studied and especially in the context of clathrin independent endocytosis (CIE) and endosomal trafficking (Donaldson, 2003). The presence of glutamine and serine residues in the effector domain regions exclusively at

ARF6 enables to control actin rearrangement, in the contrast to other members of Arf family (Al-Awar et al., 2000).

The endogenous ARF6 was localized at invadopodia in breast cancer cells (Hashimoto et al., 2004) and in melanoma cells (Tague et al., 2004) and the ARF6 activity was required for invadopodia formation. The relevance of ARF6 in ECM degradation is supported by the direct correlation between ARF6 expression levels and the invasive phenotype (Hashimoto et al., 2004). The mechanism of action of ARF6 at invadopodia, however, is not completely defined but it is likely to be manifold. Firstly, the role of ARF6 in recycling of proteins from the cells surface might influence the availability of specific integrins that are employed in invadopodia initiation and function. Furthermore, ARF6-dependent endosomal trafficking may control delivery of a bulk membrane, where it is needed as a building block of various membrane protrusions, as it is documented at the leading edge of migrating cells (Tague et al., 2004)

The ARF6 involvement in invadopodia formation comprises a complex array of downstream effectors. The ARF6-downstream effector AMAP1 and ARF6-GEF GEP100 are abnormally expressed in some breast cancers and the EGFR-GEP100-ARF6 not only stimulated matrix degradation but also disrupted E-cadherin-based cell-cell adhesion (Morishige et al., 2008; Sabe et al., 2009). Similarly, the brain exclusive ARF6-GEF EFA6A promoted cell motility and invasion through ARF6/MEK/Erk axis (Li et al., 2006).

1.2.7 Actin polymerization at invadopodia

The initiation of invadopodia by an appropriate signal is facilitated by reorganization of actin cytoskeleton. Two distinct types of F-actin network co-ordinately form invadopodia: the N-WASP-Arp2/3 complex-dependent branched actin filaments are formed at the base of invadopodia and the branched actin meshwork propels invadopodia into the underlying matrix, similarly to lamellipodia protrusions. Alternatively, the further extension of invadopodia requires parallel arrays of bundled actin filaments, which are suggested arranged perpendicularly to the substrate, along the length of invadopodia.

According to the currently accepted stepwise model of invadopodia formation and maturation, invadopodia formation starts by accumulation of actin and cortactin at sites of cell adherence to ECM, with cortactin potentially recruiting other components of invadopodia machinery (Artym et al., 2006; Oser et al., 2009), and consequently promoting the Arp2/3 complex-mediated actin polymerization. Similarly, N-WASP upstream activators are required for invadopodia formation, such as Cdc42, non-catalytic region of tyrosine kinase adaptor protein 1 (Nck1) and WASP interacting protein (WIP). Of note, on the contrary of podosomes, invadopodia formation and degradation activity was markedly suppressed by depletion of Nck1 but not Grb2 (Yamaguchi et al., 2005).

The elongation of invadopodia is driven by constant growth of parallel actin filaments present along the length of invadopodia. The extension is suggested to be aided by actin nucleation factors represented by formins (Lizarraga et al., 2009), whilst the bundling and stabilization is coordinated by actin cross-linker fascin (Li et al., 2010). Additionally, member of Ena/VASP family, Mena and its invasive-specific splicing form $Mena^{INV}$ (Lizarraga et al., 2009). Invadopodia extension is further supported by actin severing activity of cofilin, which generates free barbed ends indispensable for addition of free G-actin monomers and growth of actin filaments. Clearly, cofilin is not essential for invadopodia initiation, but it is important for the stabilization and maturation process. In particular, its depletion resulted in the formation of small, short-lived and thus poorly degrading invadopodia.

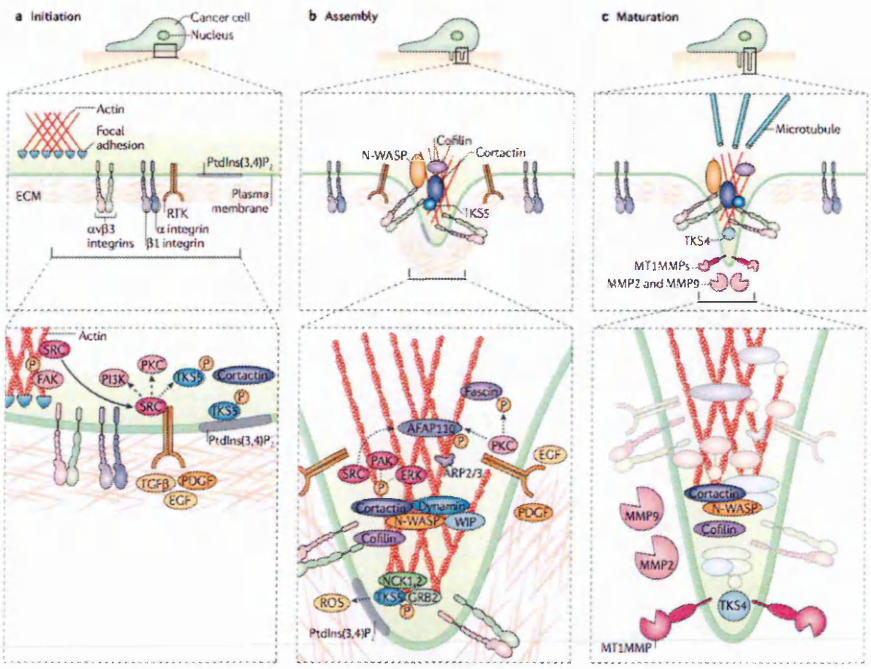

Fig. 1.4. The sequential model of invadopodia formation. The basic shape of the structure (top), a representation of key proteins in relation to the cell membrane (middle) and a molecular overview (bottom). **A)** Initiation: upon growth factor stimulation (EGF, PDGF, TGFβ), Src-phosphorylated TKS5 localize to PtdIns(3,4)P2-rich regions, which leads to recruitment of cortactin. Consequently, PI3K and PKC are activated. **B)** Formation: recruitment and activation of the actin polymerization machinery, including ARP2/3 and WIP, and the phosphorylation of key proteins , such as cortactin, TKS5, fascin, AFAP110, together withthe production of reactive oxygen species (ROS). TKS5 binds NCK1, NCK2, GRB2 and N-WASP. Cortactin associates with N-WASP and the ARP2/3 complex and generates a complex of WIP and dynamin during invadopodia formation. Phosphorylation of both cortactin and TKS5 regulate invadopodium formation. **C)** Maturation: degradation of the ECM mediated by the secretion of MMP2 and presence of MT1MMP at the tip of invadopodia. At this stage, dephosphorylated cortactin blocks the severing ability of cofilin and enables the stabilization of invadopodia. Dotted arrows indicate a regulatory pathway for which the mechanism is unknown. Dashed lines represent an enzyme–substrate interaction. P, phosphate; RTK, receptor Tyr kinase. Image taken Murphy and Courtneidge (2011)

1.2.8 Protease-dependent degradation of ECM

The main function attributed to invadopodia is that of ECM degradation, facilitated by focalized delivery of the ECM-degrading proteases. Indeed, in the initial studies on invadopodia biology, MMP2 and the surface expressed serine protease seprase were found at invadopodia, directly correlating with the invasive potential of tumour cells (Monsky et al., 1993; Monsky et al., 1994). In fact, increased protease activity is known to enhance the numbers of invadopodia (Artym et al., 2006; Branch et al., 2012; Clark et al., 2007; Steffen et al., 2008), and the broad-spectrum protease inhibitor Batimastat (BB94) blocks invadopodia formation (Ayala et al., 2008). Thus, a feedback loop appears to exist between invadopodia formation and protease activity. Among the variety of extracellular proteases expressed by human cells, matrix metalloproteases emerged as important enzymes involved in the proteolytic activity of invadopodia. Members of the MMP family (25 of them identified in humans) are multifunctional zinc-dependent enzymes that collectively degrade almost all constituents of the ECM (reviewed in Egeblad and Werb, 2002). The majority of MMPs is secreted in the extracellular environment, except for seven integral membrane proteases. The insertion of membrane-bound proteases in the membrane is facilitated either by single type I transmembrane domain (MMP14, 15, 16 and 24 or, alternatively, MT1-, MT2-, MT3- and MT5-MMP), a glycosphingolipid anchor (MMP17 and 25 or MT4- and MT6- MMP) or a type II transmembrane domain (MMP23). All MMPs share a common structure that consists of a signal peptide, a propeptide and a catalytic domain. MMPs are thus expressed as zymogens (proenzymes) and require proteolytic

cleavage of the propeptide to become active. In most cases, proteolytic activation occurs upon secretion in the extracellular milieu and is facilitated by other activated MMPs or serine proteases. MT-MMPs can also be activated by intracellular furin proteases before they reach the cell surface (Egeblad and Werb, 2002).

The paradigmatic MT1-MMP is generally considered a master regulator of protease-mediated cell invasion (Holmbeck et al., 2004; Sabeh et al., 2004; Seiki and Yana, 2003) and its key role at invadopodia-mediated degradation of the ECM has been proven repeatedly in diverse cell models (Artym et al., 2006; Branch et al., 2012; Clark et al., 2007). MT1-MMP is expressed as an enzymatically inactive 64 kDa zymogen (pro-MT1-MMP) and is further processed by furin-mediated proteolytic cleavage (Sato et al., 1996) upon its exit from Golgi prior to the arrival to the plasma membrane, originating in an enzymatically active 54 kDa fragment. Remarkably, a majority (80%) of pro-MT1-MMP is sorted to raft fractions and only a minor (20%) detergent-soluble fraction undergoes intracellular processing to the mature form (Mazzone et al., 2004). Although raft-associated pro-MT1-MMP does not directly function as a protease, it may still indirectly influence the degradation process, for example by binding of pro-MMP2 to activate it (Cao et al., 1996). Active MT1-MMP can directly degrade a variety of ECM components, such as gelatin, fibronectin, vitronectin, collagens I-III, laminin 1 and 5, fimbrin and proteoglycans. Integrins can also be cleaved by MT1-MMP, resulting in enhanced outside-in signalling.

1.2.9 Membrane trafficking to invadopodia

The trafficking of MT1-MMP to invadopodia sites serves as an excellent case in point to illustrate the complexity of the regulation of these structures and the tight balance between exocytosis and endocytosis at the sites of focal degradation. MT1-MMP is delivered to invadopodia in multiple ways (reviewed in Fritolli et al., 2010). First, targeting of MT1-MMP depends on the secretory pathway that converges on the actin cytoskeleton and the exocytic machinery. The exocyst is an octameric protein complex, consisting of Sec3, Sec5, Sec6, Sec8, Sec10, Sec15, Exo70, and Exo84, that mediates the tethering of secretory vesicles to the plasma membrane for polarized exocytosis. Importantly, activated Cdc42 and RhoA promoted binding to polarity regulator Ras-like GTPase activating protein IQGAP, and this interaction depended specifically on the exocyst subunits Sec3 and Sec8 (Sakurai-Yageta et al., 2008). The next key step in regulated exocytosis is the fusion between the donor and the acceptor membrane, facilitated by SNAREs (soluble N-ethylmaleimide-sensitive factor attachment protein receptor). At invadopodia, the vesicular SNARE TI-VAMP/VAMP-7 is required for MT1-MMP accumulation at the sites of degradation and for the efficient invadopodia formation in the breast cancer cells (Steffen et al., 2008). Accordingly, the endosomal SNAREs VAMP-3 and syntaxin 13 along with plasma membrane SNARE SNAP23 affect MT1-MMP trafficking and the invasive potential of fibrosarcoma cells (Kean et al., 2009). A fraction of MT1-MMP also originates from endocytic recycling. MT1-MMP is internalized, trafficked and recycled both through clathrin- dependent and caveolae-mediated endocytosis, and destined to endosomal and

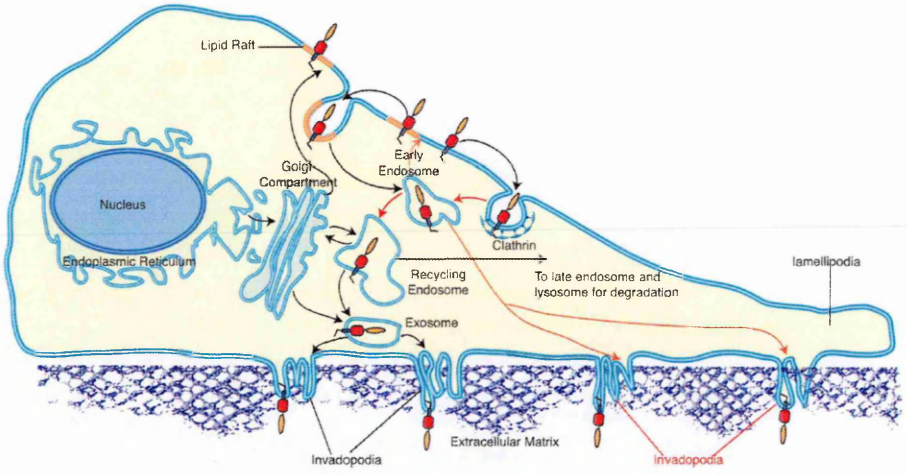

Fig. 1.5. MT1-MMP trafficking. This schematic drawing represents intersection between biosynthetic/secretory and endo-/exocytic pathways involved in the localized delivery of MT1-MMP. Adapted from Frittoli et al., 2010.

lysosomal compartments for either recycling or degradation. Additionally, MT1-MMP can be mobilized from intracellular storage by Rab8-dependent polarized exocytosis (Bravo-Cordero et al., 2007). Rab8 is a small GTPase of Rab subfamily that plays a pivotal role in the membrane traffic by determining the identity of the transported vesicles (Zerial and McBride, 2001). Another layer of complexity of proteases trafficking to the invadopodia sites has been added by a recent study on MMP2 and MMP9. In this case, small GTPase Rab40 was required for sorting of MMP2/9 in VAMP4 positive secretory vesicles and efficient degradation of matrix in breast cancer cells (Jacob et al., 2013). The authors also proposed that MMP2/9 invadopodia targeting is independent of endocytic transport.

1.2.10 Role of metabolism in the invadopodia formation

In the dense, disorganized primary tumours, cancer cells grow in low oxygen conditions. In such milieu, oxidative phosphorylation is impaired, potentially leading to adenosine triphosphate (ATP) deficiency. Cancer cells can adapt to such hypoxic conditions by switching to anaerobic metabolism, i.e., to glycolysis. Glycolytic metabolism, in turn, has lower energy yield compared to the Krebs cycle and cancer cells, indeed, exhibit a higher expression of glucose transporter GLUT (reviewed in Macheda et al., 2005) to meet increased nutrient demands. However, this metabolic adaptation presents a lethal risk to the cells due to the glycolysis-dependent increased production of H^+. The adaptive response of tumour cells to high proton concentration is

the over-expression and increased activity of pH-regulated transporters and enzymes (reviewed in Brisson et al., 2012).

A growing body of evidence suggests that hypoxic conditions might affect invadopodia biogenesis, although the key players have not been defined. The first study to analyze the functional and molecular relationship between hypoxia and invadopodia suggested that invadopodia formation is strongly affected by changes in cellular pH homeostasis, caused by Na^+/H^+ exchanger type 1 (NHE1) (Busco et al., 2010). NHE1 is involved in invadopodia formation in two ways. Firstly, NHE1 binded phosphorylated cortactin at the sites of invadopodia and the local cytosolic alkanization caused release of cofilin from cortactin to promote cofilin's severing activity (Magalhaes et al., 2011). Secondly, NHE1 activity caused acidification of the peri-cellular space around invadopodia, which is necessary for proteolysis of ECM components (Busco et al., 2010).

Diaz et al. (2013) proposed a signalling pathway that regulates invadopodia formation by coupling hypoxia inducible factor (HIF) 1α-activated cell-contact dependent signalling with paracrine activation of EGFR. In hypoxia, HIF-1-dependent induction of invadopodia formation is mediated by Notch. The subsequent Notch-dependent increase in ADAM 12 led to augmented shedding of HB-EGF, a potential ligand for EGFR (Díaz et al., 2013). Another study suggests a critical role for both Hif-1α and Hif-2α in hypoxia-induced cell motility and active invadopodia formation in melanoma cells lines derived from murine tumours (Hanna et al., 2013). In this case, Hif-1α and Hif-2α coordinately activated parallel yet distinct pathways to induce SFK activation and ECM degradation. Specifically, Hif-1α acted through platelet derived

growth factor receptor (PDGFR)-MT1-MMP axis, whereas Hif-2α induced SFK activity and ECM degradation via FAK and release of MMP-2, respectively.

1.2.11 Invadopodia in a three-dimensional world

A highly controversial aspect of invadopodia biology is whether invadopodia really exist *in vivo* and whether they contribute to the tumour cell invasion and metastasis. Most of our knowledge of invadopodia comes from studies performed using flat two-dimensional (2D) substrates, where they form below the cell body, extending a few micrometers into the ECM scaffold producing punctuate-like small lytic foci. Whether these contacts, which have been exclusively defined in some cell culture systems, are experimental artefacts or have related counterparts in three-dimensional (3D) settings either in reconstituted ECM models or *in vivo* (i.e. within tissues) is incompletely defined. This does not undermine the fundamental importance of the information gleaned by studying invadopodia biology, but has important implications in establishing the immediacy of the translational potential of such studies.

As highlighted above, invadopodia-associated proteins, such as cortactin, WASP, Arp2/3, are misregulated in some cancer types and connected to metastasis formation, suggesting a correlation between actin dynamics leading to ECM degradation *in vitro* and the invasive potential of cancer cells *in vivo* (Vignjevic and Montagnac, 2008). A current approach to gain insight into invadopodia biology in physiologically more relevant condition is the use of matrices that attempt to mimic the native environment of tumours. There are two basic patterns of ECM organization *in vivo* in mammals. Thin

and flat basement membrane, that consists primarily of type IV collagen and laminins. Underlying the basement membrane, the interstitial tissue is a thick 3D meshwork dominated by fibrillar collagen type I, which organizes into polymeric cross-linked network (Rowe and Weiss, 2009).

A initial study conducted by Friedl and Wolf (2008) using fibrillar collagen matrices or dermis slices suggested that invadopodia correspond to the lateral spikes of the migrating cells rather than to forward facing protrusions (Friedl and Wolf, 2008). However, this remains a speculation as no typically invadopodia-associated markers were used in this study. A modified version of the Boyden chamber invasion assay has also been used for the detailed study of invadopodia formation and structure. In this case, invasive colon cancer cells were plated on top of transwell filters coated with native basement membrane, and the composition and function were followed over time. Three stages were described over a period of seven days: first, formation of invadopodia and degradation of basement membrane; second, elongation of invadopodia beyond the membrane and inside the pores; and third, the maturation of invadopodia (Schoumacher et al., 2010). More recently, Magalhaes et al. (2011) used 3D matrices to show invadopodia as protrusive structures at the leading edge of migrating cells that contained invadopodial markers such as actin, cortactin and Tks5. Functionally, they were able to degrade the matrix in the direction of the movement (Magalhaes et al., 2011). The identification of lytic protrusions in 3D tissue invasion, comparable to invadopodia, and the establishment of their relevance to invasive migration and ECM remodelling, however, remains to be determined. Ultimately, one would want to know when, where, and how invadopodia contribute to 3D cell invasion and tissue

remodelling. A significant burden to 3D analysis *in vivo* and *ex vivo* is the technical one. Standard imaging approaches used in 2D settings face the problem of sample depth, focal plane, autofluorescence and signal-to-noise in 3D. Multiphoton (two-photon or non-linear) microscopy offers a good solution to aforementioned constraints of 3D imaging. Multiphoton excitation can reach substantially greater imaging depth while having reduced photobleaching and tissue damage. A by-product of multiphoton imaging is the occurrence of second and third harmonic generation (SHG and THG, respectively), that enable imaging of nonlinear scattering effects, thus allowing observation of the collagen and the tissue interface without endogenous labelling.

A major challenge of the invadopodia research field is to show that invadopodia markers indeed localize to the degradation-competent actin rich protrusions of the migrating tumour cells *in vivo*. As mentioned in the section of N-WASP, Gligorijevic et al. (2012) used a xenograft model containing the fluorescently labelled N-WASP ablated cells. In this study, 3D time-lapse imaging has been employed to follow the protrusion formation in the MTLn3 cell-derived xenograft tumours. Strikingly, these protrusions were positive for cortactin and associated with proteolytic activity, as revealed by cleaved collagen ¾ staining (Gligorijevic et al., 2012).

1.3 Cholesterol in biological membranes

Cholesterol is an essential molecular component of the eukaryotic cells, in which it is indispensable for growth and viability. Eukaryotic cells invest considerable energy to synthesize and tightly control this molecule that might be even toxic under certain circumstances. Utmost role of cholesterol is as a structural component of biological membranes that regulates diverse membrane characteristics, such as fluidity, permeability, thickness and phase order. Beside that, cholesterol serves as a precursor of bioactive molecules including steroid hormones, vitamin D, bile acid and oxysterols.

1.3.1 Biological membranes: Cholesterol and membrane viscosity

Biological membranes are circa 5 nm-thick lipid bilayers that form continuous barriers around the cell and the cellular compartments. Beside their role in cellular compartmentalization, biological membranes are fundamental platforms for signal and energy transduction, cell adhesion, cell motility and vesicular transport. Membrane lipid composition is not uniformly distributed and differs both vertically and horizontally; i.e. across the different membrane organelles, between the two bilayer leaflets of any organelle (membrane asymmetry), and within the same monolayer, where microareas enriched in specific lipids are known to exist. These regions are typically referred to as cholesterol and sphingolipid domains, or generally lipid rafts, and they are dynamic

proteo-lipid modules with specialised functions (Simons and Ikonen, 1997). Despite this complexity, lipid homeostasis is tightly maintained, as lipids are coordinately synthesised, catabolised, and shuttled from their sites of synthesis to their eventual intracellular destinations. The lipids of biological systems are either hydrophobic, containing non-polar groups only (e.g., triglycerides), or amphipathic, which means they feature both polar and non-polar groups.

The major structural amphiphathic lipids in biological membranes are glycerophospholipids, sphingolipids and cholesterol. The hydrophobic moiety of the glycerosphingolipids is diacylglycerol, which is covalently linked to two fatty acids of varying lengths. Glycerosphingolipids are subdivided in five major types depending on the polar head group: phosphatidylcholine (PC), phosphatidylethanolamine (PE), phosphatidylserine (PS), phosphatidylinositol (PI) and phosphatidic acid (PA).

The hydrophobic backbone of the sphingolipids is ceramide. The polar head group could be either phosphocholine in case of sphingomyelin, the most prominent sphingolipid in mammalian membranes, or mono-, di- or oligosaccharides in which case glycolipids are formed.

Sterols have the most atypical architecture, as they consist of a short alkyl chain and a nearly planar assembly of four rings. The only polar element of the sterols is a single hydroxyl group. In detail, cholesterol contains a single hydroxyl group at carbon 3, a double bond between carbons 5 and 6, two methyl groups at carbon 18 and 19, and an iso-octyl hydrocarbon side chain at carbon 17 (Ohvo-Rekilä et al., 2002). The 3D structure results in a rigid planar four-ring nucleus with the 3-OH group, the two

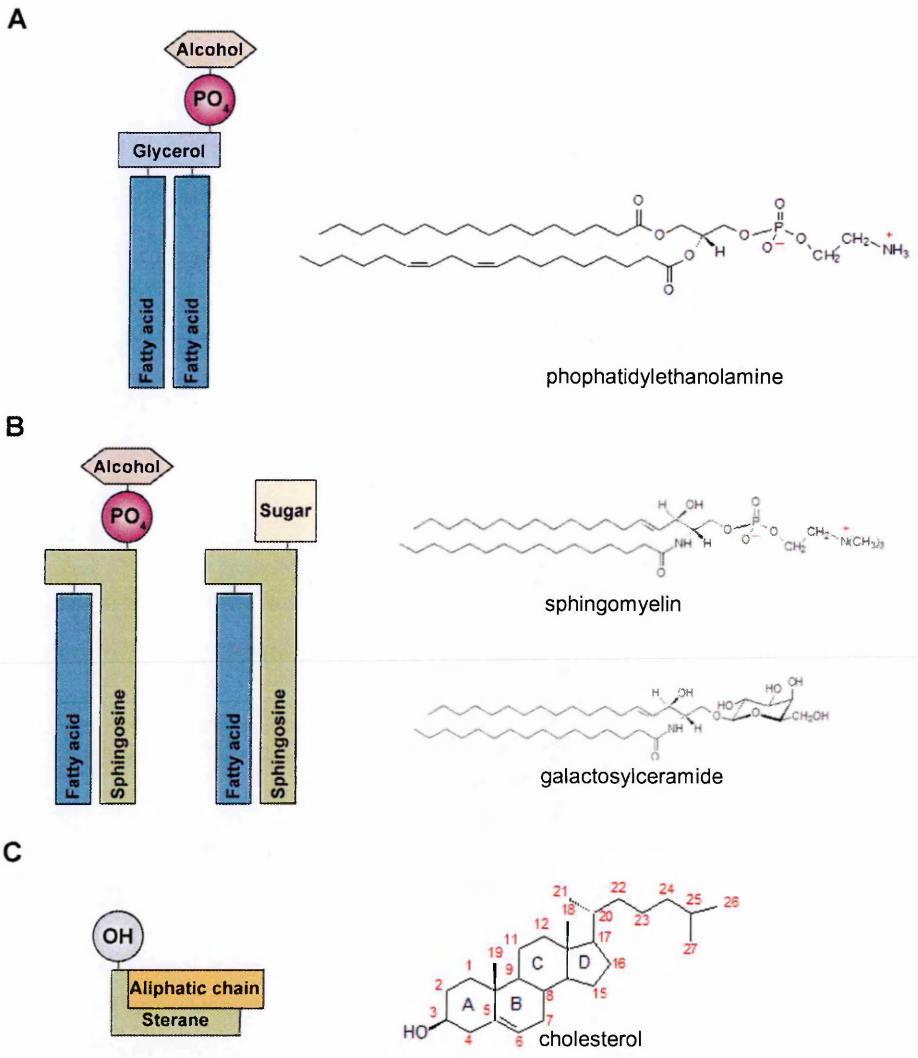

Fig. 1.6. Membrane lipids. (a) The glycerophospholipid backbone is made up of diacylglycerol, with two acyl chains, one of which (sn-2) bearing one or more *cis* double bonds. The head group can be serine, inositol, ethanolamine, choline or glycerol. (b) Sphingolipids consist of sphingosine backbone which is attached to a fatty acid and polar headgroup. In sphingomyelins, the head group is phosphocholine choline, while in glycosphingolipids (GSL) is made up of one or more sugars. (c) The polar head group of cholesterol is a single OH group, whereas the hydrophobic moiety contains an iso-octyl carbon chain linked to a sterane-derived unit. Image adapted from Fantini (2002).

methyl groups and the side chain on the same side in the β-configuration (Bittman, 1997).

Cholesterol is a major determinant of the biophysical properties of cell membranes. Membrane viscosity, as opposed to membrane fluidity, is a parameter used to describe an ease of movement of a particle within the membrane. Cholesterol modulates membrane viscosity by increasing it at higher temperatures and decreasing it at lower ones, thus acting as a membrane fluidity buffer (Nipper et al., 2008). Nevertheless, there are some indications that augmenting cholesterol might even reduce the viscosity of the plasma membrane of the aortic endothelial cells (Byfield et al., 2005). Moreover, specialized membrane domains such as the lipid rafts, influence and to certain extent spatially regulate the rigidity of the membrane. For example, inhibition of ABCA1 transporter, which is known to distribute raft cholesterol to non-raft regions, significantly alters the viscosity gradient in migrating keratinocytes, resulting in the inhibition of migration (Klein et al., 2012; Zarubica et al., 2009). Up to now, only few studies have shown a direct correlation between local microviscosity and cholesterol content in living cells, while comprehensive analysis is often burdened by imaging tools. There are a number of methods that have been developed to monitor the changes in the viscosity, amongst them fluorescence recovery after photobleaching (FRAP), environment sensitive dyes and nuclear magnetic resonance, which differ in sensitivity and robustness. Of note is the lipophilic fluorescent probe Laurdan with the distinct ability to sense the changes in the polarity of its environment. In the lipid bilayers, Laurdan undergoes a spectral shift in the presence of water, informing about water

penetration, a property related to lipid packing and membrane viscosity (Kaiser et al., 2009).

Changes in membrane viscosity represent a key tool in regulation of the membrane properties in physiological conditions and in the pathogenesis of diseases, such as atherosclerosis, hypercholesterolemia, Alzheimer disease and cancer. For example, in the cancer cell, augmentation of membrane fluidity is instrumental for cell migration and might facilitate the migratory potential of cancer cells by enhancing their deformability. Although sphingolipid/cholesterol association mediates the increased order of lipid rafts (Simons and Sampaio 2011), cholesterol fluidizes sphingolipid model membranes (Simons and Vaz 2004). Cancer cell membranes contain more cholesterol-rich lipid rafts (Li et al., 2006) and exhibit increased fluidity (Zeisig et al., 2007) relative to normal cells. It has been also shown that increased membrane fluidity correlates with changes in malignancy in experimental models.

1.3.2 Biosynthesis of cholesterol

Biosynthesis of cholesterol is a long and complex process consisting of more than 30 reactions, which were mostly unravelled by Konrad Bloch and Fyodor Lynen, who were awarded the Nobel Prize for their work in this topic in 1964. The greater part of cholesterol biosynthesis occur in the endoplasmic reticulum (ER). The initial reaction is the condensation of acetyl-coenzyme A and its derivate acetoacetyl-coenzyme A. The

product of this reaction, 3-hydroxy-3-methylglutaryl-CoA (HMG-CoA) is further reduced to mevalonate by the enzyme HMG-CoA reductase (HMGR). This step is of a particular importance as it is irreversible and rate limiting for the biosynthetic pathway. Indeed, the blood cholesterol-lowering drugs statins inhibit cholesterol synthesis at this step. Subsequently, mevalonate is converted into isopentyl pyrophosphate in three ATP-dependent reactions. Isopentyl pyrophosphate is a key precursor of all isoprenoids, which form the structural basis of many vitamins, pigments and precursors of sex hormones. In the next step of the biosynthesis, the 5-carbon isopentylpyrophosphate condenses with itself in multiple steps to form the 30-carbon squalene.

Finally, the linear squalene is cyclized to form lanosterol leading to the typical sterol tetracyclic fused ring skeleton in an aerobic reaction. Altogether, there is 19 different enzymatic reactions and 12 intermediates between the first steroid intermediate lanosterol and the final product cholesterol (Gaylor, 2002). Functionally, this complex process could be described as a progressive streamlining of the hydrophobic surface of sterol by removal of the 1-3 CH3 groups that protrude from the flat surface of the steroid ring (Mouritsen and Zuckermann, 2004). The post-lanosterol steps of cholesterol biosynthesis had been divided into Bloch and Kandutsch-Russell pathways that share the same enzymes but differ at the stage when C24 double bond is reduced. Consequently, cholesterol biosynthesis can continue with either 7-dehydrocholesterol (Kandutsch-Russell pathway) or desmosterol (Bloch pathway) as the penultimate precursor of cholesterol. The functional importance of having two distinct pathways is not well understood. Interestingly, there is evidence of an age-related differential use of the pathways. For instance, in young mice, brain cholesterol is synthesised mainly via

the desmosterol pathway, while in older mice via the 7-dehydrocholesterol pathway (Lutjohann, 2002).

1.3.3 Subcellular distribution of cholesterol

Cholesterol is not evenly distributed within the cell. The main cholesterol biosynthetic compartment, the ER, along with mitochondria and cis-Golgi, contains very little cholesterol. ER cholesterol concentration is estimated to be as low as 1% of total cholesterol, whereas the highest concentration of cholesterol is at the plasma membrane, where it constitutes about 40% of total lipids and represents 65-80% of total cellular cholesterol (Maxfield and Wüstner, 2002). Furthermore, a substantial amount of cholesterol has been detected in the membrane domains of endocytic pathway,

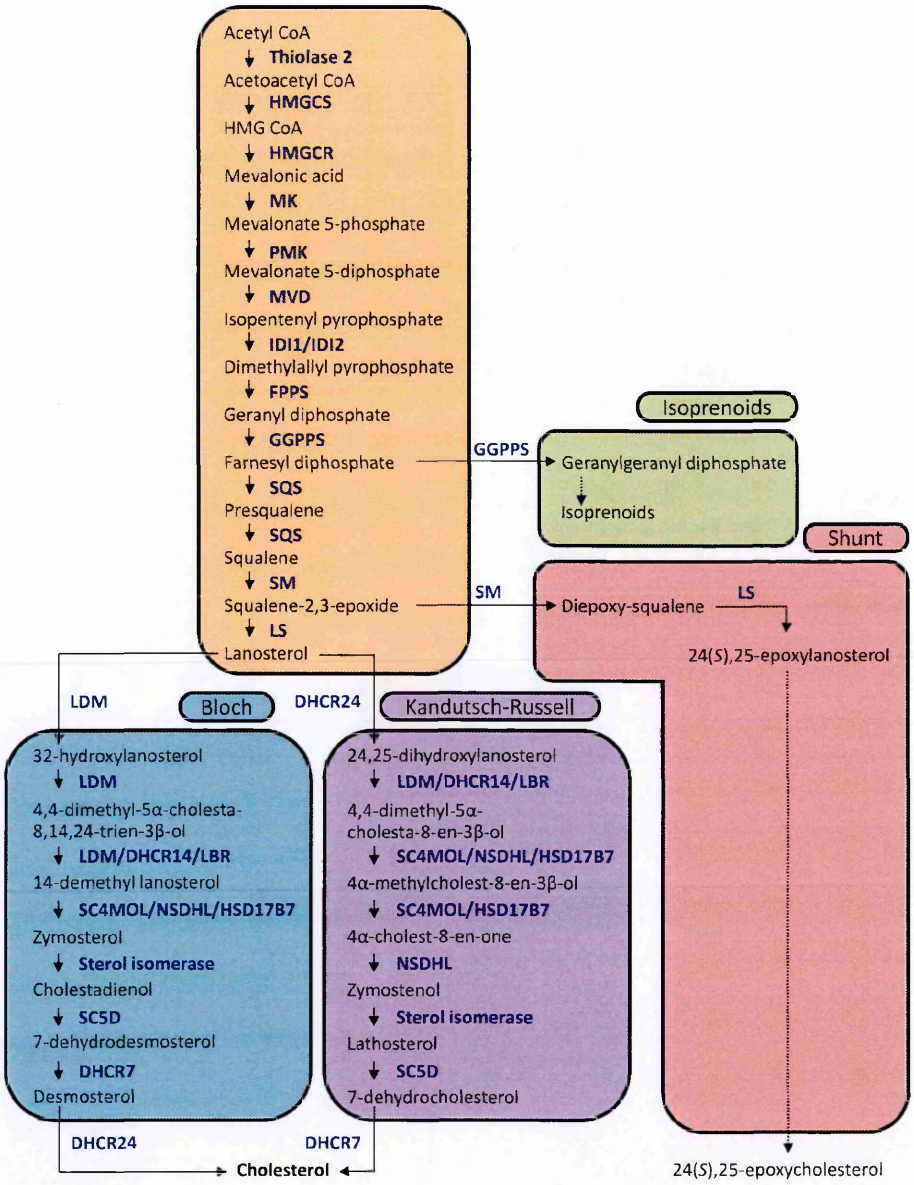

Fig. 1.7. Cholesterol synthesis pathway. Acetyl coenzyme A is finally converted to lanosterol in mevalonate pathway. Post-lanosterol cholesterol synthesis pathway is further divided in two branches, Bloch and Kandutsch pathway. Two other branches also diverge from mevalonate pathway which lead to production of isoprenoids and 24(S),25-epoxycholesterol in a shunt. Image taken from Sharpe, 2013.

specifically in the internal vesicles of multivesicular bodies (Möbius et al., 2003; Simons and Ikonen, 1997) and the endocytic recycling compartment (ERC) (Hao et al., 2002; Ohvo-Rekilä et al., 2002). Intracellular compartments in vesicular contact with the plasma membrane, such as lysosomes and trans-Golgi, have intermediate cholesterol content. How the gradient across the different membranes of the secretory pathway is maintained, remains elusive. Two main theories have been proposed. Firstly, cholesterol might be sorted into vesicles heading towards the plasma membrane but excluded from retrograde transport. Secondly, the differential distribution of cholesterol in particular membranes could depend on membrane lipid composition. According to the condensed complex model, cholesterol affinity for the different lipids varies, thus cholesterol builds more stable complexes with some lipids compared to others.

As mentioned previously, cholesterol is synthesized in the low cholesterol ER, thus a mechanism must be in place that helps to keep the cholesterol levels low. An important buffering mechanism to control the levels of unesterified cholesterol in this compartment is esterification by acetyl-coenzyme A acetyltransferase (ACAT). Esterified cholesterol is then transported to the lipid droplets or packed into lipoprotein particles.

1.3.4 Intracellular cholesterol transport

De novo synthesised cholesterol leaves the ER rapidly, in an energy dependent manner and with a halftime of 10-20 min (Bittman, 1997; DeGrella and Simoni, 1982). Brefeldin A, a well known inhibitor of anterograde transport that disrupts the Golgi

complex, has little effect on the kinetics of cholesterol arrival to the PM (Urbani and Simoni, 1990), suggesting that cholesterol is transported in a non-vesicular fashion. The non-vesicular transport of sterols and other lipids may be facilitated by a family of cytosolic lipid transfer proteins (LTPs), inter-organelle membrane contacts or combinations thereof. Further support for the non-vesicular sterol transport hypothesis comes from yeast with conditional defects in proteins involved in intracellular vesicular transport in which transport of the cholesterol yeast homologue ergosterol remained unaltered (Schnabl et al., 2005). There are many candidates for sterol transport including the oxysterol-binding protein related proteins (ORPs) (Im et al., 2005; Lutjohann, 2002) and caveolins (Smart et al., 1996; Uittenbogaard and Smart, 2000).

1.3.5 Cholesterol efflux

Because mammalian cells are unable to degrade cholesterol, they need to remove cholesterol via regulated secretion. The secretion of cholesterol by non-hepatic cells, also referred to as reverse cholesterol transport, is an important cellular homeostatic mechanism controlling the levels of free cholesterol by export to high-density lipoprotein (HDL) particles. Trans-membrane proteins from the family of ATP-binding cassette (ABC) transporters have emerged as main facilitators of this process, with the ubiquitously expressed ABCA1, the protein defective in Tangier disease (Rust et al., 1999). Binding of the circulating extracellular acceptor of cholesterol, the lipid-poor form of apoliprotein A-I (apoA-I) to the membrane-bound ABCA1 transporters triggers a multi-step process, which facilitates the transfer of phospholipids and

cholesterol to the HDL. HDL then enter the circulation and are cleared from the blood by liver and steroidogenic cells in a scavenger receptor B1 (SRB1)-dependent fashion (Valacchi et al., 2011). In the liver, the obligate heterodimers ABCG5/ABCG8 are involved in the secretion of cholesterol into bile (Graf et al., 2003).

It is worth noting that cholesterol elimination from macrophages is a crucial process in atherosclerosis. Another ABC transporter, macrophage-specific ABCG1, cooperates with ABCA1 to facilitate further loading of lipids to nascent HDL (Gelissen et al., 2006). Combined knock-out of ABCA1 and ABCG1 in mice has indicated that the synergetic action of both transporters in mediating cholesterol efflux form macrophages is of crucial importance in prevention of atherosclerosis *in vivo* (Yvan-Charvet et al., 2007).

1.3.6 Cholesterol uptake

In addition to cholesterol biosynthesis, cells can acquire cholesterol from the extracellular environment via receptor-mediated uptake of lipoprotein particles. Low-density lipoprotein receptor (LDL-R), present at the cell surface, binds low-density lipoprotein (LDL) containing esterified cholesterol and lipids. The complex is then endocytosed by clathrin-coated vesicles that pinch off from the plasma membrane. As the complex travels along the endocytic pathway, the pH of the vesicles decreases, resulting in conformational change of LDL-R and subsequent release of its cargo. At this point, LDL-R is either recycled back to the plasma membrane or targeted for degradation in lysosomes. LDL-cholesterol esters are hydrolysed in late endosomes by

acid lipase to form unesterified free cholesterol ready for cellular needs. Exit of cholesterol from the multivesicular late endosomes is mediated by late endosomal Niemann-Pick type C proteins (NPC) 1 and 2. Although the precise mechanism is not clear, loss of function of either protein leads to Niemann-Pick disease characterised by the retention of LDL-derived unesterified cholesterol in the late endosomal compartment. A soluble NPC2 binds cholesterol and delivers it to membrane-bound NPC1that incorporates the sterol in the late-endosomal/lysosomal membrane (Kwon et al., 2009).

1.3.7 Transcriptional control of cholesterol homeostasis

Cholesterol homeostasis is also regulated by two main nuclear transcriptional receptor systems, the sterol regulatory element binding proteins (SREBP) and the liver X receptors (LXR). SREBP is a transmembrane protein harboured in the ER by binding to SREBP cleavage activating protein (SCAP). In cholesterol-poor conditions, the conformational change abrogates SCAP binding with insulin-induced gene 1 (Insig 1). As a result SREBP is transported to Golgi complex, where it undergoes proteolytic cleavage. Upon transport to the nucleus, the processed fragment acts as a transcription factor that activates the expression of genes containing a sterol regulatory element, such as HMCoA and LDL, thus activating the cholesterol biosynthesis and uptake, respectively. On the contrary, activation of the LXR transcriptional system leads to reverse cholesterol transport. LXRs sense the cholesterol levels by binding the oxidized form of cholesterol, oxysterols. Upon activation, LXRs alter the transcription of

proteins involved in reverse cholesterol transport (reviewed in Tontonoz and Mangelsdorf, 2003).

1.3.8 Oxysterols

Oxysterols are the oxygenated derivates of cholesterol, which are produced by either oxidation of cholesterol itself or by an enzymatic reaction (reviewed in Brown and Jessup, 2009). Typically, they are present at 1000-fold lower concentrations compared to cholesterol. The hydroxylated sterols are more hydrophilic and can cross the biological membranes more readily than cholesterol. As first proposed by Kandutsch, certain oxysterols may serve as a sensor and modulators of cholesterol homeostasis (Kandutsch et al., 1978). The oxysterols involved in this cholesterol biosynthesis feedback regulation can be divided in four categories according to their mechanism of action: 1) suppressors of HMg-CoA reductase; 2) LXR ligands; 3) suppressors of SREB; 4) activators of cholesterol.

Of interest, 24(S), 25-epoxycholesterol is unique among oxysterols in that it is not derived from cholesterol. Instead, it is produced directly via a shunt in the mevalonate pathway. 24(S), 25--epoxycholesterol affects cholesterol homeostasis by all three main modes of cholesterol regulation: inhibition of cholesterol synthesis via stimulation of HMG-CoA reductase degradation and suppression of SREBP activation; inhibition of re-uptake via suppression SREBP activation and stimulation of efflux via LXR (Brown, 2009).

1.3.9 Cholesterol-lowering drugs and their possible implication in cancer therapy

The most prescribed cholesterol-lowering drugs, the statins (also among the most prescribed drugs in any class), are inhibitors of HMG-CoA reductase and as such studied both intensively and extensively. First isolated from fungi strain as mevastatin (also called compactin), the first chemically derived compound, lovastatin, was marketed in the late 80's with other statins soon to follow (reviewed in Gelissen and Brown, 2011). Interestingly, population studies suggested that, in addition to the beneficial effects in prevention of cardiovascular diseases, administration of statins correlates with reduced incidence of a number of pathologies, such as melanoma, breast, prostate and colon cancer (Hindler et al., 2006) and continuous administration of standard doses of statins is beneficial and might be especially helpful in preventing certain types of tumours, as first reviewed by Solomon and Freeman (Solomon and Freeman, 2008). A most studied point in case is prostate cancer (PCa) (recent reviews Krycer et al., 2013; Moon et al., 2013; Pelton et al., 2012). Early evidence of an association between cholesterol and PCa arose from studies on Japanese citizens, who had a manifold increased risk of PCa upon immigration to the United States, implicating high cholesterol as a culprit. Since then, the link between high cholesterol levels and prostate cancer risk has been studied in numerous epidemiological studies, including large population studies of cholesterol and disease, observational studies of cholesterol and PCa, observational studies of cholesterol-lowering drugs and PCa, and randomized trials of statins that report on cancer (reviewed in Pelton et al., 2012). Although the recent literature indicates that long-term statin therapy is chemopreventive against

aggressive PCa, large randomized trials of statin drugs that report on cancer (including PCa) do not support this claim. Solomon and his colleagues previously expressed several concerns about such all-cancer studies: their relatively short duration, relatively few PCa cases, inconsistency in recording of PCa grade or stage, large crossover of patients from control to statin groups, and the over-representation of least potent statin, pravastatin. In aggregate, whether or not statin-mediated lowering of cholesterol has a positive impact on cancer risk has been a subject of a numerous studies, although with conflicting results due to the diverse methodologies used in the studies, inconsistency in the duration, the prostate cancer markers and definition of terms such as low cholesterol. Nevertheless, the recent observational studies on the statins role in prostate cancer are supportive of the hypothesis that statin use reduces risk of advanced prostate cancer. In two independent studies Platz and colleagues showed in an analysis aimed specifically at prostate cancer incidence that there is no association between overall prostate cancer risk and statin use. In contrast, longer statin use was associated with advanced disease risk and development of a more dangerous, castration-resistant stage of PCa. Several more studies from independent groups largely confirmed this observation of that statins reduce the risk of aggressive PCa (Flick et al., 2007; Geybels et al., 2013; Jacobs et al., 2007). For example, a recent study revealed in 10 years follow-up a drastic reduction of prostate cancer-specific mortality in statin users. However, the study demonstrated that statins do not have an effect on progress or recurrence (Geybels et al., 2013). In conclusion, it appears that statins might not prevent risk of early stage prostate cancer, but affect progression to more agressive phenotypes and to reduce mortality.

The protective effect of statins is further supported by number of pre-clinical studies. By exploring the effect of statins on tumourigenesis at the molecular level, it has been confirmed that statins may help to keep under control a range of cellular functions involved in tumour initiation, growth and invasion. Whilst inhibiting the early step in the cholesterol biosynthetic pathway, statins inhibit synthesis of non-cholesterol synthetic intermediates, too. Most probably the beneficial effects of statins derive in vivo from lowering serum cholesterol, whereas extrahepatetic levels of statins are generally very low, and thus it is unlikely that statins accumulate in the other tissues at sufficient concentration to promote any sustained local effect (Solomon and Freeman, 2008; Solomon and Freeman, 2011). Alternatively, tumour growth might be affected by the availabity of circulating cholesterol. Epidemiological studies regarding statins thus report on the effect of lowering of circulating cholesterol, or LDL, respectively.

Currently, several clinical trials on statins (simvastatin and atorvastatin- see www.clinical-trials.gov, identifiers NCT00572468, NCT01821404, NCT01759836, NCT01220973, NCT01561482) are ongoing to assess the effect on various parameters, such as histological and circulating biomarkers (Moon et al., 2014).

In summary, critical evaluation of the epidemiological data supports the beneficial effect of statins, and enhanced cholesterol lowering, in prostate therapy, and several studies are underway. One such approach would be to employ statins, or other cholesterol lowering drugs, as an adjuvant therapy to standard cancer treatment.

1.4 C-terminal Src kinase: The regulation of Src family kinases

The Src family kinases (SFK) are vitally important for the control of an array of signalling networks involved in cell proliferation, cytoskeleton organization, metabolism, motility, differentiation and in just about any cellular activity. The SFKs represent the largest family of non-receptor kinases in mammalian cells and comprise nine members, Src, Yes, Fyn, Fgr, Lyn, Hck, Lck, Blk, Yrk, of which Src, Fyn and Yes are ubiquitously expressed. SFKs share five similar functional domain arrangements, with an N-terminal domain followed by three domains designated as Src-homology (SH) region, SH3, SH2 and SH1 (catalytic) domain and a C-terminal tail with a regulatory tyrosine.

1.4.1 Regulation of SFK activity

The structural similarities account for common mechanisms of regulation of the SFK activity: 1) fatty acylation of N-terminal domain regulates their membrane association and subcellular distribution; 2) once phosphorylated, the tail inhibitory tyrosine binds intramolecularly to the SH2 domain, thus maintaining the kinase in a closed, inactive conformation (reviewed in Ingley, 2008).

The poorly conserved N-terminal region, sometimes called unique domain, is the most divergent part of SFKs and is believed to provide functional specificity to each family member, as the status of fatty acylation has been shown to regulate their subcellular location (reviewed in Resh, 1999). All family members are co-translationally myristoylated on the terminal glycine. Myristoylation mediates attachment to the inner surface of bilayered membrane. In addition, the unique domain could bear another lipid modification, reversible post-translational palmitoylation at multiple cysteine residues.

Tyrosine phosphorylation is the most significant mode of SFK regulation. All SFKs possess two tyrosine motifs that regulate activity in opposing ways. Phosphorylation of the tyrosine within the activation loop confers full activity of the kinase, while the C-terminal residue is phosphorylated in the inactive enzyme. The latter can interact with the SH2 domain intramolecularly, which makes the SH2 domain a key regulator of allosteric kinase regulation. In summary, the complex regulatory mechanism allows multiple levels of kinase activity, starting from 1) fully active form, where the activatory tyrosine within the A-loop is phosphorylated; 2) partially active form, where the activatory tyrosine is not yet phosphorylated; 3) closed inactive conformation.

1.4.2 Csk protein structure and catalytic function

The main physiological inhibitor of SFKs is the C-terminal Src kinase (Csk), another non-receptor tyrosine kinase with a molecular mass of 50 kDa, discovered in

the late 80's (Okada and Nakagawa, 1988). The structural organization of Csk and its homologue Csk-homologue kinase (Chk) is very similar to that of SFKs. However, they are some key differences. The distinctive feature of Csk is the absence of an autophosphorylation site, inhibitory tyrosine and N-terminal fatty-acyl modification. As a consequence, Csk activity is regulated in a distinct fashion, which will be discussed in the next section.

Each domain of Csk plays a role in the interaction with various binding partners. The catalytic domain (SH1) of Csk binds and phosphorylates all nine members of the SFK family (reviewed in Ingley, 2008); the phospho-tyrosine binding SH2 domain binds various scaffolding proteins, such as the ubiquitiously expressed Csk-binding protein/Protein associated with (Cbp/PAG) (Brdicka et al., 2000; Kawabuchi et al., 2000), caveolin-1 (Cao et al., 2002), insulin receptor substrate-1 (IRS-1) (Tobe et al., 1996), paxillin (Schaller and Parsons, 1995) and LIME (Brdickova et al., 2003). The inhibitory action of Csk might be coupled with the dephosphorylation of the activatory SFK tyrosine by a phosphatase that associates with Csk.

1.4.3 Regulation of Csk activity

Csk lacks both a trans-membrane domain and fatty-acyl modification, and it is thus predominantly localized in the cytosol. Therefore, Csk seems to be primarily regulated spatially than catalytically (Howell and Cooper, 1994). The investigation of the mechanism underlying the plasma membrane localization of Csk has led to the identification of functionally related scaffolding proteins that bind Csk in a

phosphorylation dependent manner and thus bring it to the plasma membrane in close proximity to its membrane-associated substrates (Brdicka et al., 2000; Brdickova et al., 2003; Cao et al; 2002; Kawabuchi et al., 2000). This creates a negative feedback loop by associating active SFKs with their suppressor Csk. Furthermore, binding to the adaptors can fully activate the enzymatic activity of Csk by inducing a conformational change in the catalytic domain, as shown in case of binding of Csk to phosphorylated Cbp/PAG (Takeuchi, 2000).

In addition to its spatial regulation, other mechanisms are involved in the regulation of the phosphotransferase activity of Csk. Firstly, Gβγ upregulates Csk activity, probably by binding to the catalytic domain and by covalent modification (Lowry et al., 2002). Secondly, Csk is *in vitro* and *in vivo* phosphorylated on Ser 364 by protein kinase A (PKA) (Vang et al., 2001), leading to increased Csk activity due to altered interaction between the catalytic and SH3 domains (Yaqub et al., 2003).

1.4.4 Adaptor proteins – Cbp/PAG

The mechanism underlying cell membrane localization of Csk has been investigated and has led to the identification of adaptor proteins (Ingley, 2009) including the phosphoproteins Cbp/PAG (Kawabuchi et al., 2000), LIME (Brdickova et al., 2003) and caveolin 1 (Cao et al., 2002). In this section, I will discuss Cbp/PAG.

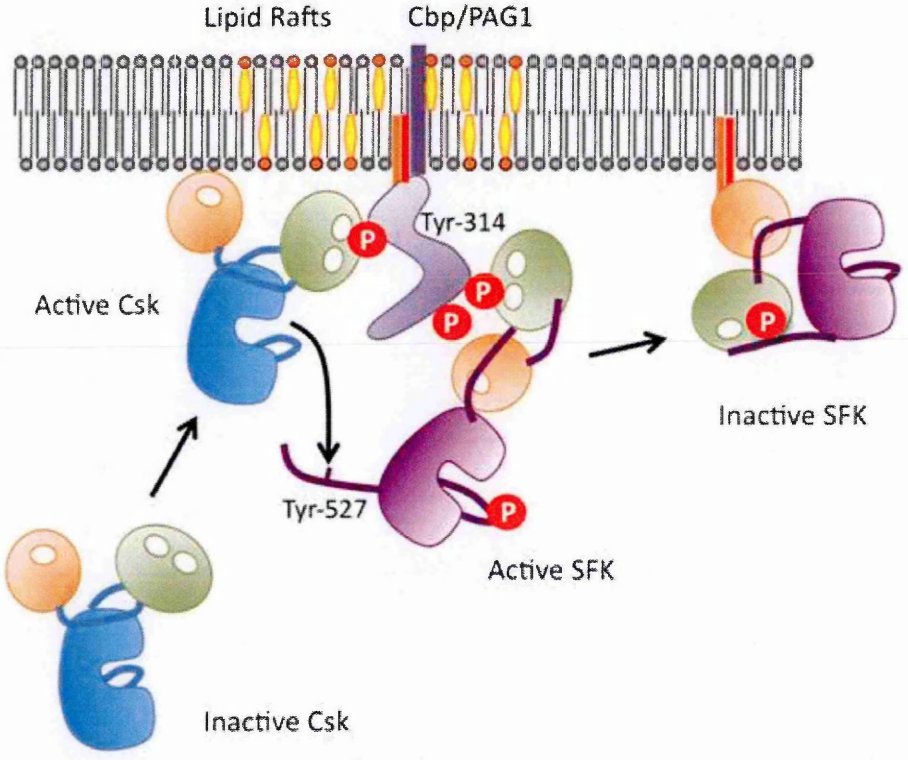

Fig. 1.8. Model of Csk activation by Cbp/PAG. Image taken from Okada (2012).

The Csk-binding protein/phosphoprotein associated with glycosphingolipid-enriched domains (Cbp/PAG) (Brdicka et al., 2000; Kawabuchi et al., 2000) is characterized by a short extracellular domain (16-18 amino acids), a single trans-membrane domain and a long intracellular part. Palmitoylation targets Cbp/PAG to the lipid rafts but this lipid modification is transient, which might allow the presence of Cbp/PAG in the membrane only in certain circumstances. A growing body of evidence points to Cbp/PAG as a strategic molecule placed at the hub of early signalling, involving regulation of SFK, monomeric Ras proteins, and modification of the cytoskeleton (reviewed in Svec, 2008). Cbp/PAG binds Csk through phosphorylated tyrosine residue 317 (Brdicka et al., 2000; Kawabuchi et al., 2000), and in addition, the formation of the Cbp/PAG-Csk complex leads to the activatory conformational change within the Csk molecule (Takeuchi, 2000). Several other interactions were discovered during the following years. Interestingly, Cbp/PAG indirectly interacts with F-actin, through binding of EBP50 (ezrin/radixin/moesin (ERM) binding phosphoprotein) (Brdickova et al., 2001). In detail, the C-terminal domain of Cbp/PAG binds the PDY domain of EBP50, which further binded to the ERM family of proteins. The interaction with ERM proteins in turn linked the Cbp/PAG-EBP50 complex to the actin cytoskeleton, which might be an important event to anchor lipid rafts to the actin cytoskeleton (Itoh et al., 2002). Interestingly, Cbp/PAG links SFK inhibition with SFK polyubiquitylation and degradation (Ingley, 2009).

1.4.5 Csk in oncogenesis

A line of evidence suggests the role of Csk in neoplastic progression via inhibition of SFKs. v-Src was identified as a first oncogene, but activating mutations of c-Src are very rare in human cancers. Despite this, Src activity is deregulated in many types of cancers, such as in pancreatic neoplasia (Shields et al., 2011). Src activation can indeed occur following a loss of regulation at inhibitory Y527 due to loss of Csk, altered Csk binding protein function or elevated phosphatase activity. The direct involvement of Csk in oncogenesis, however, is not clear (Okada, 2012).

Reduced expression of Csk might play a role in the activation of Src in some cancers. In hepatocellular carcinoma, Csk levels are reduced compared to those in normal liver tissue and this reduced expression correlates with enhanced Src activity (Masaki 1999). Moreover, over-expression of Csk appears to reduce metastatic capacitites of human colon cancer cells, accompanied by decreased invasion in Matrigel and decreased secretion of MMP2 (Nakagawa et al., 2000).

In the case of pancreatic ductal carcinoma, it has not been well understood whether increased Src activity, usually associated with poor prognosis, actually contributes to the onset of the disease. A recent study of Shields et al. (2011), with a murine model depleted of Csk, showed that Csk deletion accelerated the formation of neoplasia only in a Kras context (Shields et al., 2011). Over-expression of Csk in a mouse highly metastatic colon cancer cell line NL-17 led to decreased invasion in Matrigel and decreased secretion of MMP2 (Nakagawa et al., 2000). Another confirmation of the importance of Csk-dependent regulation of SFK activity in cancer

progression derives from experiments on the human epithelial colon cancer cell lines HCT15 and HT29. These two cell lines exhibit elevated autophosphorylation of SFKs and reduced expression of Csk in comparison with a highly differentiated adenocarcinoma cell line. Introduction of active Csk in both colon cancer cell lines reverted their invasiveness *in vitro*, accompanied by a decrease in SFK activity, an increase in E-cadherin mediated cell-cell contacts and a reduction of cell adhesion and invasiveness. Moreover, Csk has been shown to have a critical role in defining the cell sensitivity to integrin-mediated, adhesion-dependent activation of SFKs (Rengifo-Cam et al., 2013).

By contrast, the Csk's function as a tumour suppressor might depend on the expression of its adaptor proteins. A line of evidence supports Cbp/PAG as a potential suppressor of SFK-promoted tumour progression. The expression of Cbp/PAG is down-regulated in many types of cancer (Oneyama et al., 2008) which might interfere with the translocation of Csk to the plasma membrane and efficient control of SFKs. In a recent study by Mak et al. (2013), the role of an apoptosis-stimulating protein of p53 (ASPP2)-Csk-Src axis in gestional choriocarcinoma has been unveiled. In detail, ASPP2 messenger RNA (mRNA) is downregulated in choriocarcinoma cell lines and its ectopical re-introduction lead to decreased cell migration, specific induction of E-cadherin and inactivation of Src; and this specific effect was overcome by silencing of Csk (Mak et al., 2013).

CHAPTER 2: Materials and experimental procedures

2.1 General materials

Sodium dodecyl sulphate (SDS), potassium acetate, TRIZMA base, magnesium acetate, Tris[Hydroxymethyl]aminomethane (Tris), ethyl- enediaminetetraacetic acid (EDTA), KH_2PO_4, Na_2HPO_4, NaH_2PO_4, $MgSO_4$, bovine serum albumin (BSA), β–glycerol phosphate, kanamycin, porcine gelatine, sodium azide, sodium deoxycholate (DOC), methyl-β-cyclodextrin, lovastatin, mevalonate, cholesterol, sucrose, rhodamine and fluorescein 5- isothiocyanate (TRITC and FITC) were from Sigma-Aldrich (WI, USA). NaCl, $Na_2B_4O_7$, HCl, NaOH, KOH, NaF, NH_4Cl, $(NH_4)SO_4$, acetone, glacial acetic acid, ethanol, methanol, trichloroacetic acid (TCA) were from Carlo Erba (Italy). Piperazine-1,4-bis (2- ethanesulfonic acid) (PIPES), 4-(2-Hydroxy-ethyl)-piperazine-1-ethane-sulfonic acid (HEPES), glycerol, KCl, $MgCl_2$, and $CaCl_2$ were from Merck (Germany). Triton-X100 was from Fluka (Sigma-Aldrich, WI, USA). The broad-range MMP inhibitor BB-94 was from British Biotechnology (UK). Other materials will be specified under each procedure. All disposable plastic materials were from BD Falcon (NJ, USA). Filters (0,45 and 0,2 μm) were from Millipore (MA, USA).

2.2 Cell culture

2.2.1 Cells and materials

A375MM cells, a characterized human melanoma cell line, were a kind gift of Dr. G. Egea (University of Barcellona, Spain). MDA-MB-231 cells, a characterized human breast cancer cell line, were obtained from ATCC. Dulbecco's Modified Eagles Medium (DMEM), Dulbecco's Modified Eagles Medium/F12 medium (DMEM/F12 1:1) mix, opti-MEM, Foetal Calf Serum (FCS), penicillin-streptomycin (Pen Strep), trypsin/EDTA and L-glutamine were all from Gibco (NY, USA).

2.2.2 Growth medium

A375MM were maintained in DMEM/F12 1:1, supplemented with 10% FCS, 4 mM L-glutamine, 100 U/ml Pen-Strep. MDA-MB-231 were maintained in DMEM, supplemented with 10% FCS, 4 mM L-glutamine, 100 U/ml Pen-Strep.

2.2.3 Growth conditions

Cells were grown in a controlled atmosphere with 5% CO_2 at 37 °C in 100 mm Petri dishes, up to 80-90% confluence. To propagate A375MM, the medium was removed and a PBS/EDTA solution (1mM EDTA in PBS) was added until cells were detached (5 min). To propagate MDA-MB-231, the medium was removed and a trypsin/EDTA solution was added until cells were detached (5-10 min). Cells were then collected in medium-containing plastic and centrifuged for 5 min at 300x g. The pellet was resuspended in fresh medium and cells were plated.

2.3 cDNA constructs and amplification

2.3.1 Materials

"Qiagen Plasmid Maxi Kit" was from Qiagen (CA, USA). Luria Broth (LB) powder, 3-Morpholino-propane-sulfonic acid (MOPS), RbCl and MnCl2 were from Sigma Aldrich (WI, USA). Agar was purchased from BD Biosciences (NJ, USA).

Table 2.1. DNA constructs.

wt-Csk	wild-type	CFP	pEGFP-C1	Dr.M.Vielreicher (Wurzburg University, Germany)
Csk kinase dead	R222K	CFP	pEGFP-C1	Dr.M.Vielreicher (Wurzburg University, Germany)
Lat-Csk	R107K, W47A	OFP-Myc	pMX	Dr.P.Otahal (IMG CAS, Czech republic)
Cd25-Csk	R107K, W47A	OFP-Myc	pMX	Dr.P.Otahal (IMG CAS, Czech republic)
Lat-Csk-kinase dead	R107K, R222K, W47A	OFP-Myc	pMX	Dr.P.Otahal (IMG CAS, Czech republic)
cytosolic Csk	R107K, W47A	OFP-Myc	pMX	Dr.P.Otahal (IMG CAS, Czech republic)
PH-PLC	wild-type	GFP	pEGFP–C1	M.Capestrano, PhD (FMNS, Italy)
PLD2	wild-type	GFP	pEGFP–C1	M.Capestrano, PhD (FMNS, Italy)
Syntaxin 2	wild-type	GFP	pEGFP–C1	M.Capestrano, PhD (FMNS, Italy)
Syntaxin 3	wild-type	GFP	pEGFP–C1	M.Capestrano, PhD (FMNS, Italy)

2.3.2 Buffers and media

LB: 25 g/l LB powder in deionized water and autoclaved for 20 min at 121 °C. LB agar: 19 g/l agar in LB and autoclaved for 20 min at 121 °C.

2.3.3 Preparation of competent bacteria

A single colony of DH5α *E. Coli* bacteria (Stratagene, CA, USA) was picked from an LB-agar plate and used to inoculate 10 ml of LB. Bacteria were grown 16 h, the culture was diluted in 190 ml of fresh LB and incubated at 37 °C until the optical density measured at 600 nm reached 0.5. Bacteria were centrifuged at 4,000 x *g* for 10 min at 4 °C and the pellet resuspended in 64 ml of Tfb1 and left on ice for 1-2 h. After centrifugation, the pellet was suspended in 8 ml of Tbf2 and cells frozen in liquid nitrogen and stored at -80 °C in 400 µl aliquots.

2.3.4 Transformation of bacteria

DNA plasmid (10 ng) was added to 200 µl of competent bacteria (see section 2.3.3) thawed on ice. Cells were kept on ice for 30 min followed by a 90 s heat shock at 42 °C. 800 µl LB were added and cells incubated at 37 °C for 45 min. Bacteria were then plated on LB agar containing the appropriate selection antibiotic and incubated for further 16 h at 37 °C. The next day, a colony was picked to be inoculated in 2 ml of antibiotic-supplemented LB and incubated at 37 °C for 16 h with gentle shaking (200 rpm). 300 µl of 50% (v/v) sterile glycerol were added to 700 µl of the bacterial suspension and stored at -80 °C.

2.3.5 Large scale preparation of plasmid DNA (Maxiprep)

A small amount of bacteria transformed with the plasmid of interest was scraped away from the glycerol stock, inoculated in 2 ml of selection antibiotic- supplemented LB and incubated at 37 °C for 8 h. This pre-culture was inoculated in 200 ml of LB containing the selection antibiotic and incubated at 37 °C for 16 h. Bacteria were then collected by centrifugation at 6,000 x *g* in a JA14 rotor for 10 min at 4 °C and processed with the "Qiagen Plasmid Maxi Kit" according the manufacturer's protocol. The DNA obtained was resuspended in sterile water and stored at -20 °C until further use.

2.4 General biochemical procedures

2.4.1 Materials

Ponceau red, ammonium persulphate (APS), N,N,N',N'- tetramethylethylenediamine (TEMED) were from Sigma-Aldrich (WI, USA). β- mercaptoethanol was from Fluka (Sigma-Aldrich, WI, USA). Methanol and glacial acetic acid were from Carlo Erba (Italy). Secondary horse-radish peroxidase (HRP)-conjugated antibodies against mouse or rabbit IgGs were from Calbiochem (CA, USA). All electrophoresis equipment was from Hoefer Scientific Instruments (Germany).

Table 2.2. Antibodies.

Specificity	Specie	Company	Dilution WB	Dilution IF
actin	rabbit	Sigma	1:5000	n/a
Caveolin 1	rabbit	Santa Cruz	1:1000	1:300
CD147	mouse	Cell Signalling	n/a	1:150
Csk	rabbit	Santa Cruz	1:1000	1:300
MHC I	mouse	Biosource	n/a	1:50
Myc	mouse	Sigma	1:1000	1:100
PLD2	rabbit	Santa Cruz	1:1000	1:300
p-Cav 1 (Y14)	mouse	Santa Cruz	1:1000	n/a
p-FAK (Y861)	rabbit	Santa Cruz	1:1000	n/a
p-Src (Y527)	rabbit	Invitrogen	1:500	n/a

2.4.2 Solutions

Acrylamide stock solution: 30% (w/v) acrylamide-bis acrylamide (Sigma-Aldrich, WI, USA). Ten-fold concentrated running and transfer buffer stock solution were from Bio-Rad Laboratories (UK). Lysis buffer: if not otherwise indicated, cells were lysed in 1x sample buffer.

2.4.3 Sodium Dodecyl Sulphate - PolyAcrylamide Gel Electrophoresis (SDS-PAGE)

2.4.3.1 Preparation of polyacrylamide gels

Two 16 x 18 cm plates were used to assemble a polyacrylamide gel. The plates were assembled to form a chamber using two 1.5 mm plastic spacers aligned on the lateral edges of the plates. The plates were then fixed using two clamps and mounted on a bottom-sealing plastic base. The 'running' polyacrylamide gel was prepared by mixing 1.5 M Tris-HCl pH 8.8, 10% (w/v) SDS and variable amounts of H_2O and 30% (w/v) acrylamide-bisacrylamide solution, to obtain final concentration 375 mM Tris-HCl, 0.1% (w/v) SDS and the desired percentage of acrylamide, Then, 0.06% (w/v) of APS and 0.06% (v/v) TEMED were added to trigger polymerisation, the solution was poured into the gap between the plates, leaving about 5 cm for the stacking gel. Immediately after pouring, the gel was covered with a layer of deionised water and left at RT for about 1 h. The water layer was removed and a 15-well comb was inserted between the glasses. The 'stacking' polyacrylamide gel was prepared by mixing H_2O, 30% (w/v)

acrylamide-bisacrylamide solution, 0.5 M Tris-HCl pH 6.8, 10% (w/v) SDS, to obtain 4,5 % (w/v) acrylamide, 125 mM Tris-HCl, 0.1% (w/v) SDS; 0.1% (w/v) ammonium persulphate and 0.07% (v/v) TEMED were then added and the poured over the running gel and left to polymerize for 1 h at RT.

2.4.3.2 Sample preparation and run

Samples were prepared by addition to cell lysates of SDS-sample buffer, incubation at 100 °C for 5-15 min in a Multi-Block Heater (Lab-Line, IL, USA), cooled at RT, briefly centrifuged and loaded on the gel. One or two wells were loaded with 30 µl of protein molecular weight marker solution (GE Healthcare, Amersham Pharmacia Biotech, NJ, USA). The gel was then transferred into the electrophoresis apparatus (Hoefer Scientific Instruments, NJ, USA) and subjected to a constant current of 7 mA (for 16 h over night runs) or 30 mA (for short 4 h runs).

2.4.3.3 Evaluation of protein concentration

When required, protein concentration was evaluated using a commercially available protein assay kit (Bio-Rad Laboratories, UK) according to the manufacturer's instructions.

2.4.4 Western blotting

2.4.4.1 Protein transfer onto nitrocellulose membrane

Each polyacrylamide gel was soaked for 15 min in transfer buffer, placed on a sheet of

3MM paper (Whatman, NJ, USA) and covered by a nitrocellulose filter (PerkinElmer Life and Analytical Sciences, Boston, MA, USA). The filter was covered by a second sheet of 3MM blotting paper to form a "sandwich" that was subsequently transferred into the blotting apparatus (Hoefer Scientific Instruments, NJ, USA). Protein transfer occurred at 500 mA for 4 h or at 125 mA for 16 h. The sandwich was then disassembled and the nitrocellulose filter soaked in 0.2% (w/v) ponceau red and 5% (v/v) acetic acid for 5 min to stain protein bands, and then washed with 5% acetic acid to remove excess unbound dye.

2.4.4.2 Probing nitrocellulose with specific antibodies

The nitrocellulose filters were cut into strips according to appropriate molecular weight markers with a scalpel. Strips containing the proteins of interest were incubated in PBS containing 5% skim milk powder (Fluka, Sigma-Aldrich, WI, USA) or 5% BSA for 1 h at RT, and then with the primary antibody at the appropriate working concentration in blocking solution (see Table 2.2. for the working dilutions of antibodies used herein). After 1 h incubation at RT, or 16 h incubation at 4 °C, the antibody was removed and the strips washed in PBS with 0.05% Triton twice for 10 min. The strips were then incubated for 1 h with the appropriate HRP-conjugated secondary antibody diluted 1:5000 in blocking solution and washed twice in PBS with 0.05% Triton for 10 min and once in PBS for 5 min. After washing, the strips were incubated with reagents for enhanced chemiluminescence- (ECL) based detection from Amersham Pharmacia Biotech (NJ, USA), according to the manufacturer's instructions and directly exposed to BioMax Films (Kodak, NY, USA).

2.5 Density Gradient

2.5.1 Solutions

TNE buffer: 50 mM Tris-HCl, 150 mM NaCl, 2 mM EDTA, pH 8.0. Lysis buffer: 1% (v/v) TX100 in TNE buffer containing a cocktail of protease inhibitors (Roche).

2.5.2 Optiprep density gradient

The flotation assay on TX100-insoluble material was performed using previously published protocols (Arreaza, Melkonian et al. 1994) with the following modifications. Cells ($2,5\times10^6$) were plated on 100 mm Petri dishes. The day after cells grown to 80% confluence were washed in ice-cold PBS and lysed with 1 ml of 1% TX100 in TNE buffer for 10 min on ice. Lysates were scraped from dishes, adjusted with OptiPrep density gradient medium (a 60% (w/v) solution of iodixanol in water from Sigma-Aldrich, Germany) to a final 35%, and then placed at the bottom of a centrifuge tube. A discontinuous Optiprep gradient (5-30% in TNE) was layered on top of the lysates and the samples were ultracentrifuged at 120,000 x *g* for 16 h in a swinging- bucket rotor (model SW41, Beckman, CA, USA). 1 ml fractions were harvested from the top of the gradient.

2.5.3 TCA-based protein precipitation

10% TCA and 0.4 mg/ml DOC were added from a 5X TCA/DOC stock to each fraction. The mixture was mixed and incubated on ice for 1 h. After a 10 min centrifugation at 13,000 x *g* at 4 °C, the supernatant was collected and the pellet was washed twice, by

adding cold acetone, centrifuging as indicated above and removing the supernatant. Finally, the pellet was dried under gentle aspiration, resuspended in 1xSDS-sample buffer, incubated at 100 °C for 5 min and the pH was adjusted by addition of 1M Tris. Eventually, the samples were subjected to SDS-PAGE followed by western blot.

2.6 Immunofluorescence microscopy procedures

2.6.1 Materials

Alexa 488-, Alexa 546- and Alexa 633-conjugated phalloidin, goat anti- rabbit, anti-mouse antibodies were from Molecular Probes (OR, USA) and were used at a final dilution 1:300. Paraformaldehyde stock solution (8% aqueous solution) was from Electron Microscopy Sciences (PA, USA), and saponin from Sigma-Aldrich (WI, USA). Mowiol was from Calbiochem (CA, USA).

2.6.2 List of antibodies used for morphological studies

See Table 2.2 for the working dilutions of antibodies used in immunofluorescence experiments.

2.6.3 Solutions

Paraformaldehyde 4% in PBS: 10 ml paraformaldehyde 8%, 2 ml 10-fold concentrated PBS stock solution and 8 ml deionized water. Blocking solution: 0.05 % saponin, 0.5 % BSA, 50 mM NH4Cl in PBS. Mowiol: 20 mg of mowiol were dissolved in 80 ml of PBS, stirred over night and centrifuged for 30 min at 12,000 × *g*.

2.6.4 Procedure

Cells were fixed by adding one volume of 4% paraformaldehyde for 15 min at RT, and incubated in blocking solution for 30 min at RT. The cells were subsequently incubated with the specified antibodies diluted in blocking solution (see Table 2.2 for the list and dilutions of antibodies) for 1 h at RT or 16 h at 4 °C. After incubation with the primary antibody, cells were washed three times in PBS and incubated with a fluorescent-probe-conjugated secondary antibody directed against the constant region of the primary IgG molecule for 1 h at RT. Secondary antibodies were diluted 1:300 in blocking solution. Alexa 488- and Alexa 546- or 633- conjugated antibodies were used in double-labelling (rabbit/mouse) experiments in all possible combinations. Coverslips were mounted in mowiol on microscope slides. Immunofluorescence samples were observed with a T.I.L.L. Photonics video microscope (T.I.L.L. Photonics, Germany) or a LSM 510 confocal microscope equipped with 63x objectives (Zeiss, Germany). Optical confocal sections were taken at 1 Airy unit with resolution of 512 x 512 pixels and exported as TIFF files.

2.7 Gelatine degradation assay

2.7.1 Preparation of fluorophore-conjugated gelatine

This preparation was performed according to Mueller and Chen 1991, with the following modifications. 2 mg/ml of porcine gelatine were dissolved in a buffer containing 61 mM NaCl and 50mM $Na_2B_4O_7$ (pH 9.3) and incubated at 37 °C for 1 h.

After this time, 1.8 mg/ml of FITC (or rhodamine) were added and gently mixed for 2 h in complete darkness. This preparation was then dialysed 16 h at RT in PBS in complete darkness. Dialysis was usually continued for 2 days with 2-3 buffer changes per day. After a quick spin to remove insoluble material, small aliquots, containing 2% (w/v) sucrose, were stored in the dark at 4 °C.

2.7.2 Preparation of fluorophore-conjugated gelatine-coated coverslips

Fluorescent gelatine coated coverslips were prepared and the assay carried out as described (Mueller and Chen 1991; Baldassarre, Pompeo et al. 2003). Briefly, glass coverslips were sterilized in 70% ethanol for 15 min at RT. Air-dried coverslips were then coated with pre-warmed fluorophore-conjugated gelatine, using enough to cover the surface. Each coverslip was inverted onto a 100 µl drop of 0.5% ice-cold glutaraldehyde in PBS and incubated on ice for 15 min. Each coverslip was then transferred to each well of a standard 12-well plate with the gelatine-coated side up, gently washed three times with PBS and finally incubated with sodium borohydride (5 mg/ml) in PBS for 3 min at RT. Washed coverslips were sterilized again in 70% ethanol for 5 min, dried for 5 min under a sterile hood and then quenched in complete cell medium for 1 h at 37 °C. Coverslips were thus ready for seeding cells.

2.7.3 ECM degradation assay

The ECM degradation assay was performed according to the previously published protocol, referred to as invadopodia synchronization protocol. Briefly, cells were plated on gelatine-coated coverslips with 5 µM BB94. After 16 h, BB94 was washed out to

allow synchronous invadopodia formation and cells were fixed at 3 h and processed for immunofluorescence as described above. Most experiments were analyzed with the 63x oil-immersion objective of a T.I.L.L. Photonics video microscope, considering at least 30 random fields (containing about 100 cells). TIFF-formatted images were thresholded to remove noise and enhance the contrast of structures of interest. Areas of degradation to the total area for each condition was then normalized for cell number and expressed as a arbitrary units. Each experiment was repeated at least three times.

2.8 Cell treatments

2.8.1 Lipid-mediated transfection

Cells were plated at 50% confluence. The day after 0.45 μg/cm2 DNA and 2 μl/μg TransFast (Promega, WI, USA) in medium without FCS were added for 1 h at 37 °C. Complete medium was then added. Experiments to evaluate the effects of transfection were performed at least 16 h later.

2.8.2 Retroviral transfection

Retroviruses (RV) were prepared by transfection of Phoenix- Ampho cells (Origene, Rockville, MD) with plasmid DNA using Lipofectamine 2000 (Invitrogen, Karlsbad, CA) in six-well plates. RV- containing supernatant was centrifuged to remove debris and then used to spin-infect (1200×g/90 min at room temperature) A375MM and MDA-MB-231 in the presence of Polybrene (10 μg/ml, Sigma-Aldrich, St. Loius, MO). Cells

were allowed to expand in culture and then were sorted using FA Vantage cell sorter (BD Biosciences, San Jose, CA) to isolate infected OFP+ cells.

2.8.3 RNA interference (RNAi)

2.8.3.1 Materials

Smart pool reagents for human Csk, Seladin1/DHCR24 and PLD2 were purchased from Sigma (CA, USA). Stock solutions were aliquoted and stored at -20 °C. siRNAs were employed at the final concentration of 100 nM. Lipofectamine 2000 was from Invitrogen (CA, USA).

2.8.3.2.Procedures

To perform RNAi, cells (2×10^5) were seeded in 12 well plates. The following day a solution A (10 µl of an siRNA solution plus 90 µl of opti-MEM) and a solution B (1 µl of Lipofectamine 2000 plus 100 µl of opti-MEM) were prepared. After 5 min A and B were mixed and incubated for 20 min at RT. 200 µl of the mix were added to cells in 800 µl of complete medium without ATB. Silencing was evaluated by western blot (see section 2.4.4) 96 h after transfection. To perform degradation assays (see paragraph 2.7.3) cells were plated on gelatine-coated coverslips 72 h after siRNA treatment. For rescue experiments, transient expression of the DNA plasmid of interest was performed 72 h after siRNA treatment.

2.8.4 Cholesterol manipulation

2.8.4.1 Depletion procedure

Cholesterol depletion was performed as previously published (Keller and Simons 1998) with some modifications. To evaluate the effect of cholesterol depletion on gelatine degradation, cells were seeded on gelatine-coated coverslips. Once attached, fresh complete medium was added in the presence or absence of 4 μM lovastatin and 0.25 mM mevalonate. After 16 h, cells were treated or not with 10 mM methyl-β-cyclodextrin in FCS-free medium for 30 min. Methyl-β-cyclodextrin was washed-out with fresh complete medium and cells fixed after 3 h. Control and treated cells were processed for immunofluorescence microscopy (see section 2.6). To test the consequence of cholesterol depletion on invadopodia biogenesis we associated this procedure to the use of the invadopodia synchronization protocol (see paragraph 2.7.3). In detail cells were plated on gelatine-coated coverslips with BB94. The inhibitor was kept during the entire cholesterol depletion procedure and washed-out following cell treatment with methyl-β-cyclodextrin. Cells were replenished with fresh complete medium, fixed after 3 h and assayed for ECM degradation.

2.8.4.2 Re-addition procedure

Cholesterol re-addition was performed as previously published (Furuchi and Anderson 1998) with some modifications. 20 μl of cholesterol (20 mg/ml in ethanol) were solubilized in 10 ml of DMEM/F12 1:1 containing 1% methyl-β-cyclodextrin, while mixing at 40 °C to achieve a final 0,04 mg/ml cholesterol concentration. One ml of this

cholesterol/methyl-β-cyclodextrin mix was added for 1h at 37 °C to cells plated on gelatine-coated coverslips with BB94 soon after cholesterol-depletion. BB94 was then washed out with complete medium and cells fixed after 3 h. Control and cholesterol-depleted and-replenished cells were assayed for ECM degradation as reported above.

2.8.4.3 Triparanol treatment

To evaluate the effect of inhibiting of DHCR24 by Triparanol on gelatine degradation, cells were seeded on gelatine- coated coverslips. Once attached, fresh complete medium was added in the presence or absence of 4 μM lovastatin and 0.25 mM mevalonate. After 16 h, cells were treated or not with 3-10 μM Triparanol in dFCS-medium for 4 h. BB94 was washed out and FCS-containing medium with 3-10 μM Triparanol was added. Control and treated cells were fixed after 3 h (A375MM) or 1 h (MDA-MB-231) and processed for immunofluorescence microscopy (see section 2.6).

2.8.4.4 24(S), 25-epoxycholesterol treatment

To evaluate the effect of inhibiting of DHCR24 by 24(S), 25-epoxycholesterol (EC) on gelatine degradation, cells were seeded on gelatine-coated coverslips. Once attached, fresh complete medium was added in the presence or absence of 4 μM lovastatin and 0.25 mM mevalonate. After 16 h, cells were treated or not with 10 μM EC in dFCS-medium for 4 h. BB94 was washed out and FCS-containing medium with 10 μM (EC) was added. Control and treated cells were fixed after 3 h (A375MM) or 1 h (MDA-MB-231) and processed for immunofluorescence microscopy (see section 2.6).

2.8.5 Transport assays: antibody uptake and recycling

2.8.5.1 Materials

See table 2.2.

2.8.5.2 Antibody recycling assay

To assess internalisation and recycling of the major histocompability complex 1 (MHC1) and CD147 antibody, the following procedure was followed: The cells were initially subjected to binding of MHC1 antibody or Alexa 546-transferrin to the plasma membrane, as reported here: the cells were and incubated with 1 mg/ml monoclonal antibody against human MHC class 1 or CD147 for 30 min at 37 °C. The cells were then washed three times with low pH buffer (acid wash) to remove the unbound antibody. For the uptake assay, upon the previous binding step, the cells were incubated in prewarmed (37 °C) complete medium for varying times, to allow the specific antibody internalisation.

2.8.6 Wound healing assay

To perform wound healing assay, silicone Culture Inserts were used that create two cell culture reservoirs divided by thick wall. In each reservoir, $6x10^4$ cells were plated in final volume 100 µl. After 16 h, Culture Inserts were carefully removed with a tweezer and the cells were washed 3 times with fresh medium. The images were taken of control and treated cells at indicated times up to 24 h.

Statistics

All data in the text and figures are expressed as mean (SEM) and 2-way analysis of variance statistical analyses were carried out with Excel Student's t-test. A *P* value of less than 0.05 was considered significant (*P < 0.05, **P < 0.01, ***P < 0.001).

CHAPTER 3: Regulation of cholesterol homeostasis at invadopodia

3.1 Introduction

There are many indications suggesting that invadopodia present the features of, or are enriched in, cholesterol-enriched microdomains, also known as lipid rafts. Local actin polymerization, mediated by the Arp2/3 complex, is required for invadopodia initiation and assembly of invadopodial core actin structure (Yamaguchi et al., 2005). And indeed, it has recently been suggested that lipid rafts are preferential sites for N-WASP Arp2/3 dependent actin polymerization, possibly because of efficient recruitment of these actin nucleators (Golub and Caroni, 2005). Also, the majority of the MT1-MMP, a protease crucial for focal matrix degradation at invadopodia, has been shown to be preferentially sorted to lipid rafts (Mazzone et al., 2004).

In our laboratory, we have previously shown that invadopodia formation and efficient ECM degradation depends on appropriate levels of cholesterol at the cell surface. Moreover, we have demonstrated a pivotal role of caveolin in the regulation of cholesterol homeostasis at invadopodia in A375 melanoma cells (Caldieri et al., 2009). Another report has confirmed the importance of cholesterol and caveolin 1 in MDA-MB-231 breast cancer cells (Yamaguchi et al., 2009).

To further analyze the lipid raft features of invadopodia, I investigated the role of a specific downstream cholesterol biosynthesis enzyme, Seladin1/DHCR24, on invadopodia formation, random migration and eventually recycling of plasma membrane proteins.

3.2 Results

3.2.1 Exchange of cholesterol for desmosterol

Desmosterol is a cholesterol biosynthesis intermediate form that differs from cholesterol only in a double bond at carbon 24 (C24). Desmosterol, when exchanged for cholesterol, supports normal functions in cell growth and viability. However, desmosterol has lower affinity for lipid rafts and fails to support lipid raft-dependent signalling as effectively as cholesterol (Vainio et al., 2005), as documented in a report on insulin receptor lipid raft association and activation (Sánchez-Wandelmer et al., 2009). Therefore, it could be a useful tool for perturbing these specific membrane domains. I applied a modification of a published protocol based on the use of methyl-β-cyclodextrin (MβCD) to extract plasma membrane cholesterol. From the chemical point of view, cyclodextrins are composed of seven glucose units. The unique property of MβCD (and other cyclodextrins) results from its characteristic cylindrical structure with a hydrophilic surface and hydrophobic cavity (Betzel et al., 1984), that is capable of accommodating lipophilic molecules, such as cholesterol, by formation of an inclusion

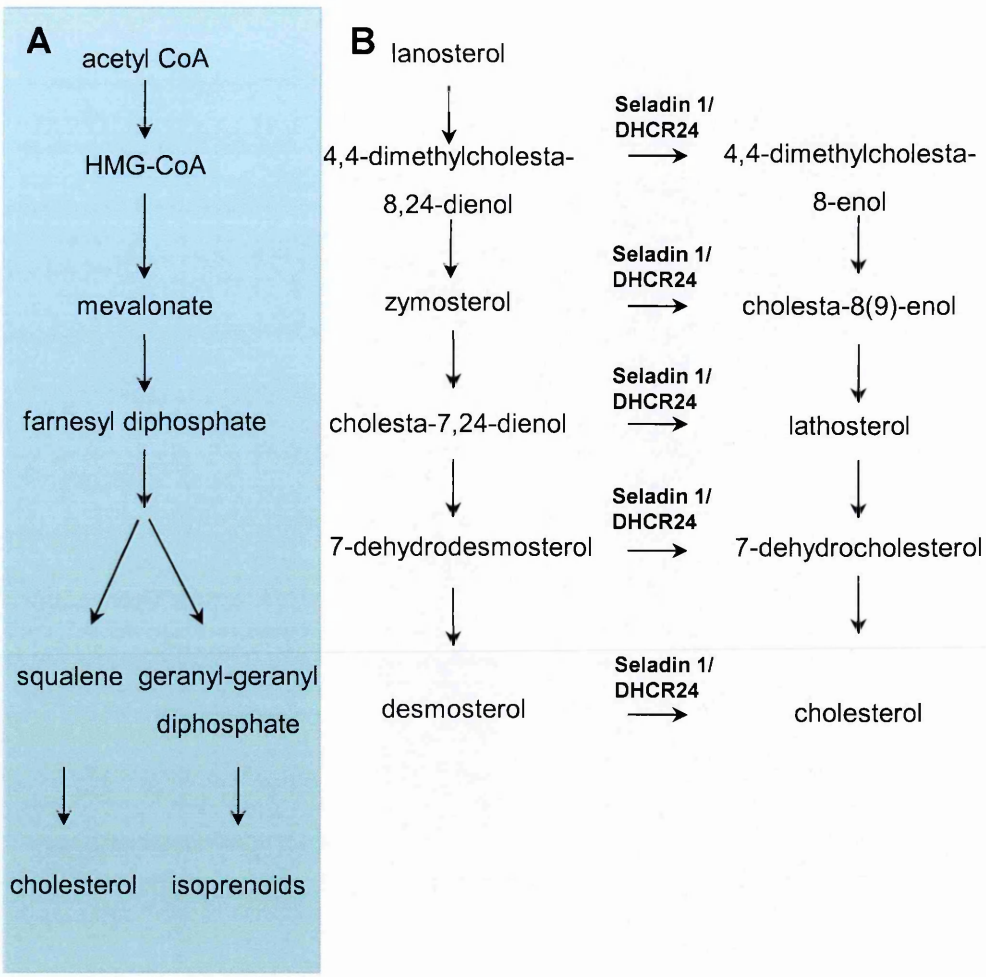

Fig. 3.1. Biosynthesis of cholesterol. A) The schematic model of branched pathway of mevalonate metabolism in mammalian cells. B) The post-lanosterol steps of cholesterol synthesis in mammalian cells. The biosynthesis of cholesterol can proceed either through the Bloch pathway (left) or Kandutsch-Russell pathway (right). Hypothetically, the C24 double bond can be reduced at each stage by Seladin 1/DHCR24.

complex. As the intracellular pool of cholesterol can continuously replenish plasma membrane cholesterol, extraction by MβCD was preceded by a treatment with lovastatin, one of the commercially available cholesterol lowering drugs statins, potent inhibitors of HMG-CoA reductase. HMG-CoA reductase is a rate-limiting enzyme of the mevalonate pathway of cholesterol biosynthesis. In my experiments, mevalonate was used as well, to minimize the side effects on production of the isoprenoid precursors (Brown and Goldstein, 1980), the non-sterol products of the mevalonate pathway (Fig. 3.1 A).

Cholesterol is the key lipid component of lipid rafts and the extraction of cholesterol from the plasma membrane results in the dispersion of such domains. In a first experimental set, I combined the depletion of cholesterol by MβCD with a re-addition of a saturated complex of MβCD and cholesterol or desmosterol in the degradation assay on adherent cells plated on fluorophore-conjugated gelatine in the presence of broad spectrum inhibitor of metalloproteases batistamat (BB94). Tumour cells plated on the appropriate substrate, such as gelatine, form spontaneously degradation-competent invadopodia, in some cases right after attachment, well before the spreading process is completed. This represents technical and interpretative problems when applying experimental approaches that require longer pre-treatment times. One would ideally wish to uncouple cell attachment and spreading from invadopodia formation. To solve this issue, I took advantage of a degradation assay protocol previously set up in my laboratory to allow synchronous formation of invadopodia. This approach makes use of broad-spectrum metalloprotease inhibitor

BB94 which functions reversibly and competitively by occupying the active site of the enzyme and reversibly blocks invadopodia formation without affecting cell behaviour in any other aspect. Cells are plated and the desired treatment is applied in the presence of BB94, hence cells are not allowed to form invadopodia and degrade the ECM during the pre-treatment. BB94 is then washed out and cells are allowed to degrade the ECM for appropriate times depending on the cell type (Ayala et al., 2008). After the treatment, I assayed the ability of cells to degrade the ECM after BB94 wash out. As we have strong evidence that invadopodia have features of lipid rafts, I would have expected cholesterol but not desmosterol to rescue the MβCD-induced phenotype. Surprisingly, I observed that both desmosterol and cholesterol were able to do so (Fig. 3.2). This might be due to the fact that desmosterol is an intermediate of cholesterol metabolism and can be converted rapidly into cholesterol via the reaction catalysed by the ubiquitous enzyme 24-dehydroxysterol reductase (DHCR24), that catalyses the reduction of the delta-24 double bond of sterol intermediates during cholesterol biosynthesis (Fig. 3.1 B).

Initially identified as a gene down-regulated in Alzheimer's disease vulnerable brain regions, DHCR24 was initially named Selective Alzheimer's disease Indicator 1 (Seladin 1) (Greeve et al., 2000). Moreover, missense mutations of Seladin1/DHCR24 have been reported to cause desmosterolosis, a rare autosomal recessive disorder biochemically characterized by elevated plasma levels of desmosterol and accumulation of desmosterol in the plasma membrane. *In vitro*, only desmosterol was present in untreated J774 murine macrophage-like cells that are defective in Seladin1/DHCR24 (Zerenturk et al., 2011).

I thus reasoned that inhibition of DHCR24 was essential to better understand the effects of desmosterol in my experimental conditions.

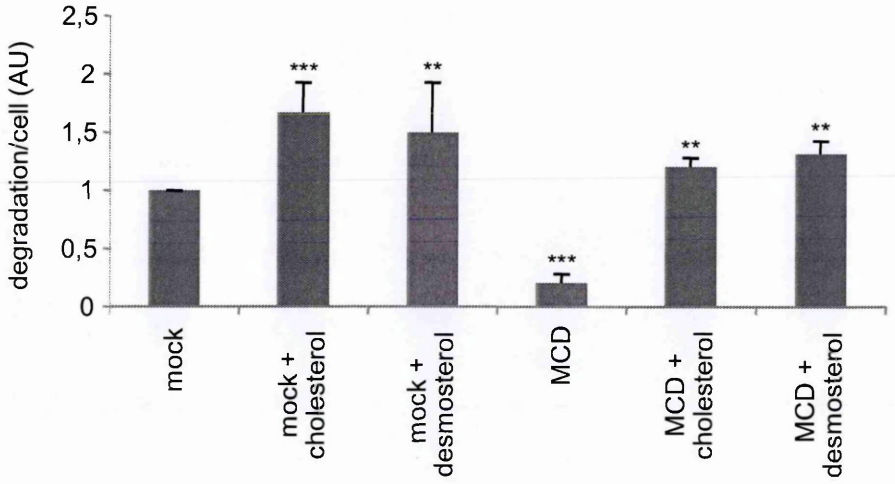

Fig. 3.2. Cholesterol depletion blocks invadopodia formation. A375MM cells were plated on gelatine in the presence of BB94 and the lovastatin/mevalonate mix (L+M), and were left untreated or subjected to acute cholesterol extraction with MCD (MCD) 30 minutes prior to BB94 washout. Samples were fixed after 3 hours. Quantification of ECM degradation revealed an 80% decrease in MCD-treated as compared to lovastatin/mevalonate-treated cells. Both cholesterol and desmosterol readdition to depleted cells prior to BB94 washout restored the normal phenotype. Error bars are standard deviations of the mean. Three independent experiments were performed.$^{**}P < 0.01$, $^{***}P < 0.001$.

3.2.2 Inhibition of Seladin1/DHCR24 1 by Triparanol

Therefore, I explored strategies to inhibit Seladin1/DHCR24 to achieve accumulation of desmosterol at the expense of cholesterol. My first choice was an inhibitor of DHCR24 commercially available under the name Triparanol, which inhibits DHCR24 in non-competitive fashion (Bae and Paik, 1997). Triparanol is not widely used but few studies convincingly described its effects on desmosterol accumulation due to DHCR24 inhibition. Functionally, in 3T3-L1 adipocytes, Triparanol disrupts caveolae-dependent insulin-receptor signalling and co-incubation with cholesterol rescued IR signalling to the control values (Sánchez-Wandelmer et al., 2009).

I plated the A375MM cells on gelatine coverslips in the presence of lovastatin, mevalonate and BB94. The next day, I pre-treated the cells with Triparanol at concentrations ranging from 3 μM to 10 μM. After 4 h, I added cholesterol to the cells in the complex with MβCD in serum free medium in the presence of BB94 and Triparanol. After 1 h, I washed out BB94 and allowed the cells to degrade the matrix for 3 h in complete medium, in the continuous presence of Triparanol. As A375MM cells treated with higher concentrations of Triparanol were not viable after addition of cholesterol, only experiments after pre-treatment with 3 μM Triparanol were quantified. Clearly, even this lower concentration of inhibitor was sufficient to block gelatine degradation and its effect was overcome by cholesterol addition, validating the specificity of the Triparanol effect (Fig. 3.3 A).

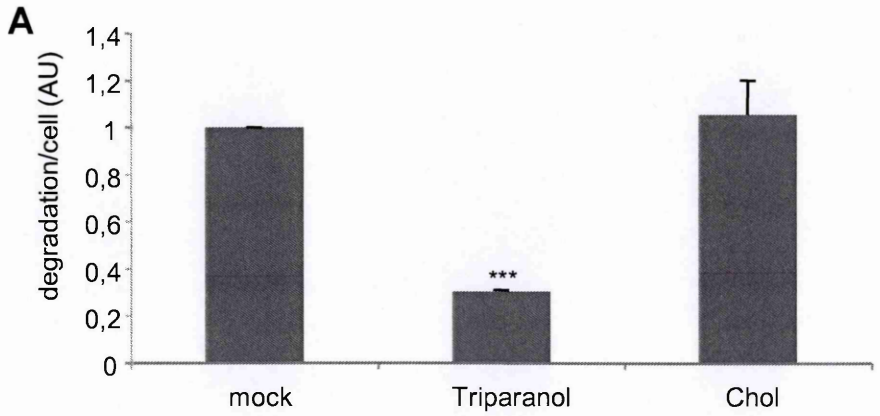

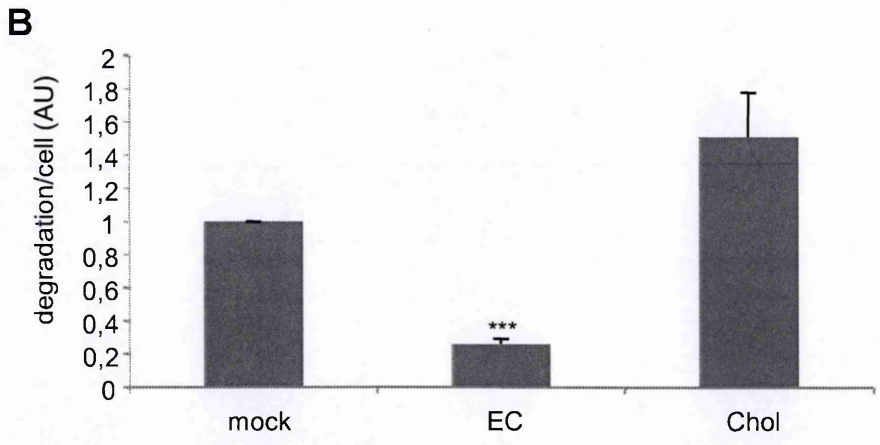

Fig. 3.3. Inhibition of Seladin1/DHCR24 blocks ECM degradation. A375MM cells were plated on gelatine in the presence of BB94 and the lovastatin/mevalonate mix (mock), and were left untreated or subjected to A) Triparanol or B) 24(S),25-epoxycholesterol treatment (EC) (B) treatment for 4 h prior to BB94 wash out. Cholesterol was re-added in saturated complexes with MCD to the treated cells (Chol). Cells were fixed after 3 h and ECM degradation quantified. Error bars are standard deviations of the mean. Three independent experiments were performed. $P < 0.001$.

3.2.3 Inhibition of Seladin1/DHCR24 by 24(S), 25-epoxycholesterol

According to the so-called "Oxysterol Hypothesis of Cholesterol Homeostasis", which was first formulated by Kandutsch and colleagues in 1978 (Kandutsch et al., 1978), the suppressive effect of cholesterol synthesis might be mediated by endogenously produced oxysterols. Among the many oxysterols 24(S), 25-epoxycholesterol (24(S), 25-epoxy-cholest-5-en-3b-ol; 24,25-EC for brevity EC from here on) is unique because it is synthesised via a shunt of the mevalonate pathway of cholesterol biosynthesis in cholesterogenic cells rather than being derived from cholesterol like the other oxysterols. The likely physiological role of EC is to control cholesterol homeostasis at different levels.

Interestingly, EC has recently been shown to inhibit Seladin1/DHCR24, causing an increase in desmosterol levels at the expense of cholesterol (Zerenturk et al., 2011). Based on this knowledge, I decided to use EC to confirm the role of cholesterol and more specifically the role of Seladin1/DHCR24 in the invasive behaviour of tumour cell lines. As in the previous experiment, I plated A375MM cells on fluorophore-conjugated gelatine coverslips in the presence of BB94 and incubated them with a mixture of lovastatin and mevalonate overnight.

The next day, I pre-treated cells with 10 μM EC for 4 hours prior to the addition of a saturated MβCD/cholesterol complex. Four hours after re-addition, I washed out BB94 and allowed the cells to degrade for 3 h. I fixed the cells and quantified the degradation. I observed that gelatine degradation inhibited by EC, was rescued by cholesterol replenishment. As in the case of Triparanol, the phenotype rescue suggests

the specificity of the effect on EC and confirms that inhibition of ECM degradation was due to lack of cholesterol (Fig. 3.3B).

3.2.4 Inhibition of Seladin1/DHCR24 in an alternative cell model

In parallel, and to help validate my findings, I applied the same approaches to an additional cell model, the breast cancer cell line MDA-MB-231, with some minor modifications. I observed that MDA-MB-231 cells, unlike A375MM cells, are viable even in the presence of higher concentration of Triparanol (10 μM). I applied the same protocol as described above, only with shorter degradation times of 1,5 h. I confirmed the same effect of both inhibitors on ECM degradation (Fig. 3.4).

Next, I explored the consequences of Seladin1/DHCR24 inhibition on the migration of MDA-MB-231 cells, since the role of lipid rafts in migration is clearly established. Cell migration is a multistep, highly integrated process, which is key for the invasion of tumour cells. Directional migration can be measured in the so-called wound healing assay. Cells were plated in silicone inserts, called Culture Inserts, with defined cell-free gap, and incubated overnight in the presence of lovastatin and mevalonate. The next day, the inserts were removed and the confluent cells were allowed to migrate and close the gap between two cells patches for 16 h in the presence of 10 μM Triparanol or 10 μM EC (thus the same concentration as above in the degradation assay) (Fig. 3.5 A). The characteristic parameter in this assay is the change in the cell-covered area, over

time. Both inhibitors block migration significantly by 50 per cent, suggesting a role of Seladin1/DHCR24 in migration of tumour cells (Fig. 3.5 B).

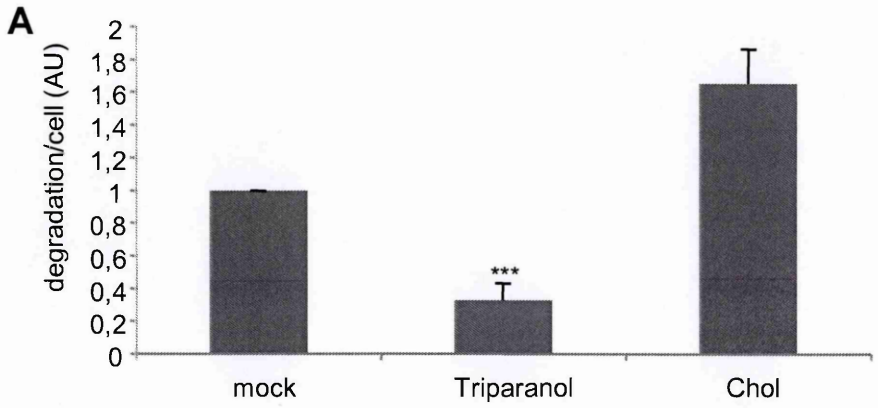

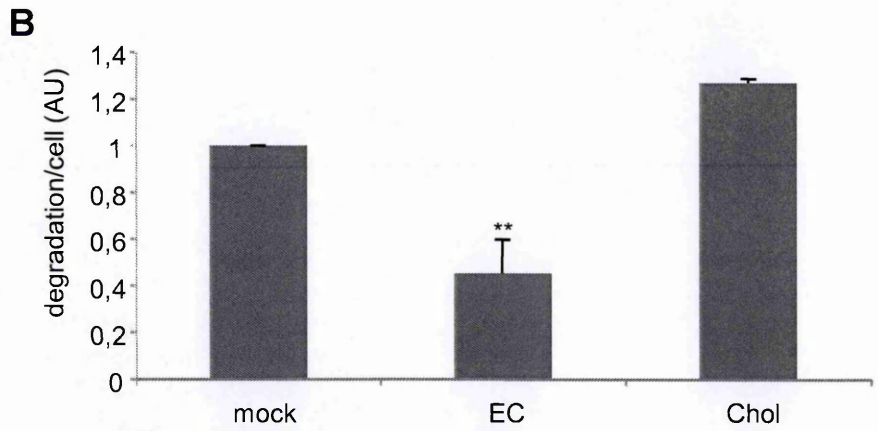

Fig. 3.4. Inhibition of Seladin1/DHCR24 blocks ECM degradation. MDA-MB-231 cells were plated on gelatine in the presence of BB94 and the lovastatin/mevalonate mix (mock), and were left untreated or subjected to A) Triparanol or B) 24(S),25-epoxycholesterol treatment (EC) (B) treatment for 4 h prior to BB94 wash out. Cholesterol was re-added in saturated complexes with MCD to the treated cells (Chol). Cells were fixed after 1 h and ECM degradation quantified. Error bars are standard deviations of the mean. Three independent experiments were performed. $^{**}P < 0.01$, $^{***}P < 0.001$.

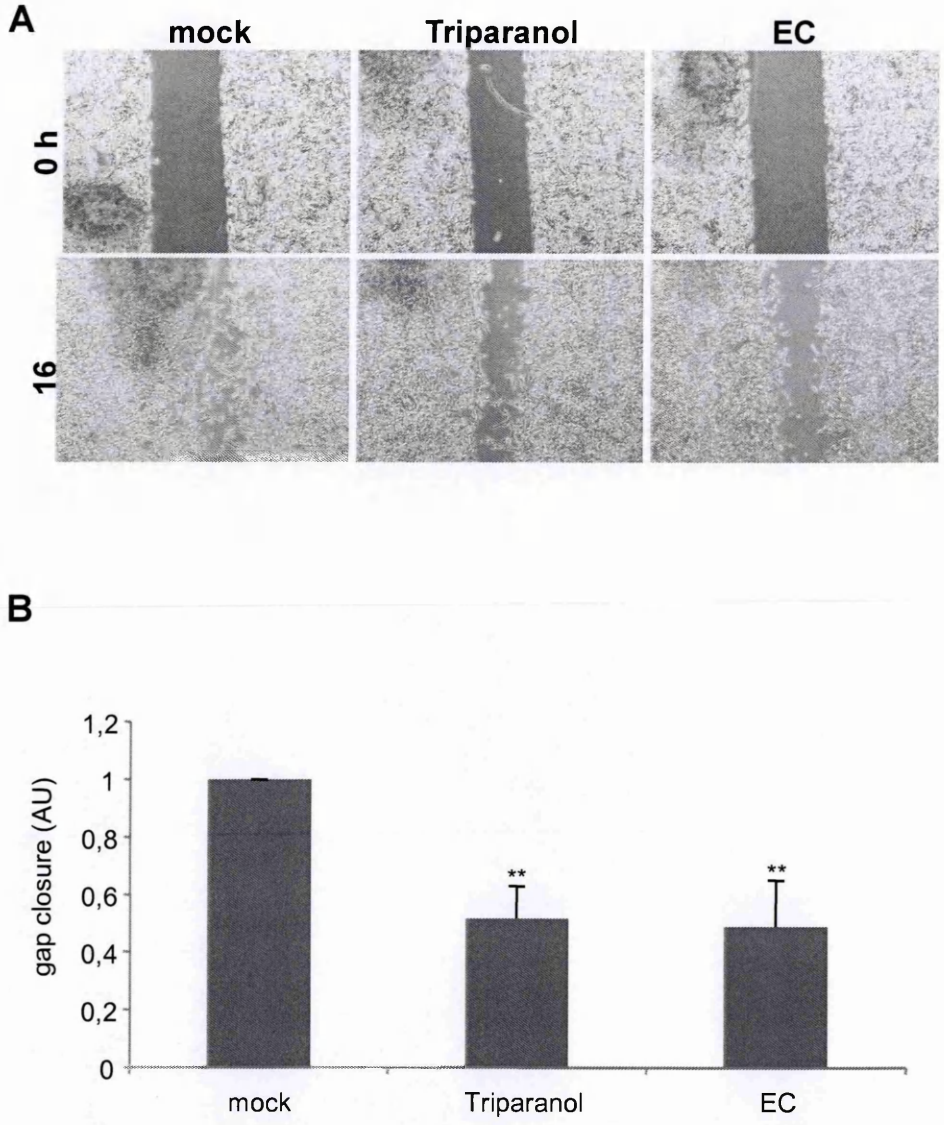

Fig. 3.5. Inhibition of Seladin1/DHCR24 by Triparanol and 24,25-epoxycholesterol inhibits the gap closure in wound healing assay. MDA-MB-231 cells were plated in the culture inserts in the presence of the lovastatin/mevalonate mix (mock), and were left untreated or subjected to Triparanol or 24(S),25-epoxycholesterol (EC) treatment for 4 h prior to the insert removal. Cells were fixed after 16 h and ECM degradation quantified. Error bars are standard deviations of the mean. Three independent experiments were performed. $P < 0.01$.

3.3 Discussion

Invadopodia are platforms where signalling events, membrane traffic and actin remodelling integrate towards the efficient focal degradation of the ECM. It has been previously shown that invadopodia formation and efficient ECM degradation depends on appropriate levels of cholesterol at the cell surface (Caldieri et al., 2009; Yamaguchi et al., 2009). The evidence that cholesterol homeostasis is essential for invadopodia formation suggests a tight control of cholesterol homeostasis in invadopodia-forming cells.

I took advantage of the regulator of the ultimate step of cholesterol synthesis, Seladin1/DHCR24, which catalyzes the conversion of desmosterol to cholesterol. Emerging studies have suggested that desmosterol is not able to fully substitute cholesterol in the lipid rafts. Indeed, it is documented that loss of Seladin 1/DHCR24 impaired lipid raft-dependent signalling events due to the accumulation of membrane desmosterol.

I also tested the Seladin1/DHCR24 substrate desmosterol to gain further insight into the cholesterol-dependence of invadopodia. To achieve this, I used two known inhibitors of Seladin1/DHCR24, Triparanol and EC. The latter one is a potent oxysterol regulator, which is known to regulate cholesterol levels via multiple ways. Importantly, it has been shown that EC shuts down cholesterol synthesis at Seladin1/DHCR24 without affecting its protein levels (Zerenturk et al., 2011).

I showed that in the both cell lines, A375MM and MDA-MB-231, Triparanol and EC caused decrease in gelatine degradation. This effect was further abolished by addition of cholesterol, which also confirmed the specificity of the effect of Seladin1/DHCR24 inhibitors. Consequently, in MDA-MB-231 cells inhibition of Seladin1/DHCR24 slowed down random migration.

The cholesterol-synthesis enzyme Seladin1/DHCR24 is not widely studied in the context of cancerogenesis but a few studies have implied its role in the prostate cancer (Battista et al., 2010; Bonaccorsi et al., 2008; Hendriksen et al.; 2006). The level of Seladin1/DHCR24 expression is a hallmark of prostate cancer, with the levels inversely correlating with grade of prostate cancer. Moreover, decreased gene expression has been connected to the elevation of metastasis incidence. This gene down-regulation is further linked to increase in androgen secretion and cell proliferation.

CHAPTER 4: Regulation of Src family of tyrosine kinase (SFK) activity at invadopodia

4.1 Introduction

The importance of SFK-derived signalling in invadopodia formation has been repeatedly demonstrated through a variety of approaches including RNA interference, expression of mutants and the use of inhibitors. Nevertheless, there is less known about regulation of SFK. Among the plethora of SFK substrates, tyrosine phosphorylated Caveolin 1 acts inhibitory towards invadopodia formation (Caldieri et al., 2009). SFK-dependent tyrosine 14 phosphorylation of Caveolin 1 forms a docking site for C-terminal Src kinase (Csk), thus recruiting it from the cytosol to the cholesterol-rich lipid rafts in the plasma membrane to exert its function. Csk specifically phosphorylates the C-terminus tail inhibitory tyrosine (Y527 in Src) of the non-receptor SFKs, thereby inhibiting their activity (Ingley, 2008). Csk is ubiquitously expressed and shares 40 per cent sequence identity with SFKs, with a similar domain structure but lacking any N-terminal fatty acid modification. Unlike SFKs, Csk is not phosphorylated on activating or inhibitory sites in line with the notion that Csk is regulated sterically rather than catalytically. The mechanism underlying cell membrane localization of Csk has been investigated and has led to the identification of lipid raft-associated adaptor proteins (Ingley, 2009), including the phosphoproteins Cbp/PAG (Kawabuchi et al., 2000),

LIME (Brdickova et al., 2003) and Caveolin 1 (Cao, 2002). Thus, I investigated the role of Csk and effect of its membrane localization at the degradation capability of invadopodia.

4.2 Results

4.2.1 Csk knock-down stimulates invadopodia formation

In our laboratory, we have previously shown that Y14-phosphorylated caveolin 1 is inhibitory towards invadopodia biogenesis and we hypothesized that this was probably by removing cholesterol from the plasma membrane and possibly via inhibition of SFK-dependent signalling (Caldieri et al., 2009). Indeed, the pY14 of caveolin 1 serves as a docking site for the SH2 domain of Csk (Cao, 2002), the endogenous SFK inhibitor (Ingley, 2008). Hence, I directly explored the function of Csk in invadopodia formation and function. Csk specifically phosphorylates the inhibitory tail tyrosine of SFKs (Y530 in human Src) and thus inhibits their activity. 72 h after siRNA treatment, Csk-depleted A375MM cells or MDA-MB-231 cells (Csk-KD) were plated on FITC-conjugated gelatine in presence of BB94 to block invadopodia formation. The following day, a degradation assay was performed. Csk was knocked-down with more than 60 per cent efficiency (Fig. 4.1 A) leading to a more than two-fold increase in the degradation per cell in A375MM melanoma cells and MDA-MB-231 breast cancer cells (Fig. 4.1 B). In parallel, 72 h after siRNA treatment,

Csk-depleted A375MM cells were plated on gelatine in the presence of BB94 to block invadopodia formation. The following day, BB94 was washed out to allow invadopodia formation and after 5 h cells were lysed in 1 x sample buffer and subjected to Western blotting. Membranes were stained with antibodies against Csk to reveal the level of knock-down and against phosphorylated inhibitory tyrosine of Src (Y530) and Src-substrate phospho-FAK (Y421) (Fig. 4.2 A). After the Csk knock-down, I observed lower levels of inhibited Src and increased phosphorylation of the prominent SFK substrate FAK (Fig. 4.2 B). This would suggest that the role of Csk in invadopodia biogenesis is dependent on its catalytic activity. To further confirm this conclusion, I performed phenotype rescue after siRNA-mediated knock-down of Csk by over-expressing wild-type and kinase dead Csk. The Csk kinase dead mutant bears a K 222 to-R mutation that makes it kinase defective. Indeed, only wt-Csk efficiently decreased the level of ECM degradation of siRNA-treated cells to mock levels (Fig.4.3).

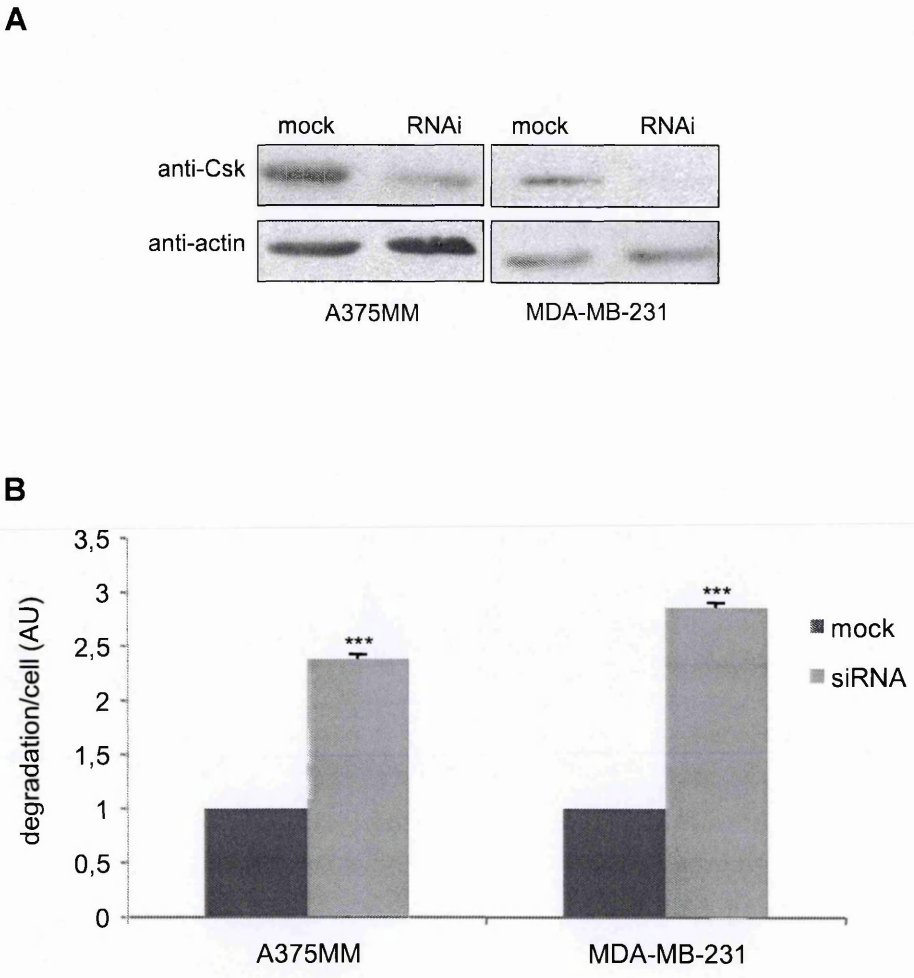

Fig. 4.1. Csk-knock down affects ECM degradation. A) Efficiency of Csk knock-down. A375MM and MDA-MB-231 cells were treated without (mock) or with (RNAi) siRNA targeting Csk for 96 hours. RNAi reduced Csk expression up to 70% as shown in western blots of lysates using antibodies against Csk and actin as a loading control. B) Quantification of ECM degradation revealed an almost three-fold increase in degradation per cell in A375MM and MDA-MB-231 Csk knock-down cells compared to mock-transfected (mock). Error bars represent standard deviation of the mean. Three independent experiments were performed. $P < 0.001$.

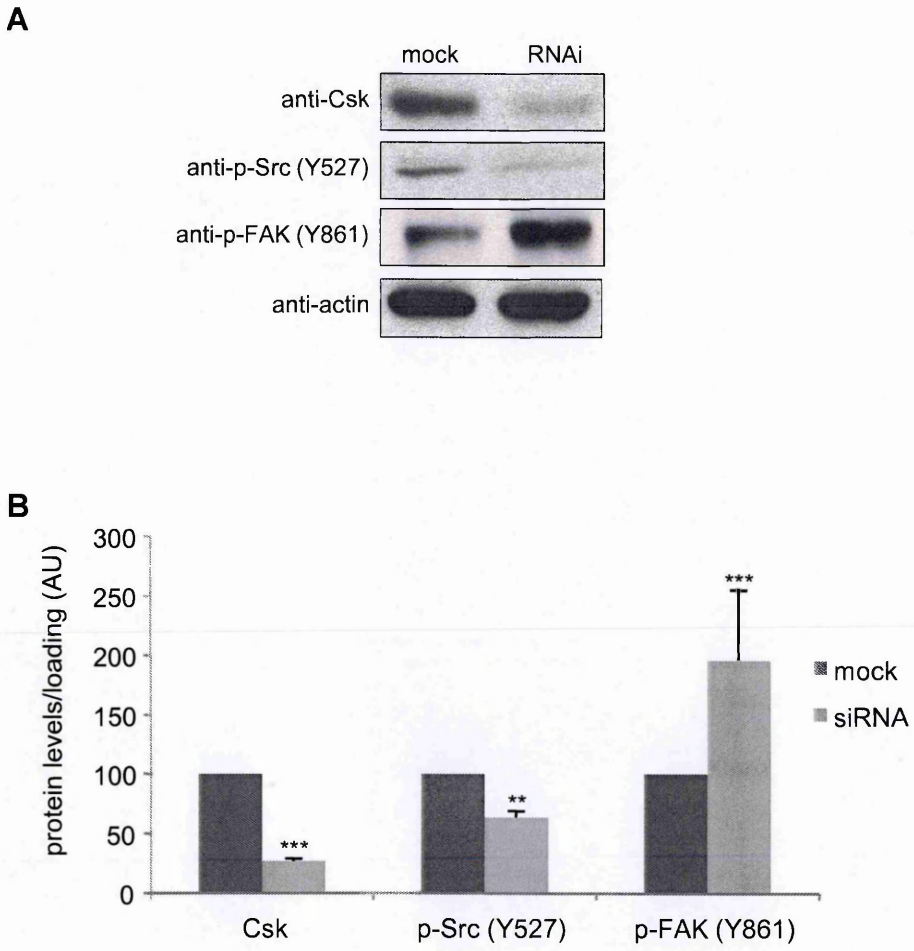

Fig. 4.2. Src-dependent phosphorylation after Csk knock-down.

A375MM cells on gelatine were treated without (mock) or with (RNAi) siRNA targeting Csk for 96 hours. Image shows western blots of lysates using antibodies against Csk, pSrc (Y527), pFAK (Y861) and actin as a loading control. B) After 96 hours of siRNA treatment cells were lysed and subjected to Western blotting. Membranes were stained with antibodies against Csk to reveal the level of knock-down and against pSrc (Y527) and pFAK (Y861). The ablation of Csk resulted in decreased phosphorylation of inhibitory tyrosine of Src and increased phosphorylation of FAK. Error bars represent standard deviation of the mean. Three independent experiments were performed. $**P < 0.01$, $***P < 0.001$.

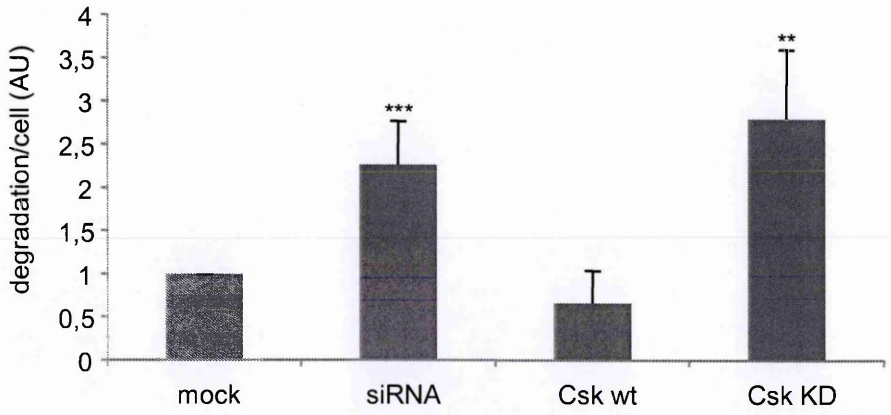

Fig. 4.3. Csk knock-down stimulates invadopodia formation and the phenotype is efficiently rescued upon wt Csk overexpression. Quantification of ECM degradation revealed a 150 per cent increase in Csk knock-down A375MM cells (siRNA) compared to mock-transfected cells (mock). The phenotype was efficiently rescued by overexpression of wild type Csk (Csk wt) but not catalytically inactive kinase dead Csk (Csk KD). Error bars represent standard deviation of the mean. Three independent experiments were performed. $^{**}P < 0.01$, $^{***}P < 0.001$.

4.2.2 Csk is not involved in EGF stimulation

Invadopodia formation has been shown to be initiated by EGF that in turn leads to activation of the actin polymerization machinery (Yamaguchi et al., 2005). The importance of EGF signalling for invadopodia biogenesis is not very clear, since invadopodia formation in many cell models does not necessarily require EGF receptor (EGFR) activation. It is well established that EGF binding activates c-Src (Biscardi et al., 1999a; Biscardi et al., 1999b), which then phosphorylates Tyr 845 of EGFR to enhance the EGF-dependent response. It has been suggested that also Csk might have a role in EGF signalling. Upon EGF stimulation of Cos-1 cells, Csk is transiently translocated to SFK-phosphorylated Cbp in the membrane ruffles. This connection leads to downregulation of SFK in the early stage of EGF signalling (Matsuoka, 2003). Over-expression of Csk catalytic mutants has been used as a tool to inactivate SFKs in a study on the effect of EGF-dependent migration of human pancreatic carcinoma cells. Expression of wt- but not kinase dead Csk disrupted the EGF-induced activation of SFKs and cell migration on vitronectin (Ricono et al., 2009). Moreover, EGF-dependent signalling in breast cancer cell lines has a biphasic character. At low concentration, EGF activates SFKs by Y416 phosphorylation, whereas higher concentration suppresses their activity via inhibitory tyrosine phosphorylation (Y527). Based on this evidence, I decided to explore the function of Csk in EGF stimulation of MDA-MB-231 cells. I performed RNAi of Csk as described above and after 72 h I plated the mock and Csk-KD cells on transparent-gelatine coated wells in FCS-free medium. The next day, I stimulated the starved cells with EGF for indicated time (0, 5 and 30). I lysed the cells in sample buffer and performed Western blot analysis. I probed the membranes with

anti-p-Erk 1/2 antibody. Erk 1/2 are down-stream effectors of EGFR, therefore phosphorylation Erk 1/2 is a reliable indicator of stimulation of EGFR-MAPK/Erk pathway. I reported no difference between stimulation of Erk 1/2 in mock and Csk-knock down cells, suggesting that Csk has no role in EGF signalling in our cell system (Fig. 4.4).

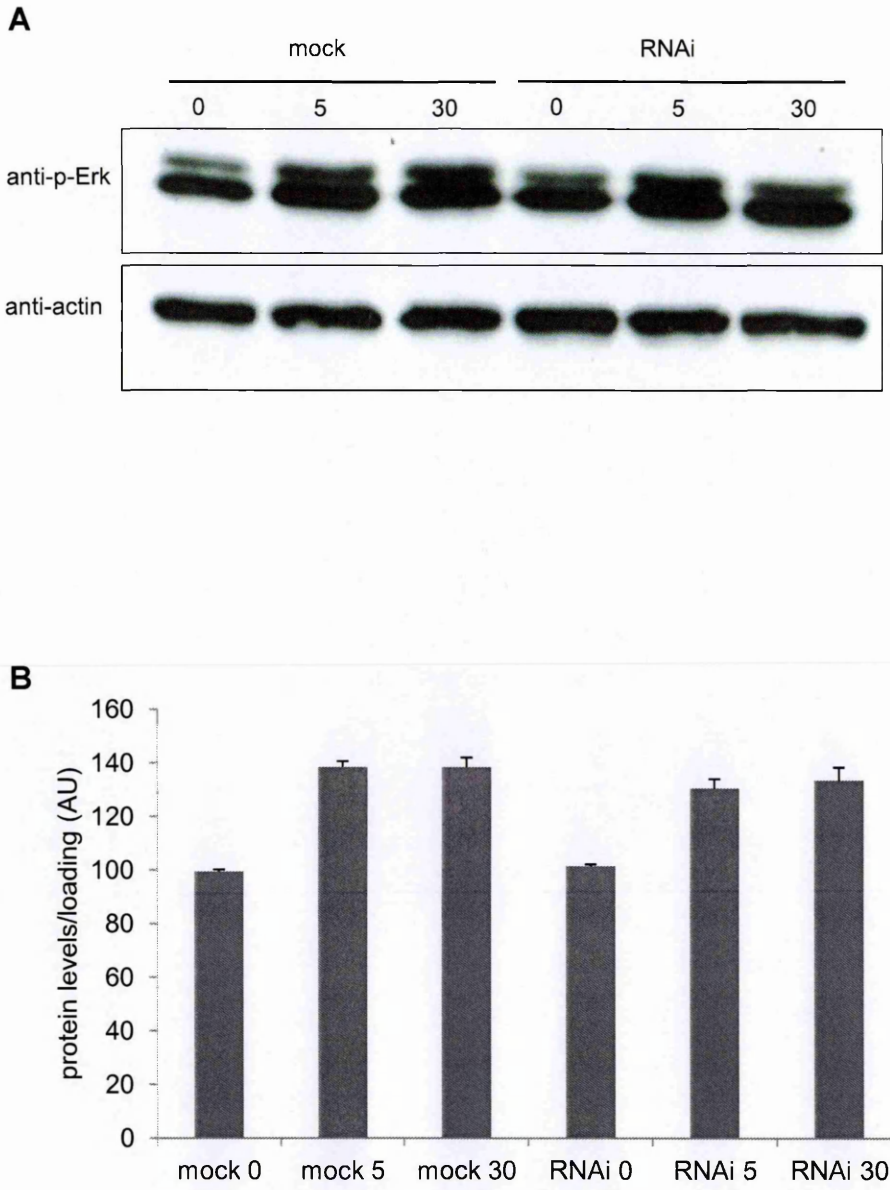

Fig. 4.4. Csk is not involved in EGF stimulation. MDA-MB-231 cells on gelatine were treated without (mock) or with (RNAi) siRNA targeting Csk for 96 hours. Image (A) shows western blots of lysates using antibodies against Csk, pERK and actin as a loading control. B) Levels of pErk after 5 min and 30 min of EGF stimulation. Error bars represent standard deviation of the mean. Two independent experiments were performed. No significant difference between mock and RNAi cells was reported.

4.2.3 Csk chimaeras with different membrane anchors

I showed in the previous chapter that acting on cholesterol biosynthesis by blocking the specific reductase DHCR24 leads to inhibition of ECM degradation and migration of tumour cells. I reasoned that if invadopodia are enriched in lipid rafts (Caldieri et al., 2009; Yamaguchi et al., 2009) and Csk is inhibitory towards their formation and function, then targeting Csk specifically to lipid rafts could directly affect ECM degradation.

To find out how targeting of Csk to different membrane compartments affects ECM degradation, through collaboration with Dr. Tomas Brdicka (IMG, AS, Prague) I obtained C-terminally modified Csk constructs with distinct targeting motifs. These constructs code for fusion proteins containing a membrane-specific targeting sequence, constitutively active Csk, a Myc tag and orange fluorescent protein (OFP). Lipid raft-targeted kinase-dead Csk and cytosolic Csk were included as controls (Fig. 4.5). To minimize possible complicating effects of interactions of Csk Src-homology domains 2 and 3 (SH2 and SH3) with other proteins, such as adaptor proteins and substrates, Csk was mutated to inactivate these domains (R107K mutation to inactivate the SH2 domain and W47A to inactivate the SH3 domain) (Otáhal et al., 2011).

4.2.4 Effect of transient transfection of Csk chimaeras on ECM degradation

I started with a transient transfection approach. All the constructs are cloned into the pMXs retroviral vector, thus primarily designed for the introduction in the cells via retroviral transfection but they are also amenable to standard lipid-mediated transient transfection protocols. For this reason, I adjusted the method used in our laboratory by using higher amounts of plasmid DNA than usual. In this way I was able to achieve a level of transfection of A375MM cells that allowed me to perform immunofluorescence but not biochemical analysis. I was not successful with MDA-MB-231 cells as they are more difficult to transfect and did not obtain levels of transfection high enough to perform experiments with a sufficient number of cells.

In my transient transfection experiments, I observed that lipid-raft targeted Csk (Lat-Csk), but not the other forms, inhibited ECM degradation in A375MM cells. This is in accord both with my findings on the inhibitory effect of Csk on invadopodia function and with our previous results suggesting that invadopodia organize into cholesterol-enriched lipid raft domains.

4.2.5 Retrovirus-mediated transfection of Csk chimaeras

After the observation in transiently transfected A375MM cells I decided to follow up by using stably transfected cell lines. I expected that this approach would allow me to perform a biochemical analysis along with better control of expression levels of the respective chimaeras. Moreover, stable transfection would enable me to use MDA-MB-231 cells. In collaboration with Dr. Tomas Brdicka we created stably transfected A375 and MDA-MB-231 cells lines by retroviral transfer. Briefly, retroviruses were prepared by transfection of the cells with DNA plasmids. Upon the centrifugation of retroviruses-containing supernatant, the cleared supernatant was used to spin-infect A375MM and MDA-MB-231 cells. The infected cells were then FACS-sorted to obtain the OFP-positive population (Fig. 4.6).

4.2.6 Membrane domain localization of Csk chimaeras in stably transfected cells

To validate the obtained stably transfected cell lines, I verified the predicted localization of each single Csk construct in the specific membrane domains. The primary biochemical approach to separate lipid rafts involves the discontinuous high-speed density gradient equilibrium assay. The unique lipid composition of lipid rafts endows them with resistance to solubilisation in non-ionic mild detergents, as opposed to the bulk cellular membrane material that is readily dissolved in such conditions. Upon separation in the discontinuous high density gradient made up of varying concentrations of sucrose or iodixanol (marketed as OptiPrep), the non-solubilised lipid

raft fraction floats with respect to solubilised and insoluble non-lipid material when separated in such gradient assay. To this end, A375MM cells stably expressing the Csk chimaeras were lysed in a TNE buffer containing 1% Triton X-100 and subjected to a floatation assay on a discontinuous Optiprep gradient. After over-night ultracentrifugation, fractions were collected and processed for Western blotting. Membranes were probed with antibodies against Myc to detect the Csk chimaeras and Caveolin 1 as a bona fide marker of lipid rafts. I observed that clearly only the lipid raft-targeted constructs, Lat-Csk and Lat-kinase-dead Csk were found in the gradient fraction with highest abundance of Cav-1, thus to be considered bona fide lipid rafts. Conversely, non-lipid raft targeted CD25-Csk and cytosolic Csk were only found in the lower, i.e. heavier fractions (Fig. 4.7). I repeated the same experiments and obtained similar results with stably transfected MDA-MB-231 cells.

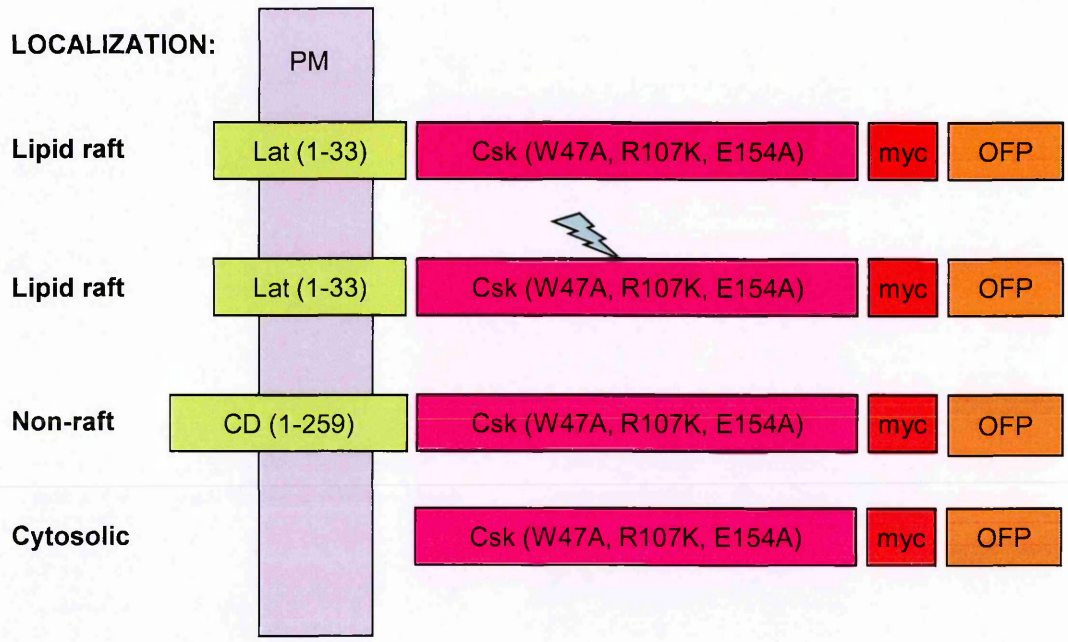

Fig. 4.5. Construct scheme and subcellular localization of Csk-OFP constructs. Abbreviation: PM, plasma membrane; OFP, orange fluorescent protein; the numbers in the constructs denote the respective amino acid segments. Colour coding:green-membrane anchor, violet-Csk, red-a Myc tag, orange-orange fluorescent protein

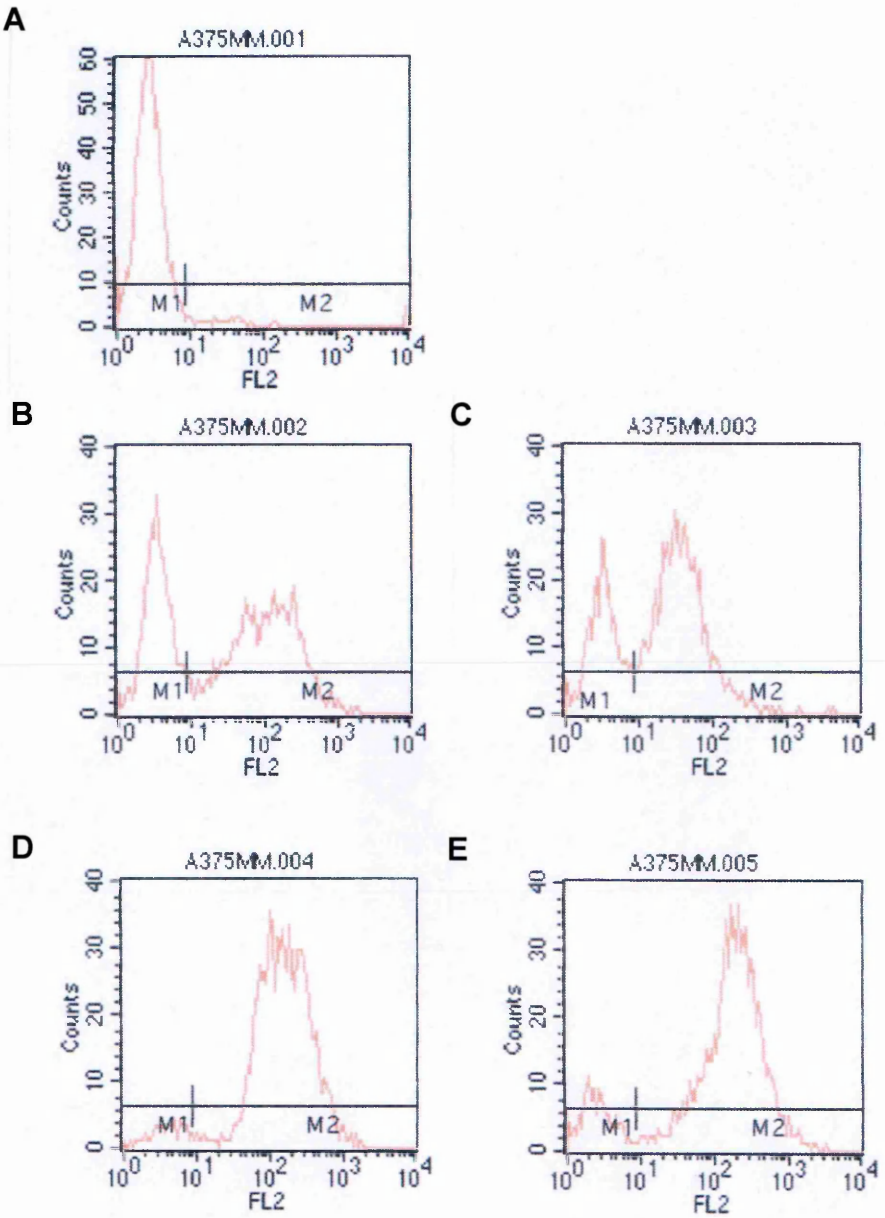

Fig. 4.6. FACS analysis of A375MM cells stably over-expressing Csk-Myc-OFP chimaeras. Cells were detached and 300.000 cells were analyzed by FACS to measure the level of transfection. Number of cells was plotted (y) against wavelength (x). (A) control cells; (B) Lat-Csk: 57,36% OFP^+ cells; (C) CD25-Csk: 70,64% OFP^+ cells; (D) Lat-Csk kinase dead: 96,88% OFP^+ cells; (E) cytosolic Csk: 90,04% OFP^+ cells.

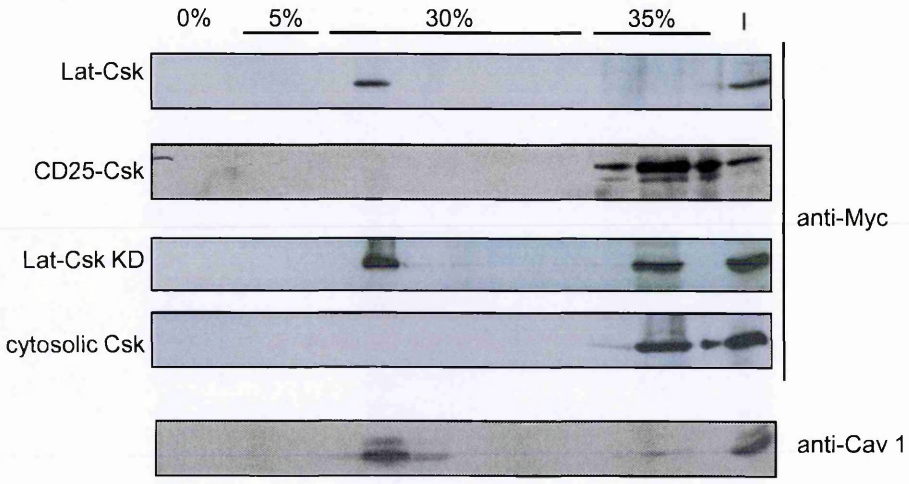

Fig. 4.7. Floatation assay in a discontinuous Optiprep gradient. A375MM cells were lysed in Triton X-100-containing buffer. Fractions were collected and subjected, together with initial lysates (I) to Western blotting and probed with anti-Myc antibody to stain Csk-Myc-OFP chimaeras. Caveolin 1 was used as a bona fide marker of lipid rafts. Clearly, only Lat-Csk and Lat-Csk kinase dead were detected in the lighter fraction of Optiprep gradient, together with Cav 1. CD25-Csk and cytosolic Csk were found in the heavier fraction, as expected.

4.2.7 Effect of Csk compartmentalization on ECM degradation

Finally, having confirmed the proper localization of Csk constructs in the discontinuous Optiprep gradient, I evaluated whether the specific membrane localization of Csk had any effect on the cells' ability to degrade the ECM.

I performed the ECM degradation assays as described above. In the A375MM cells, the results were similar to those obtained with transient transfection of Csk chimaeras, i.e. inhibition of degradation after over-expression of lipid-raft targeted Csk (Fig. 4.9 A). In line with the result in A375MM cells, the stably transfected MDA-MB-231 displayed similar behaviour. When MDA-MB-231 cells were plated on the gelatine, the degradation was significantly lowered in cells stably transfected with lipid-raft targeted (Lat-Csk) (Fig. 4.9 B).

4.2.8 Effect of Csk compartmentalization on cell migration

Csk has been shown to play a regulatory role in cell migration. Adenovirus-mediated over-expression of wild type Csk attenuates cell motility in colon cancer cell lines HCT15 and HT29 (Rengifo-Cam et al., 2013). Gs-linked G protein–coupled receptor activation of cAMP-dependent protein kinase (PKA) in endothelial cells suppresses cell migration via a Csk-mediated regulation of SFK (Bae and Paik, 1997; Jin et al., 2010). Also, as mentioned above, expression of a wt-, but not kinase dead Csk disrupted the EGF-induced activation of SFKs and cell migration on vitronectin (Ricono et al., 2009). Hence, I followed up on these studies by investigating whether the

compartmentalization of Csk function in different membrane domains has an effect.

I plated FACS-sorted MDA-MB-231 cells in the culture inserts and allowed them to attach overnight. The second day, I removed the inserts and allowed the cells to migrate for 16 h. Then, I measured the gap at time 0 and end time. I could clearly observe an effect of lipid raft targeted Csk on migration, as compared to different controls, including mock, cytosolic Csk and kinase dead lipid raft targeted Csk. Lipid raft targeted Csk inhibited migration by 50 per cent, while expression of bulk membrane targeted Csk did not affect migration (Fig. 4.9).

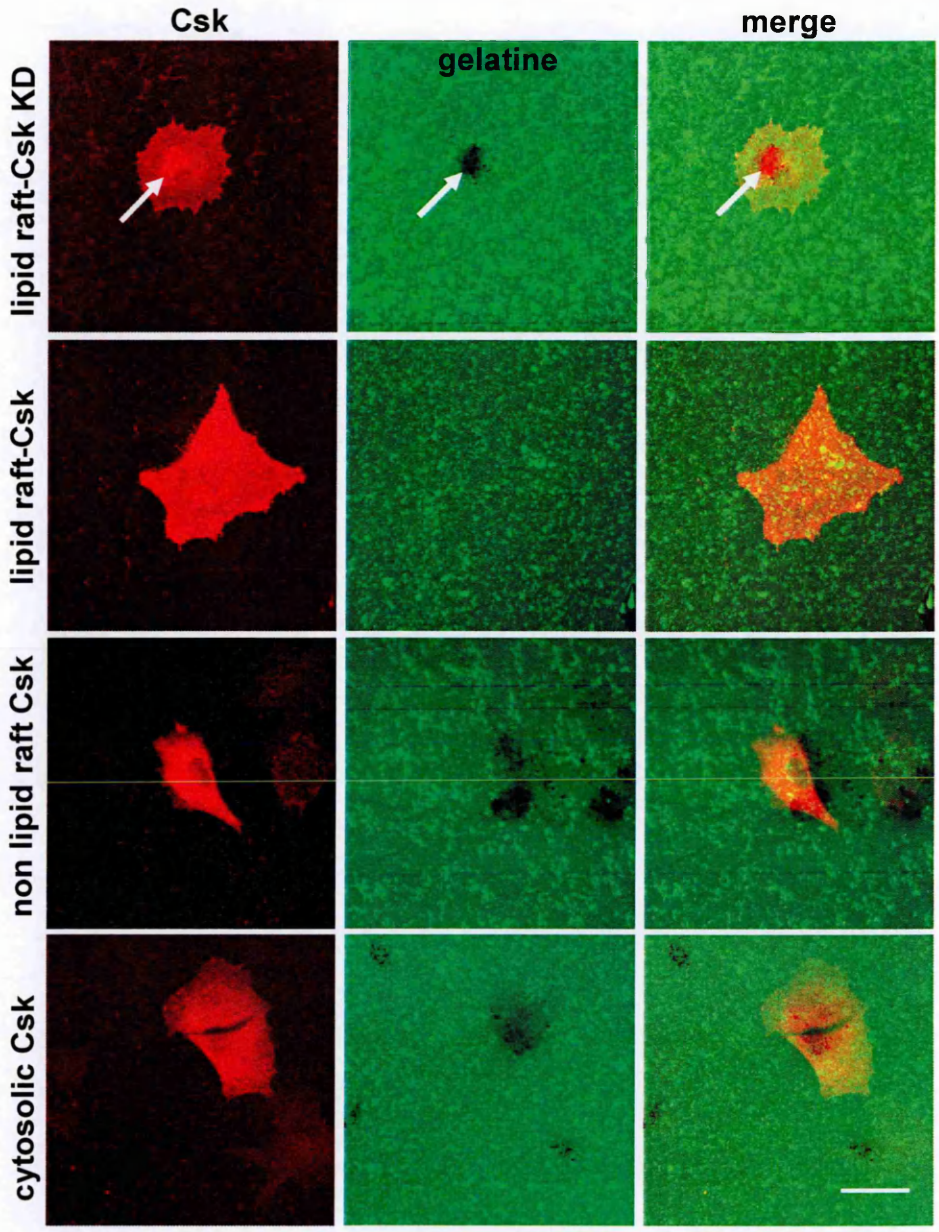

Fig. 4.8. Subcellular localization of Csk-OFP constructs. Stably transfected A375MM cells were plated on the FITC-conjugated gelatin (green). The following day, cells were fixed and stained with anti-Myc antibody to reveal the Csk construct (red). White arrow shows the colocalization of lipid raft targeted kinase dead Csk (Csk KD) with the degradation site. Scale bar 10 μm.

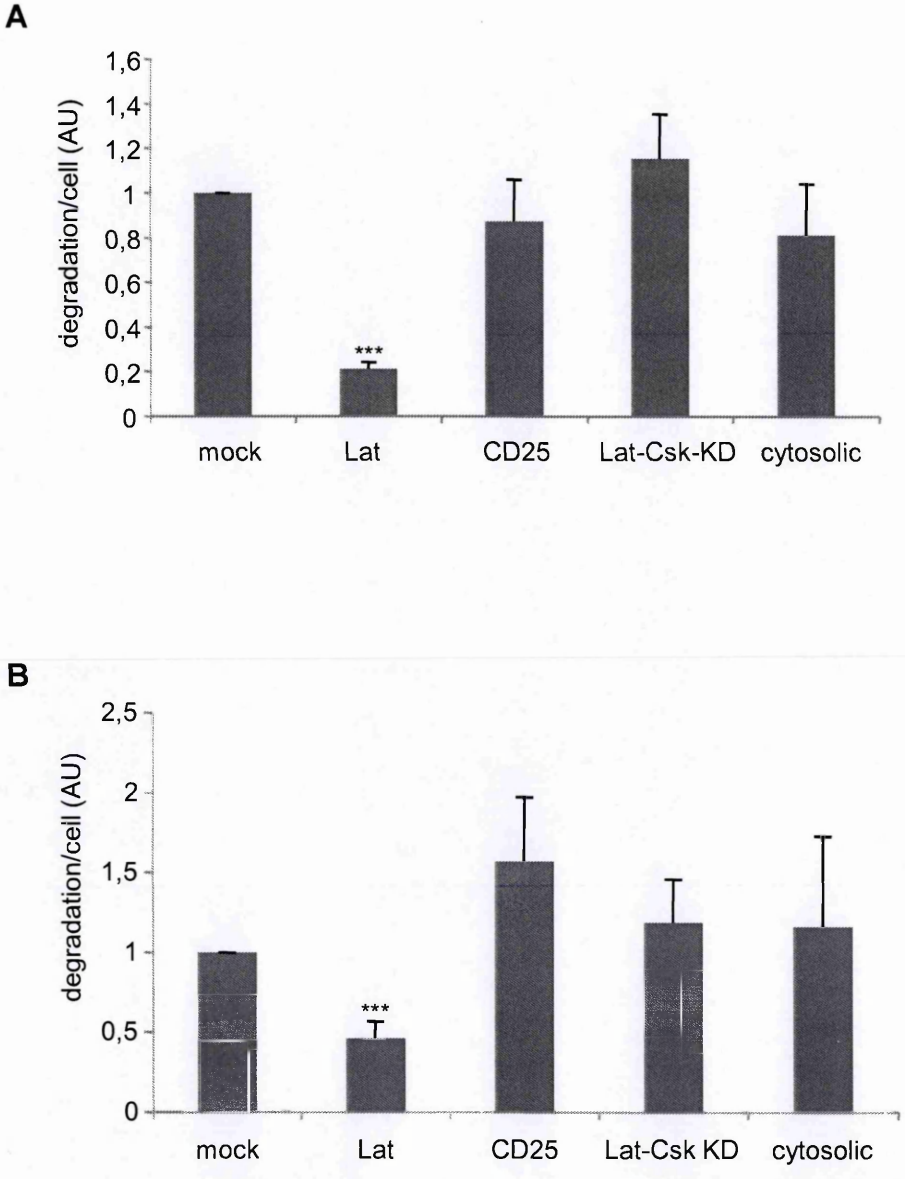

Fig. 4.9. ECM degradation after over-expression of Csk chimaeras targeted to different membrane domains. Stably transfected A375MM (A) and MDA-MB-231 (B) cells were plated on the FITC-conjugated gelatin in the presence of BB94 to block invadopodia formation. The following day, a degradation assay was performed. Only lipid raft targeted Csk (Lat-Csk) was able to inhibit ECM degradation. Error bars represent standard deviation of the mean. Three independent experiments were performed. $P < 0.001$.

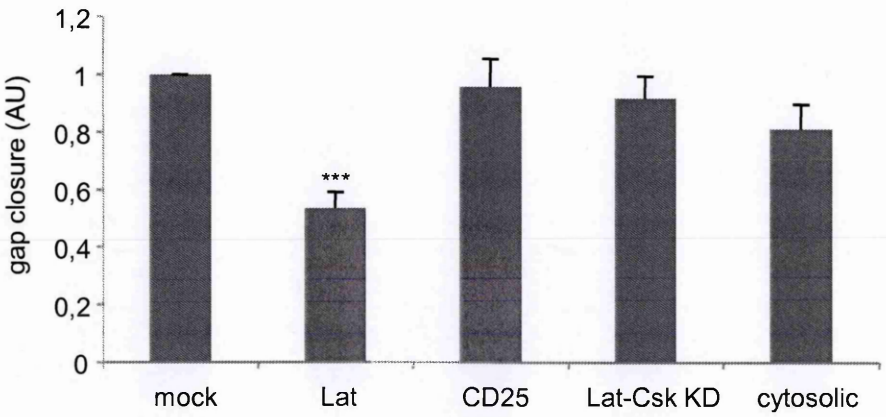

Fig. 4.10. Lipid raft-targeted Csk slows down the gap closure in wound healing assay. Stably transfected MDA-MB-231 cells were plated in the culture inserts prior to the insert removal. Cells were observed after 16 h. Error bars represent standard deviation of the mean. Three independent experiments were performed. $P < 0.001$.

4.3 Discussion

Invadopodia were first indentified in v-Src fibroblasts and later described as Src activation-dependent structures. Invadopodia formation initiates upon Src activation in response to inputs such as EGF, PDGF or integrin-mediated adhesion (Destaing et al., 2011) to promote invasive migration. Src is both necessary and sufficient for invadopodia formation, as has been repeatedly demonstrated. Indeed, Src targets a number of substrates to orchestrate invadopodia formation, maturation and disassembly (reviewed in Boateng and Huttenlocher, 2012) by involvement in different processes: a) actin polymerization; b) MT1-MMP endocytosis and c) calpain-mediated proteolysis. Hence, full understanding of SFK regulation at invadopodia is of central interest in the invadopodia biology.

Although there has been a substantial progress in understanding the molecular machinery of invadopodia, surprisingly little is known about regulation of Src activity at these structures. Recently, it has been suggested that ROS, such as hydrogen peroxide, are generated locally at invadopodia by Tks5-mediated activation of Nox complex and that they are indispensible in the initiation of invadopodia formation (Diaz et al., 2009). Although direct evidence is still lacking, it is an intriguing possibility that ROS modulate Src activity via phosphorylation of cysteine (Cys) residue. In addition, phosphatase PTP1B activates Src by dephosphorylation of C-terminal inhibitory tyrosine during invadopodia assembly (Cortesio et al., 2008).

In this study, I focused on the negative regulator of Src, C-terminal Src kinase (Csk). Csk specifically phosphorylates the N-terminal tyrosine Src to induce intramolecular binding and inhibition. I demonstrated the inhibitory action of Csk at

invadopodia formation using RNA interference. Moreover, I provided evidence that the enhanced gelatine degradation per cell after Csk ablation coincided with activation of SFK due to decreased phosphorylation of the inhibitory tyrosine of SFK, accompanied by higher phosphorylation of SFK substrates. In line with this evidence, only catalytically active wild-type Csk efficiently restored the phenotype induced by Csk knock-down. Moreover, I showed that the activity of Csk at invadopodia is confined to the lipid rafts, as only the lipid rafts targeted wt Csk efficiently blocked invadopodia formation and consequent degradation.

These results complement the evidence of invadopodia as lipid raft-rich membrane. In the normal cellular context, Csk is delocalized to specific membrane compartments by binding to phosphorylated scaffold proteins, such as Cbp/PAG (Kawabuchi et al., 2000) or caveolin 1 (Cao et al., 2002). In my laboratory, we have previously shown that caveolin 1 phosphorylation on tyrosine 14 acts inhibitory towards invadopodia formation, probably due to decrease of plasma membrane cholesterol levels and partial contribution of SFK inhibition (Caldieri et al., 2009). It would be challenging for the future research to investigate whether axis Csk-Cav1-Src contributes to invadopodia regulation, and if so, how the complex is regulated spatiotemporally. Although the detection of spatiotemporal changes in Src activity has been difficult due to lack of reliable tools, the recent development of new biosensors might help to get further insight to Src-dependent signalling events at invadopodia (Gulyani et al., 2011).

CHAPTER 5: ARF6-mediated trafficking is involved in invadopodia formation and function

5.1 Introduction

ARF6 is a small molecular weight GTPase that localizes to the plasma membrane and endosomal compartment where it regulates endocytic membrane trafficking and actin remodelling (Donaldson, 2009; Grant and Donaldson, 2009). Over the last few years, ARF6 GTPase is emerging also as an important regulator of invadopodia formation.

Studies investigating the role of ARF6 in melanoma and breast tumour cell invasion have shown that endogenous ARF6 localized at invadopodia and that ARF6 activity is required for invadopodia formation (Tague et al., 2004). These effects, together with the well known ability of ARF6 to regulate endosomal membrane recycling, may suggest that the ARF6-dependent recycling compartment regulates bulk membrane available for the formation of invadopodia (Schweitzer et al., 2011). Moreover, ARF6 influences the deposition and distribution of membrane proteins, such as $\alpha 6\beta 1$ integrin, which has been shown to be important for the initiation of invadopodia (Nakahara et al., 1998).

The ARF6 recycling compartment is organized in long tubules that develop from the perinuclear recycling compartment and are generally extended toward the leading edge of the cells (Weigert et al., 2004). Such tubules contain many other associated

proteins such as Rab22, PLD2, PIP5K (Porat-Shliom et al., 2008) and are enriched in certain lipids, such as cholesterol and PtdIns(4,5)P_2.

In this section, I focused on the constituents and cargo of ARF6-dependent pathway. I proved to show that both the constituents and cargo are localized and recycled, respectively at invadopodia. Moreover, inhibition of PLD2, a component of ARF6 pathway led to decrease in the level of gelatine degradation.

5.2.1 Constituents of ARF6 pathway are present at invadopodia

I resorted to an immunofluorescence (IF) approach to examine whether the ARF6 recycling compartment could be connected to the invadopodia sites. ARF6 is the only member of the small ARF GTPases to localize at the PM where it regulates membrane trafficking through phospholipase D2 (PLD2) and PIP5K, resulting in the generation of phosphatidic acid and PIP2.

PLD2 colocalizes with ARF6 at the plasma membrane and on endosomal membranes and, more importantly, PLD2 is selectively activated by ARF6 (Hiroyama and Exton, 2005). Upon activation, PLD2 catalyzes the hydrolysis of phosphatidylcholine (PC) to form choline and phosphatidic acid (PA), a signaling lipid that can be further converted to diacylglycerol (DAG) (Porat-Shliom et al., 2008).

ARF6 can interact with, and activate PIP5K in the presence of PA to produce PtdIns(4,5)P_2 and over-expression of ARF6 increases PtdIns(4,5)P_2 levels at the plasma membrane (Honda et al., 1999; Martin et al., 1996). Similarly to the over-expression of a constitutively active form of ARF6 (Q67L), over-expression of PIP5K induces the formation of large internal vesicle structures, probably through the fusion of endocytic vesicles that are prevented from recycling back to the plasma membrane (Aikawa and Martin, 2005). While PIP5K-induced vesicle formation is not blocked by a dominant-negative form of ARF6, PIP5K probably acts downstream of ARF6 to induce CIE.

In my analysis, cells plated on gelatine were transfected with GPF-tagged variants of mentioned proteins and then subjected for IF. The results revealed that all examined accessory proteins of the ARF6 recycling pathway, PLD2 (Fig. 5.1), syntaxin 2 (Fig. 5.2.) and 3 (Fig. 5.3) localize at the actin-rich degradation sites. In addition, I used a construct encoding the PH domain of PLC-δ that specifically binds PtdIns(4,5)P_2, the product of PIP5K (Fig. 5.4).

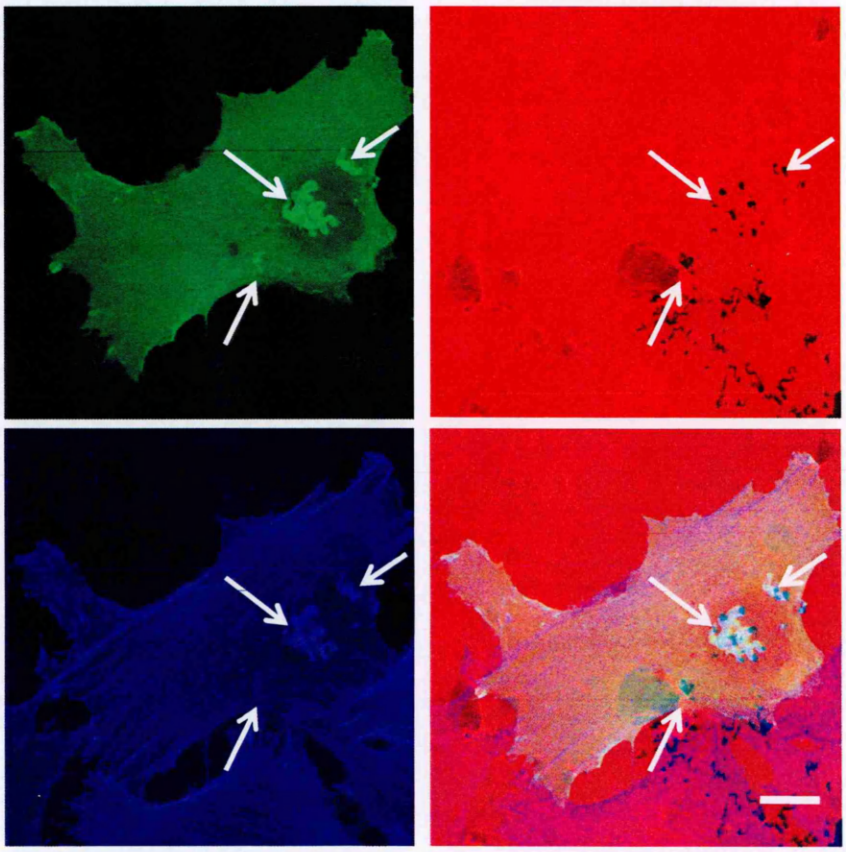

Fig. 5.1. PLD2 localization in the actively degrading cells. A375MM cells transfected with PLD2-GFP were detached, plated on fluorophore conjugated gelatine coated coverslips and fixed after over night degradation. Colocalization with underlying degradation is shown (white arrows). Green: GFP construct, red: gelatine, blue: F-actin. Merge image also shown. Three independent experiments were performed. Scale bar 10 μm.

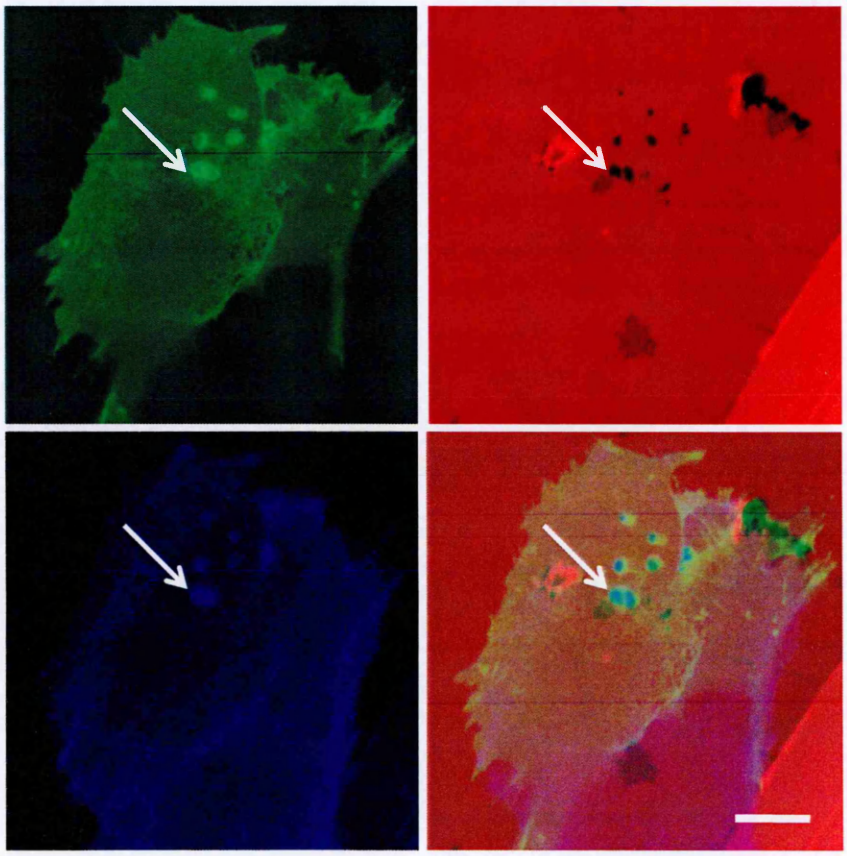

Fig. 5.2. Syntaxin 2 localization in the actively degrading cells. A375MM cells transfected with syntaxin 2-GFP were detached, plated on fluorophore conjugated gelatine coated coverslips and fixed after over night degradation. Green: GFP construct, red: gelatine, blue: F-actin. Colocalization with underlying degradation is shown (white arrows). Merge image also shown. Three independent experiments were performed. Scale bar 10 μm.

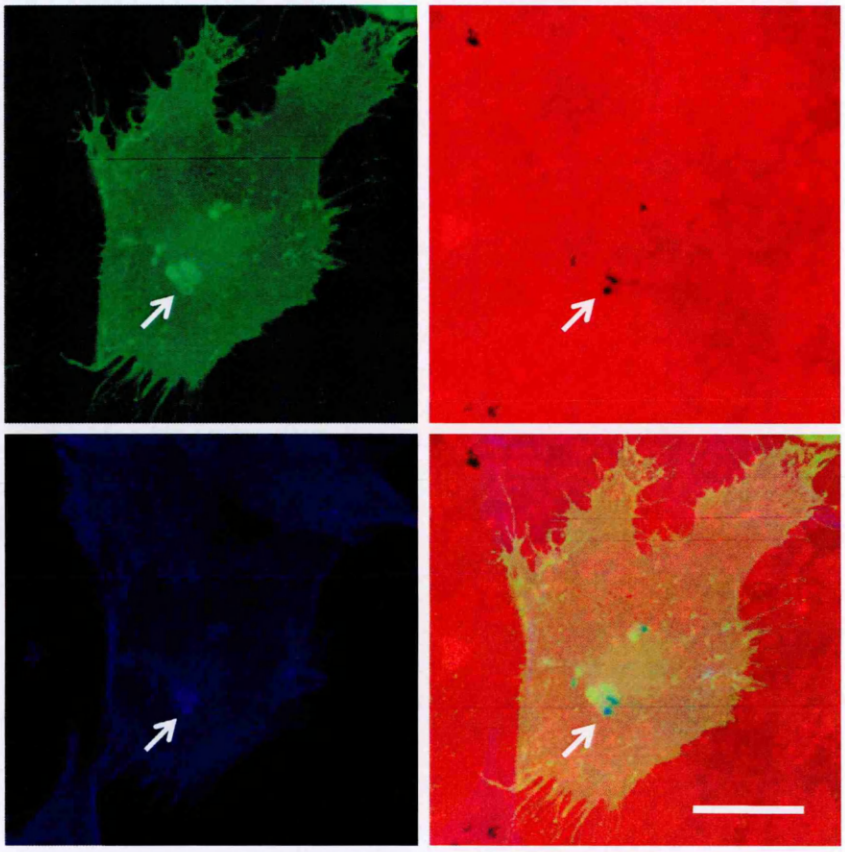

Fig. 5.3. Syntaxin 3 localization in the actively degrading cells. A375MM cells transfected with PH-PLC-GFP were detached, plated on fluorophore conjugated gelatine coated coverslips and fixed after over night degradation. Green: GFP construct, red: gelatine, blue: F-actin. Colocalization with underlying degradation is shown (white arrows). Merge image also shown. Three independent experiments were performed. Scale bar 10 μm.

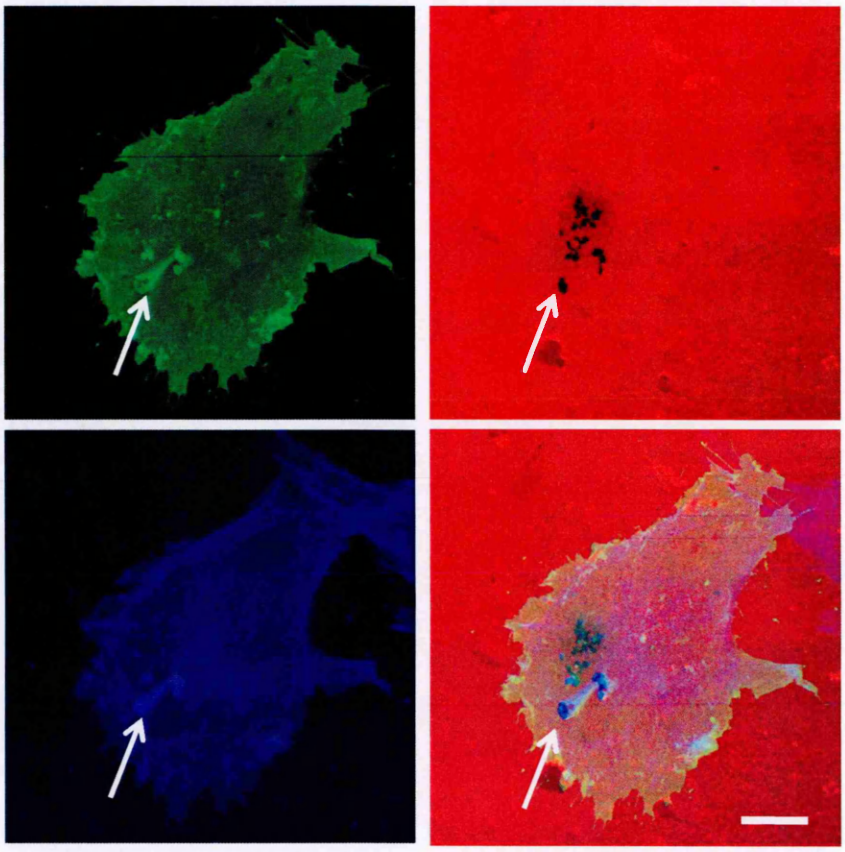

Fig. 5.4. PH-PLC localization in the actively degrading cells. A375MM cells transfected with PH-PLC-GFP were detached, plated on fluorophore conjugated gelatine coated coverslips and fixed after over night degradation. Green: GFP construct, red: gelatine, blue: F-actin. Colocalization with underlying degradation is shown (white arrows). Merge image also shown. Three independent experiments were performed. Scale bar 10 μm.

5.2.2 PLD2 inhibition blocks ECM degradation

To follow up on the IF analysis of the ARF6 recycling compartment accessory proteins, I chose to examine role of PLD2 in invadopodia-mediated ECM degradation. For that, I used a small molecular weight compound, 5-fluoro-2-indolyl des-chlorohalopemide (FIPI), which had been identified in an *in vitro* chemical screen as a strong PLD2 inhibitor, consequently blocking the synthesis of the lipid second messenger PA (Monovich et al., 2007; Su et al., 2009). Briefly, I performed a degradation assay in the presence of 750 nM FIPI for 5 h. Strikingly, ECM degradation in cells treated with FIPI was almost completely blocked as compared to control cells (Fig. 5.5 A).

Furthermore, I performed loss of function experiments by down-regulating PLD2 with siRNA (Fig. 5.5 B), and similarly I observed inhibition of gelatine degradation, albeit less striking as compared to the FIPI effect (Fig. 5.5 C).

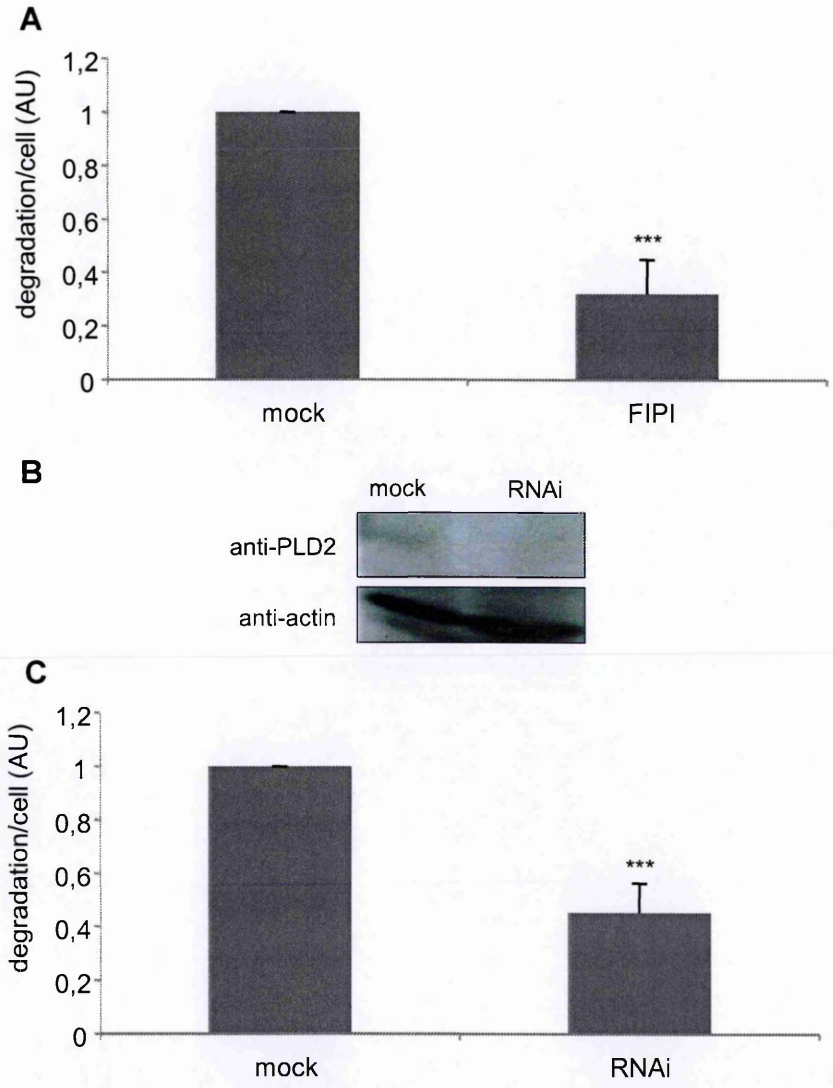

Fig. 5.5. PLD2 inhibition leads to a decrease in ECM degradation. Quantification of ECM degradation revealed more than 50% decrease in degradation per cell in FIPI-treated (FIPI) compared to mock (mock)-treated A375MM cells. A) Efficiency of PLD2 knock-down. A375MM cells were treated without (mock) or with (RNAi) siRNA targeting PLD2 for 96 hours. RNAi reduced PLD2 expression up to 85% as shown in western blots of lysates using antibodies against PLD2 and actin as a loading control. B) Quantification of ECM degradation revealed more than 50 decrease in degradation per cell in PLD2 knock-down (RNAi) compared to mock-transfected (mock) A375MM cells. Error bars represent standard deviation of the mean. Three independent experiments were performed. $P < 0.001$.

5.2.3 ARF6-dependent cargo CD147 is delivered to the sites of matrix degradation

As shown above, constituents of ARF6-associated endocytic pathway are evidently localized at invadopodia. Thus, I decided to explore the fate of ARF6-associated cargo. The list of proteins that enter cells via the ARF6-pathway includes the well-characterized cargo MHC I and the recently identified ones CD44, CD98 and CD147 (also known as EMMPRIN or basigin) (Eyster et al., 2009). I chose CD147 for the next analysis, since it has been recently shown to enhance matrix degradation by breast cancer cells at invadopodia (Grass et al., 2012). CD147 (also known as emmprin or basigin) is a single pass integral membrane protein, which is normally expressed at low levels in the most of the tissues, but it is highly upregulated during tissue remodeling and tumour progression. CD147, and its overexpression in the cancer-related role is associated with induction of expression of MMPs, such as MMP-1, MMP-2, MMP-3, MMP-9 and MMP-11 (Weidle et al., 2010)

First, I performed an IF analysis of actively degrading cells on gelatine by staining the cells with antibody against endogenous CD147. Clearly, CD147 colocalized with actin at the degradation sites (Fig. 5.6).

To explore whether recycling of the plasma membrane pool of CD147 is involved in delivery to invadopodia, I employed an antibody binding and internalization assay. In this assay, cells are first incubated with antibody-containing complete medium to allow the binding and consequent uptake of the antibody. After incubation, cells are washed briefly with an acidic buffer. Through a washing step, the surface pool of antibody is removed and thus any further antibody detected at the plasma membrane

will have derived from recycling, not residual binding. I combined this assay with the degradation assay. Briefly, cells plated on gelatine were incubated with the antibody against CD147 at 37 °C in the presence of BB94 for 30 min and then washed with low pH buffer. After this acid wash, cells were left to degrade matrix for the indicated time. I performed IF analysis, showing that the majority of the internalized anti-CD147

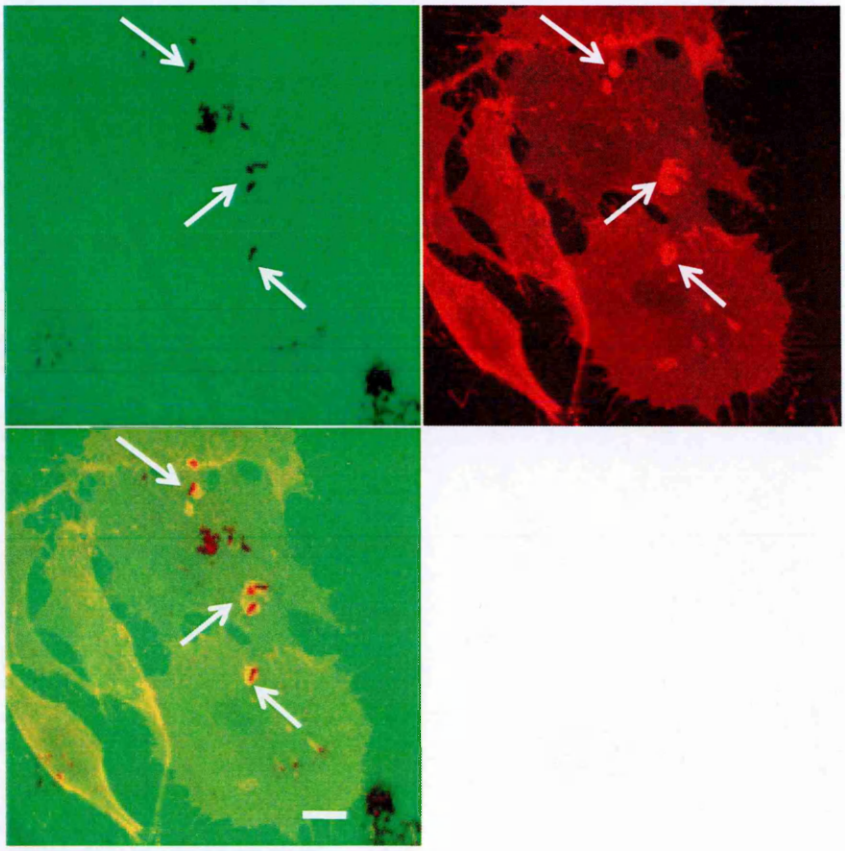

Fig. 5.6. CD147 localization in the actively degrading cells. A375MM cells plated on FITC-gelatine (green) were fixed after the 30 min uptake of anti-CD147 antibody and stained without permeabilization (red). Colocalization with underlying degradation is shown (white arrows). Three independent experiments were performed. Scale bar 10 μm.

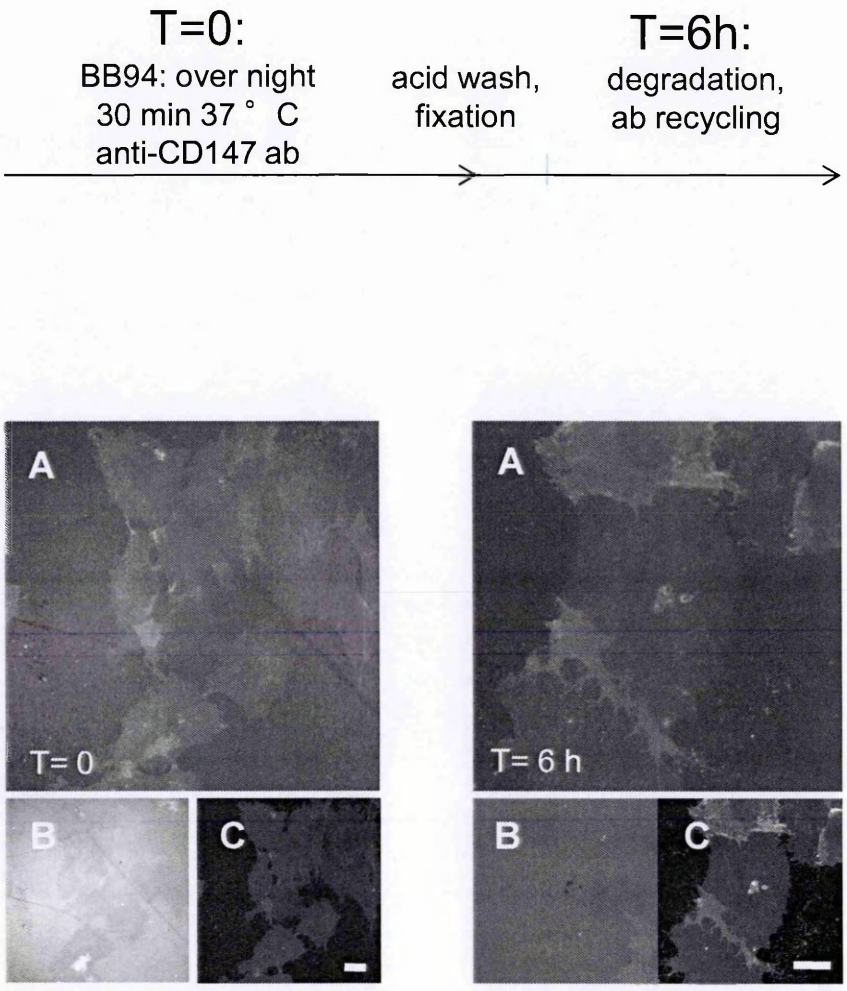

Fig. 5.7. Plasma membrane bound CD147 antibody is recycled to degradation sites. The uptake of anti-CD147 antibody was performed on the A375MM cells plated on the FITC gelatine-coated coverslips in the presence of BB94 at 37 °C for 30 min. The non-internalized antibody was washed out with low pH buffer (acid wash) and cells were fixed after 6 h of gelatine degradation. Uptake of anti-CD147 antibody was performed for 6 h on A375MM cells plated on fluorophore-conjugated gelatine-coated coverslips. Cells were fixed 6 h after acid wash. A) merge; B) gelatine; C) CD147. Three independent experiments were performed. Scale bar 10 μm.

antibody is delivered to invadopodia (Fig. 5.7). This confirms that the plasma membrane pool of CD147 was recycled and preferentially delivered to invadopodia. At this point, it is important to mention that the internalization of antibody was performed in the presence of BB94, i.e. in the condition when invadopodia are not formed. Therefore, the accumulation of CD147 antibody cannot be an artifact of the assay but derives from intracellular recycling.

5.2.4 Effect of Seladin1/DHCR24 inhibition on the ARF6-dependent endocytic pathway

Proteins and lipids that reside in lipid rafts seem to be prominently internalised via clathrin-independent endocytosis (CIE). The widely studied ARF6-dependent trafficking is of a particular interest in the context of CIE as it regulates a wide range of events of relevance in tumour biology, including cell migration, adhesion and invasion. The ARF6-dependent pathway is mainly responsible for the endocytosis of cell surface integral proteins that lack adaptor protein localisation sequences. Among these are the major histocompatibility complex class I (MHC I) proteins (Radhakrishna and Donaldson, 1997), syndecan 1 (Zimmermann et al., 2005), β1-integrin (Brown et all.,2001) and the GPI-anchored protein CD59 (Naslavsky et al., 2004). Following internalization, vesicles containing these cargo proteins traffic to the early endosomes, where they meet the clathrin-dependent cargo. From there, the cargo is either transported via a degradative pathway to the late endosomes and lysosomes or recycled back to the plasma membrane (Donaldson et al., 2009). In addition, ARF6-dependent

endosomal trafficking impacts cholesterol homeostasis and is free cholesterol dependent (Schweitzer et al., 2011). Therefore, I wondered whether the inhibition of Seladin 1/DHCR24, and consequent block of cholesterol biosynthesis, might affect the Arf-6 dependent pathway and trafficking of cargo.

I based my experiment on the trafficking of MHC I, a well-known ARF6-dependent cargo (Radhakrishna and Donaldson, 1997). First, I examined whether the uptake of MHC I is affected by Seladin1/DHCR24 inhibition. A375MM cells were plated on uncoated coverslips in the presence of lovastatin and mevalonate. The second day, antibody uptake was performed after pre-treatment with inhibitors in medium containing dFCS. Briefly, cells were incubated with MHC-I antibody at 37 °C and fixed at different time-points. I did not observe any significant difference between the control and treated cells. Thus, I decided to use a modified protocol, where the uptake of MHC-I antibody is preceded by antibody binding on ice. Uptake itself was performed again at 37 °C and followed by an acid wash. This wash removes the antibody bound on the cell surface, while the route of internalized antibody remains intact. Using this approach I observed an impairment of the recycling route, especially striking in the Triparanol-treated cells. I also found that most MHC I antibody remains in the early endosomes, as confirmed by increased co-localization of MHC I and Early Endosome Autoantigen 1 (EEA-1), a well-known marker of early endosomes (Fig. 5.8 A). This would suggest that the inhibition of DHCR24 causes impairment in the recycling via the ARF6-dependent CIE pathway back to the membrane. To confirm the specificity of the treatments, I performed a phenotype rescue experiment by replenishing cholesterol as described previously. I observed the loss of accumulation of internalized MHC I in the

early endosomes in both Triparanol- and EC-treated cells (Fig. 5.8 B). Interestingly, I also observed an increase in number and location (closer to the plasma membrane) of early endosomes in all the cholesterol replenished cells (Fig. 5.8 C). One might suggest that this change is due to acute cholesterol overload-connected stimulation of ARF6-associated endocytosis. This is a speculation at this stage and would require further experiments, such as testing different cholesterol concentrations and/or modifying treatment times to observe longer-term effects. Another possibility could be cholesterol tracking by using some of its fluorescent analogues, eg. Bodipy-cholesterol.

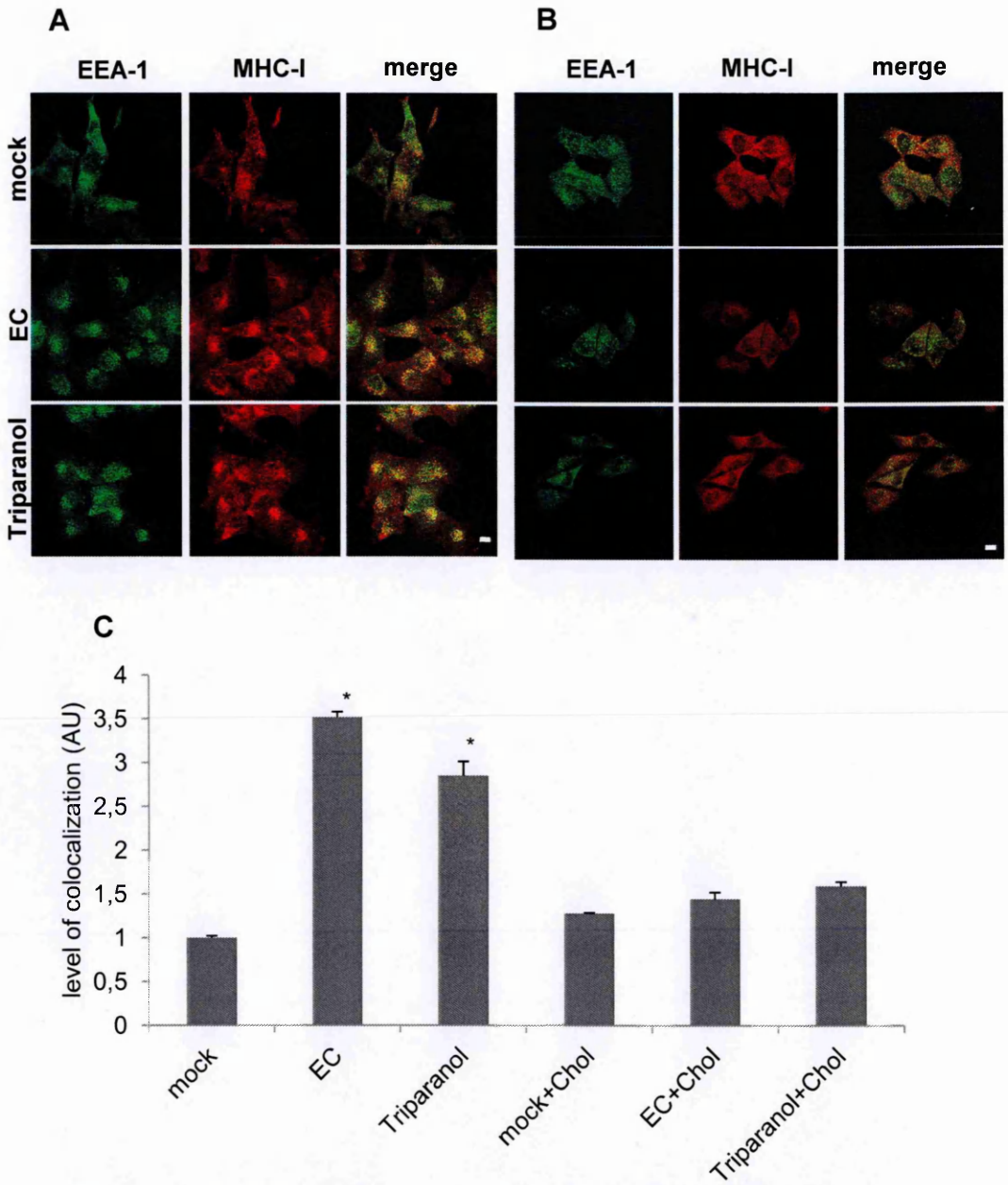

Fig. 5.8. Inhibition of Seladin1/DHCR24 blocks recycling of MHC I. A375MM cells were plated with lovastatin/mevalonate mix (mock) and were treated with 24(S),25-epoxycholesterol (EC) or Triparanol or left untreated (mock) 4h prior the uptake of anti-MHC-I antibody (A) or cholesterol addition followed by MHC-I-ab uptake (B). Cells were fixed 30 min after acid wash and stained with anti-EEA-1 (green) and anti-MHC I (red) antibody. Merged images are also shown. Scale bar 10 μm. C) Colocalization of EEA-1 and MHC-I was quantified using ImageJ software. Error bars represent standard deviation of the mean. Two independent experiments were performed. $P < 0.05$.

5.3 Discussion

Invadopodia are cellular structures that confine different cellular processes, such as signalling, cytoskeleton remodelling and proteolysis, at discrete areas of the cell surface. A current challenge is to understand how the invadopodia components are precisely delivered to discrete sites of matrix degradation. Much of the effort to elucidate the trafficking to invadopodia has focused on MT1-MMP. The delivery of MT1-MMP to the plasma membrane and its activation likely include many pathways. At any given time, at least two pools of MT1-MMP exist within the cell: a) a pool of newly synthesized protein in route from Golgi compartment to the PM and b) a second pool of PM localized MT1-MMP which is constantly internalized through clathrin-dependent and -independent mechanisms (Remacle et al., 2003) and eventually routed to early and late endosomes before being recycled back to the PM (Frittoli et al., 2010; Poincloux et al., 2009). Whether and how the secretory/biosynthetic and endo/exocytic pathways are coordinately regulated, is currently unknown.

In my work, I focused on the small GTPase ARF6, an important regulator of clathrin-independent endocytosis and actin remodelling. A role of ARF6 at invadopodia has previously been indicated. However, a direct demonstration of the involvement of the ARF6-associated pathway in invadopodia assembly has been lacking. Here I show that typical components of ARF6-associated recycling pathway, including PLD2, syntaxin 2 and syntaxin 3, are localized at invadopodia. Furthermore, I show that the recently discovered ARF6-pathway cargo, CD147 (Eyster et al., 2009) is localized at

invadopodia and is continuously recycled to invadopodia during active degradation. CD147, also known as the extracellular matrix metalloproteinase inducer (EMMPRIN) or basigin, is enriched on the surface of tumour cells and stimulates adjacent stromal cells to produce several matrix MMPs, including MT1-MMP.

On one hand, the role of ARF6 in recycling of proteins from the cell surface might be to modulate the availability of specific proteins that are employed in invadopodia initiation and function. Such recycled cargo might include specific integrins, CD44 and/or CD147. Delivery of these protein components of invadopodia might in turn affect the activity and delivery of MT1-MMP at invadopodia. On the other hand, ARF6-dependent endosomal trafficking may control delivery of bulk membrane, wherever it is needed as a building block for various membrane protrusions, as documented for the leading edge of migrating cells.

An additional possibility is that recycling of MT1-MMP itself is ARF6-dependent. Hence, it would be of particular interest to explore the role of ARF6 recycling compartment in the recycling of MT1-MMP to the invadopodial membrane, and some of the approaches presented in this thesis could be employed together with ARF6 knock-down and cytochalasin D treatment.

CHAPTER 6: Final discussion

Invasive tumour-derived or transformed cells, cultured on a flat extracellular matrix substratum, extend specialized proteolytically active plasma membrane protrusions. These structures, termed invadopodia, are responsible for the focal degradation of the underlying substrate. Invadopodia are subcellular structures specialised in the focalised proteolysis of the ECM *in vitro*. Their formation and function requires the simultaneous coordination of different cellular processes, such as signalling, membrane traffic and cytoskeleton remodelling, at discrete areas of the cell surface. How the localisation and the function of all components required for these activities, such as integrins and proteases, are spatially and temporally confined to specific cell-ECM contacts is not known.

Although the description of the ultrastructural features of invadopodia is still rather incomplete, many recent developments have uncovered a tight structure-function relationship that is helping us understand how the many invadopodia components are recruited, and ultimately, how ECM degradation is so precisely directed. My PhD project has been focused on the working hypothesis that these functional features are tightly connected to cholesterol homeostasis at the plasma membrane and might be achieved through the polarized delivery of invadopodia components to sites of degradation. I manipulated cholesterol levels by inhibition of Seladin1/DHCR24, an enzyme known to catalyze the reduction of the double bond of intermediates of cholesterol biosynthesis pathway. More importantly, inhibition of this enzyme has been

shown to lead to accumulation of desmosterol that differs from cholesterol only by the presence of a C24 double bond. Interestingly, desmosterol cannot fully substitute cholesterol in lipid rafts. I showed here that the decrease of ECM degradation caused by Seladin1/DHCR24 inhibition could be fully reversed by addition of cholesterol.

Tyrosine phosphorylated Caveolin 1 is inhibitory towards invadopodia biogenesis and function in its capacity as a regulator of cholesterol homeostasis at the plasma membrane and possible regulation of SFK activity (Caldieri et al., 2009). Indeed, the phosphorylated caveolin 1 binds the SH2 domain of the SFK-inhibitory kinase Csk (Cao et al., 2004), that inhibits SFK-dependent signalling, which is required for invadopodia formation. In accordance, I found that ablation of the SFK-inhibitory kinase Csk led to increased invadopodia formation and ECM degradation. To exert its inhibitory effect, Csk must localize to cholesterol-rich lipid rafts but not to other membrane domains, as indicated by experiments using differentially targeted wild type and mutant Csk chimeras in transient and stable transfectants.

Furthermore, I provided evidence of a role for the ARF6-associated clathrin-independent endocytic and recycling pathway. The cargo that travels along this pathway includes both lipid raft and non-lipid raft proteins but cholesterol homeostasis appears to be crucial for the functional endocytosis and recycling. In my work, I showed that constituents such as syntaxin 2 and 3, PLD2 and PtdIns(4,5)P_2 of the ARF6-associated pathway are all localized at degradation sites. Moreover, the recently discovered ARF6-pathway cargo CD147 is recycled to the active invadopodia. Along with the inhibitory effect of PLD2 ablation on ECM degradation, this provides proof of the direct involvement of ARF6-associated recycling at invadopodia.

In aggregate, my work contributes to further understanding of the intertwine of signalling and membrane trafficking at invadopodia, and shows the dependence of this process for the cholesterol homeostasis at the plasma membrane.

These results are further complemented by another project in my laboratory, wherein I actively participated. The evidence that invadopodia are specialized, cholesterol-rich membrane domains suggest an existence of apical-like raft-dependent trafficking, similar to epithelial cells. The plasma membrane of epithelial cells is typically organised into apical and basolateral domains separated by tight junctions, and characterised by different lipid and protein composition. Similarly, non-polarised cells have an ability to establish a clear segregation between diverse functions, by creating membrane compartments characterized by a different molecular composition exposed to a different milieu.

We found that glycosylphosphatidylinositol-anchored green fluorescent protein (an apical model protein), but not vesicular stomatitis virus G-protein or influenza virus hemagglutinin (both basolateral model cargoes), was transported to sites of ECM degradation. Also, RNAi-mediated knock-down of proteins known to specifically regulate polarised apical transport, such as caveolin 1 and annexin XIIIB or basolateral transport in epithelial cells, such as clathrin, demonstrated that the selective inhibition of the apical, but not the basolateral, transport route impairs invadopodia formation and ECM degradation. Invadopodia thus appear to be apical-like membrane domains, where signal transduction and local membrane remodelling events might be temporally and spatially confined via selective raft-dependent apical transport routes (Caldieri et al., 2012).

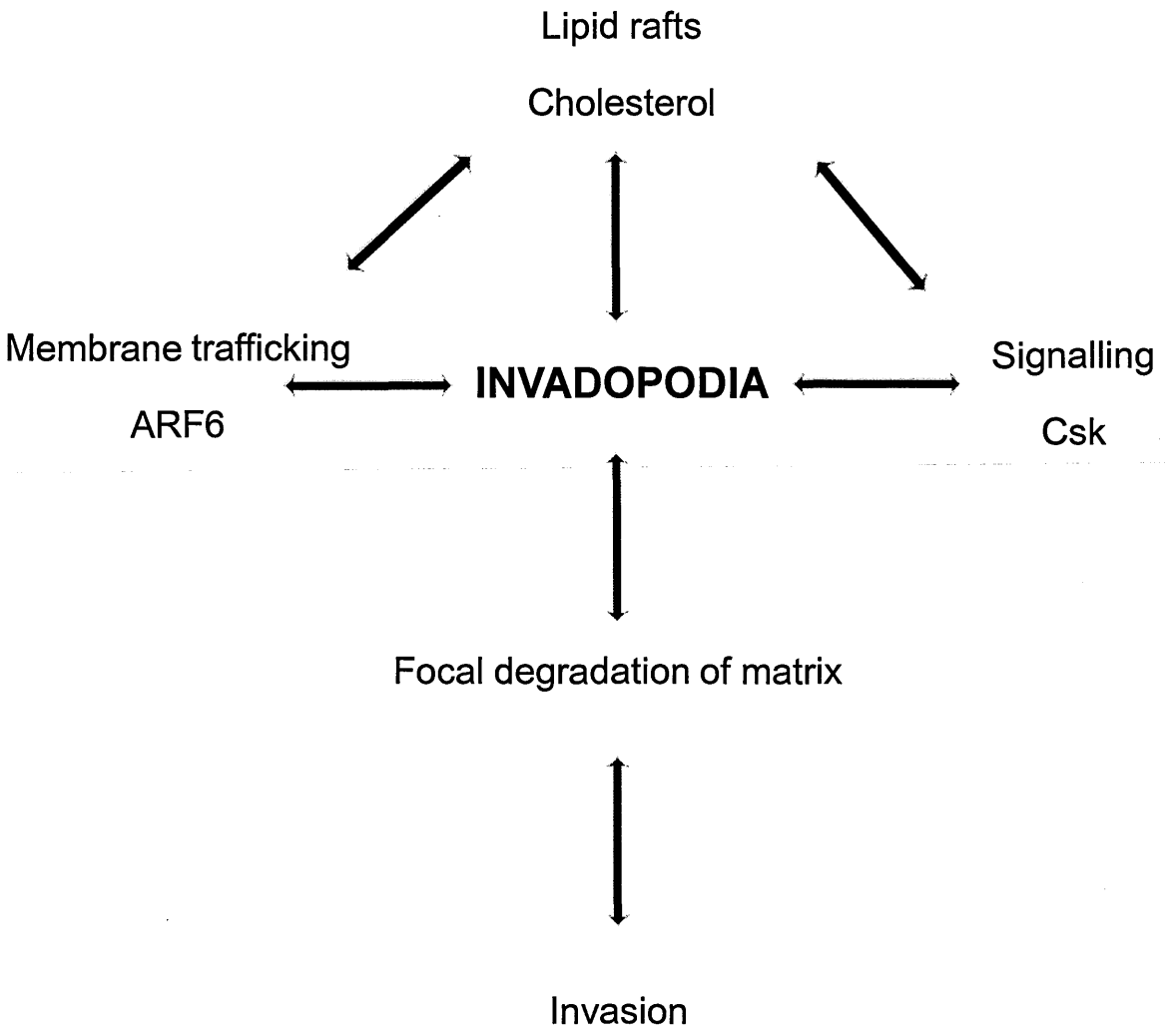

Fig. 3.5. Graphical abstract.

CHAPTER 7: Future perspectives

My findings converge on the hypothesis that cholesterol influences the metastatic process of the tumoural cells. Intriguingly, the solid tumors were show to be highly enriched in cholesterol by Swyer in 40s, who found that the cholesterol content almost doubled between the normal prostate and prostatic hyperplasia. Since then, the interest in the association of cholesterol and cancer has been resuscitated with a seminal observation showing that cholesterol lowering drugs statins might be linked with the prostate cancer diagnosis. However, the association between cancer and dietary cholesterol is not clear (Hu et al., 2011) and the hypothesis might be valid only for some types of cancer, such as prostate and breast.

The potential roles of cholesterol in cellular functions supporting tumourigenesis are multiple, including the cellular growth, inflammation, membrane organization and steroidogenesis. Indeed, the rapid growth and high metabolic rate of tumour cells has to be supported by abundance of the essential building blocks, cholesterol among them. At advanced disease stage, the tumour cells are even reported to reduce the circulating cholesterol, with low serum cholesterol as an effect of progressing cancer (reviewed in Solomon and Freeman, 2011).

Cholesterol is an essential component of cell membranes and in complex with membrane glycosphingolipids plays a regulatory role by forming a platforms in asymmetric membrane domains, aka lipid rafts (Lingwood and Simons 2010). These

domains are more ordered relatively to bulk plasma membrane and variably accumulate proteins involved in cell signalling (Levental et al. 2010), such that membrane rafts become foci for bio-information transduction. Our current understanding of lipid rafts is still rather incomplete, such as their actual size and lifetime is under debate (Simons and Lingwood, 2011). Lipid rafts are increased (Li et al., 2006) and key in the aberrant signalling and adhesion of cancer cells (Staubach and Hanisch, 2011). Hypercholesterolemia in mice model lead to accumulation of lipid rafts and consequent altered plasma membrane signalling and membrane trafficking, accompanied by increased phosphorylation of Akt and increased tumour growth in transgenic prostate cancer mice (Oh et al., 2010; Zhuang et al., 2005). Intriquingly, higher tumour membrane cholesterol in the lipid rafts may help the neoplastic and cancer stem cells to avoid the immunodetection by hindering the glycosphospholipids, too. In the lipid raft rich plasma membrane of tumour cells, cholesterol makes glycosphingolipids' epitopes unavailable for active antibody recognition (Novak et al., 2013).

The oxidation and deposition of cholesterol in the atherosclerotic lesions is a common pathological consequence of the hypercholesterolemia and it is a common cause of inflammatory response that leads to cardiovascular disease. Given that certain pool of human cancer is thought to develop as a consequence of inflammation, the role of oxidized cholesterol in promoting inflammatory responses could be a factor in initiation of carcinogenesis (Pelton et al., 2012).

The abberant tumour cells' demand for cholesterol is satisfied both by loss of feedback regulation, leading to enhanced enhanced cholesterol synthesis and uptake via upregulated LDL receptors (Chen and Hughes-Fulford 2001; Hentosh et al., 2001).

As a vital part of body's chemistry, cholesterol serves as a precursor of steroid hormones; it is then likely that cholesterol promotes the growth of hormone dependent tumours by this virtue. Prostate tumor cells respond to androgen through the action of the androgen receptor (AR), a nuclear receptor that controls PCa cell proliferation at all stages of disease, including late-stage, castration-resistant disease. The xenograft prostate cancer tumours express all the enzymes necessary for the de novo synthesis of androgens of cholesterol, and the cholesterol levels correlate with expression of CYP17A. Thus, cholesterol acts merely not only as an essential precursor, but also as an agonist of androgen synthesis. Secondly, cholesterol is a precursor of estrogen, which has a clearly established role in the etiology of the breast cancer. The results of recent research on the breast cancer imply that increased cholesterol levels help tumour cells to feed the tumour with estrogen, leading to the tamoxifen resistance (Nelson et al., 2013).

Accumulating evidence on the pathological role of invadopodia provides a rationale to study them as a possible therapeutical target. They represent excellent model structures to study ECM degradation, a key step to in invasion and metastatic process, and might provide new avenues into novel anti-cancer therapeutics. My results support the idea that the pharmacological alteration of cholesterol biosynthesis, or alteration of Csk localization in the cholesterol-rich lipid rafts, or ARF6-associated membrane trafficking events regulates the invadopodia biogenesis and function. The findings discussed in my thesis suggest a role for cholesterol in proteolytic degradation of ECM, deriving from its role in the membrane organization.

Although the mechanisms of the association of cholesterol and cancer have not yet been unequivocally elucilated, it is becoming clear that cholesterol is able to affect key attributes of tumour biology. Given the abundance of cholesterol in the Western diet, the ability to effectively target this molecule or its metabolism and moderate its downstream effectors would be a tremendous advance cancer prevention and treatment. One such approach would be to employ enhanced cholesterol lowering drugs as adjuvant therapy to conventional therapies. Also other stategies aimed at dysregulated cholesterol regulation in cancer cells emerge as a possible avenue to combat the cancer.

Acknowledgements

Foremost, I would like to express my thanks to my two supervisors, Roberto Buccione and Gareth Jones, for leading me through my PhD studies ang giving me a valuable opportunity to be a part of T3Net network, where I met a lot of great scientists and new friends.

Many thanks go to all my colleagues, especially Francesca Attanasio, Mariagrazia Capestrano, Aurora Fusella, Rosanna Di Toro, Vinoth and Neelam Khandelwal, and of course Paolo Ciufici, for encouraging me and being good collaborators and even better friends. I thank Rosanna Tucci, too, to be a great support to our lab.

I would also like to thank my extended family in Italy, Cissi and Thomas Gardmo with their daughter Sara and Noelle Walsh-Wallis and her husband Mitch for their constant support. Many thanks goes also to Valeria and Paolo.

I want to thank my family, which has supports me on the distance and allows me to be what I am.

I owe a special thanks to Mimmo, who stands by me, in good times bad times.

References

Abram, C. L., Seals, D. F., Pass, I., Salinsky, D., Maurer, L., Roth, T. M. and Courtneidge, S. A. (2003). The adaptor protein fish associates with members of the ADAMs family and localizes to podosomes of Src-transformed cells. *J. Biol. Chem.* **278**, 16844–16851.

Aikawa, Y. and Martin, T. F. J. (2005). ADP-ribosylation factor 6 regulation of phosphatidylinositol-4,5-bisphosphate synthesis, endocytosis, and exocytosis. *Meth. Enzymol.* **404**, 422–431.

Al-Awar, O., Radhakrishna, H., Powell, N. N. and Donaldson, J. G. (2000). Separation of membrane trafficking and actin remodeling functions of ARF6 with an effector domain mutant. *Molecular and Cellular Biology* **20**, 5998–6007.

Albiges-Rizo, C., Destaing, O., Fourcade, B., Planus, E. and Block, M. R. (2009). Actin machinery and mechanosensitivity in invadopodia, podosomes and focal adhesions. *Journal of Cell Science* **122**, 3037–3049.

Alexander, N. R., Branch, K. M., Parekh, A., Clark, E. S., Iwueke, I. C., Guelcher, S. A. and Weaver, A. M. (2008). Extracellular Matrix Rigidity Promotes Invadopodia Activity. *Current Biology* **18**, 1295–1299.

Artym, V. V., Kindzelskii, A. L., Chen, W.-T. and Petty, H. R. (2002). Molecular proximity of seprase and the urokinase-type plasminogen activator receptor on malignant melanoma cell membranes: dependence on beta1 integrins and the cytoskeleton. *Carcinogenesis* **23**, 1593–1601.

Artym, V. V., Zhang, Y., Seillier-Moiseiwitsch, F., Yamada, K. M. and Mueller, S. C. (2006). Dynamic interactions of cortactin and membrane type 1 matrix metalloproteinase at invadopodia: defining the stages of invadopodia formation and

function. *Cancer Research* **66**, 3034–3043.

Artym, V. V., Matsumoto, K., Mueller, S. C. and Yamada, K. M. (2010). Dynamic membrane remodeling at invadopodia differentiates invadopodia from podosomes. *European Journal of Cell Biology* 1–9.

Attanasio, F., Caldieri, G., Giacchetti, G., van Horssen, R., Wieringa, B. and Buccione, R. (2011). Novel invadopodia components revealed by differential proteomic analysis. *European Journal of Cell Biology* **90**, 115–127.

Ayala, I., Baldassarre, M., Giacchetti, G., Caldieri, G., Tetè, S., Luini, A. and Buccione, R. (2008). Multiple regulatory inputs converge on cortactin to control invadopodia biogenesis and extracellular matrix degradation. *Journal of Cell Science* **121**, 369–378.

Ayala, I., Giacchetti, G., Caldieri, G., Attanasio, F., Mariggiò, S., Tetè, S., Polishchuk, R., Castronovo, V. and Buccione, R. (2009). Faciogenital dysplasia protein Fgd1 regulates invadopodia biogenesis and extracellular matrix degradation and is up-regulated in prostate and breast cancer. *Cancer Research* **69**, 747–752.

Badowski, C., Pawlak, G., Grichine, A., Chabadel, A., Oddou, C., Jurdic, P., Pfaff, M., Albiges-Rizo, C. and Block, M. R. (2008). Paxillin phosphorylation controls invadopodia/podosomes spatiotemporal organization. *Molecular Biology of the Cell* **19**, 633–645.

Bae, S. H. and Paik, Y. K. (1997). Cholesterol biosynthesis from lanosterol: development of a novel assay method and characterization of rat liver microsomal lanosterol delta 24-reductase. *Biochem. J.* **326 (Pt 2)**, 609–616.

Baldassarre, M., Pompeo, A., Beznoussenko, G., Castaldi, C., Cortellino, S., McNiven, M. A., Luini, A. and Buccione, R. (2003). Dynamin participates in focal extracellular matrix degradation by invasive cells. *Molecular Biology of the Cell* **14**, 1074–1084.

Baldassarre, M., Ayala, I., Beznoussenko, G., Giacchetti, G., Machesky, L. M., Luini, A. and Buccione, R. (2006). Actin dynamics at sites of extracellular matrix degradation. *European Journal of Cell Biology* **85**, 1217–1231.

Battista, M.-C., Guimond, M.-O., Roberge, C., Doueik, A. A., Fazli, L., Gleave, M., Sabbagh, R. and Gallo-Payet, N. (2010). Inhibition of DHCR24/seladin-1 impairs cellular homeostasis in prostate cancer. *Prostate* **70**, 921–933.

Beaty, B. T., Sharma, V. P., Bravo-Cordero, J. J., Simpson, M. A., Eddy, R. J., Koleske, A. J. and Condeelis, J. (2013). β1 integrin regulates Arg to promote invadopodial maturation and matrix degradation. *Molecular Biology of the Cell* **24**, 1661–75– S1–11.

Betzel, C., Saenger, W. and Hingerty, B. E. (1984). Topography of cyclodextrin inclusion complexes, part 20. Circular and flip-flop hydrogen bonding in. beta.-cyclodextrin undecahydrate: a neutron diffraction study. *Journal of the American ....*

Biscardi, J. S., Maa, M.-C., Tice, D. A., Cox, M. E., Leu, T.-H. and Parsons, S. J. (1999a). c-Src-mediated phosphorylation of the epidermal growth factor receptor on Tyr845 and Tyr1101 is associated with modulation of receptor function. *J. Biol. Chem.* **274**, 8335–8343.

Biscardi, J. S., Tice, D. A. and Parsons, S. J. (1999b). c-Src, receptor tyrosine kinases, and human cancer. *Adv. Cancer Res.* **76**, 61–119.

Bittman, R. (1997). Has nature designed the cholesterol side chain for optimal interaction with phospholipids? *Subcell. Biochem.* **28**, 145–171.

Boateng, L. R. and Huttenlocher, A. (2012). Spatiotemporal regulation of Src and its substrates at invadosomes. *European Journal of Cell Biology* **91**, 878–888.

Boivin, D., Labbé, D., Fontaine, N., Lamy, S., Beaulieu, E., Gingras, D. and Béliveau, R. (2009). The Stem Cell Marker CD133 (Prominin-1) is Phosphorylated on Cytoplasmic Tyrosine-828 and Tyrosine-852 by Src and Fyn Tyrosine Kinases.

Biochemistry **48**, 3998–4007.

Bonaccorsi, L., Luciani, P., Nesi, G., Mannucci, E., Deledda, C., Dichiara, F., Paglierani, M., Rosati, F., Masieri, L., Serni, S., et al. (2008). Androgen receptor regulation of the seladin-1/DHCR24 gene: altered expression in prostate cancer. *Lab. Invest.* **88**, 1049–1056.

Bowden, E. T., Barth, M., Thomas, D., Glazer, R. I. and Mueller, S. C. (1999). An invasion-related complex of cortactin, paxillin and PKCmu associates with invadopodia at sites of extracellular matrix degradation. *Oncogene* **18**, 4440–4449.

Bowden, E. T., Onikoyi, E., Slack, R., Myoui, A., Yoneda, T., Yamada, K. M. and Mueller, S. C. (2006). Co-localization of cortactin and phosphotyrosine identifies active invadopodia in human breast cancer cells. *Experimental Cell Research* **312**, 1240–1253.

Boyd, N. F., Rommens, J. M., Vogt, K., Lee, V., Hopper, J. L., Yaffe, M. J. and Paterson, A. D. (2005). Mammographic breast density as an intermediate phenotype for breast cancer. *Lancet Oncol.* **6**, 798–808.

Branch, K. M., Hoshino, D. and Weaver, A. M. (2012). Adhesion rings surround invadopodia and promote maturation. *Biol Open* **1**, 711–722.

Bravo-Cordero, J. J., Marrero-Diaz, R., Megías, D., Genís, L., García-Grande, A., García, M. A., Arroyo, A. G. and Montoya, M. C. (2007). MT1-MMP proinvasive activity is regulated by a novel Rab8-dependent exocytic pathway. *EMBO J.* **26**, 1499–1510.

Bravo-Cordero, J. J., Oser, M., Chen, X., Eddy, R., Hodgson, L. and Condeelis, J. (2011). A novel spatiotemporal RhoC activation pathway locally regulates cofilin activity at invadopodia. *Curr. Biol.* **21**, 635–644.

Brdicka, T., Pavlistova, D., Leo, A., Bruyns, E., Korinek, V., Angelisova, P., Scherer, J., Shevchenko, A., Shevchenko, A. and Hilgert, I. (2000).

Phosphoprotein associated with glycosphingolipid-enriched microdomains (PAG), a novel ubiquitously expressed transmembrane adaptor protein, binds the protein tyrosine kinase csk and is involved in regulation of T cell activation. *J. Exp. Med.* **191**, 1591–1604.

Brdickova, N., Brdicka, T., Anděra, L., Spicka, J., Angelisova, P., Milgram, S. L. and Hořejší, V. (2001). Interaction between two adapter proteins, PAG and EBP50: a possible link between membrane rafts and actin cytoskeleton. *FEBS Lett.* **507**, 133–136.

Brdickova, N., Brdicka, T., Angelisova, P., Horvath, O., Spicka, J., Hilgert, I., Paces, J., Simeoni, L., Kliche, S., Merten, C., et al. (2003). LIME: A New Membrane Raft-associated Adaptor Protein Involved in CD4 and CD8 Coreceptor Signaling. *Journal of Experimental Medicine* **198**, 1453–1462.

Brisson, L., Reshkin, S. J., Goré, J. and Roger, S. (2012). pH regulators in invadosomal functioning: Proton delivery for matrix tasting. *European Journal of Cell Biology.*

Brown, A. J. (2009). 24(S),25-Epoxycholesterol: A messenger for cholesterol homeostasis. *Int. J. Biochem. Cell Biol.* **41**, 744–747.

Brown, A. J. and Jessup, W. (2009). Oxysterols: Sources, cellular storage and metabolism, and new insights into their roles in cholesterol homeostasis. *Molecular Aspects of Medicine* **30**, 111–122.

Brown, M. S. and Goldstein, J. L. (1980). Multivalent feedback regulation of HMG CoA reductase, a control mechanism coordinating isoprenoid synthesis and cell growth. *J. Lipid Res.* **21**, 505–517.

Buschman, M. D., Bromann, P. A., Cejudo-Martin, P., Wen, F., Pass, I. and Courtneidge, S. A. (2009). The novel adaptor protein Tks4 (SH3PXD2B) is required for functional podosome formation. *Molecular Biology of the Cell* **20**, 1302–1311.

Busco, G., Cardone, R. A., Greco, M. R., Bellizzi, A., Colella, M., Antelmi, E., Mancini, M. T., Dell'Aquila, M. E., Casavola, V., Paradiso, A., et al. (2010). NHE1 promotes invadopodial ECM proteolysis through acidification of the peri-invadopodial space. *The FASEB Journal* **24**, 3903–3915.

Byfield, F.J., Aranda-Espinoza, H., Romanenko, V.G., Rothblat, G.H., Levitan, I., 2004. Cholesterol depletion increases membrane stiffness of aortic endothelial cells. Biophysical Journal 87, 3336–3343.

Caldieri, G., Giacchetti, G., Beznoussenko, G., Attanasio, F., Ayala, I. and Buccione, R. (2009). Invadopodia biogenesis is regulated by caveolin-mediated modulation of membrane cholesterol levels. *Journal of Cellular and Molecular Medicine* **13**, 1728–1740.

Caldieri, G., Capestrano, M., Bicanova, K., Beznoussenko, G., Baldassarre, M. and Buccione, R. (2012). Polarised apical-like intracellular sorting and trafficking regulates invadopodia formation and degradation of the extracellular matrix in cancer cells. *European Journal of Cell Biology.*

Corbeil, D., Röper, K., Hellwig, A., Tavian, M., Miraglia, S., Watt, S. M., Simmons, P. J., Peault, B., Buck, D. W. and Huttner, W. B. (2000). The human AC133 hematopoietic stem cell antigen is also expressed in epithelial cells and targeted to plasma membrane protrusions. *J. Biol. Chem.* **275**, 5512–5520.

Cao, J., Rehemtulla, A., Bahou, W. and Zucker, S. (1996). Membrane type matrix metalloproteinase 1 activates pro-gelatinase A without furin cleavage of the N-terminal domain. *J. Biol. Chem.* **271**, 30174–30180.

Cao, H. (2002). A Phosphotyrosine-dependent Protein Interaction Screen Reveals a Role for Phosphorylation of Caveolin-1 on Tyrosine 14. RECRUITMENT OF C-TERMINAL Src KINASE. *Journal of Biological Chemistry* **277**, 8771–8774.

Chander, H., Truesdell, P., Meens, J. and Craig, A. W. B. (2012). Transducer of

Cdc42-dependent actin assembly promotes breast cancer invasion and metastasis. *Oncogene* **32**, 3080–3090.

Chen, W. T. (1989). Proteolytic activity of specialized surface protrusions formed at rosette contact sites of transformed cells. *J. Exp. Zool.* **251**, 167–185.

Chen, Y., Fulford, M.H., 2001. Human prostate cancer cells lack feedback regulation of low-density lipoprotein receptor and its regulator, SREBP2. Int. J. Cancer.

Chuang, Y.-Y., Tran, N. L., Rusk, N., Nakada, M., Berens, M. E. and Symons, M. (2004). Role of synaptojanin 2 in glioma cell migration and invasion. *Cancer Research* **64**, 8271–8275.

Colicelli, J. (2010). ABL tyrosine kinases: evolution of function, regulation, and specificity. *Science Signaling* **3**, re6.

Cortesio, C. L., Chan, K. T., Perrin, B. J., Burton, N. O., Zhang, S., Zhang, Z. Y. and Huttenlocher, A. (2008). Calpain 2 and PTP1B function in a novel pathway with Src to regulate invadopodia dynamics and breast cancer cell invasion. *The Journal of Cell Biology* **180**, 957–971.

Courtneidge, S. A. (2012). Cell migration and invasion in human disease: the Tks adaptor proteins. *Biochem. Soc. Trans.* **40**, 129–132.

Deakin, N. O. and Turner, C. E. (2008). Paxillin comes of age. *Journal of Cell Science* **121**, 2435–2444.

DeGrella, R. F. and Simoni, R. D. (1982). Intracellular transport of cholesterol to the plasma membrane. *J. Biol. Chem.* **257**, 14256–14262.

Deryugina, E. I., Ratnikov, B. I., Postnova, T. I., Rozanov, D. V. and Strongin, A. Y. (2002). Processing of integrin alpha(v) subunit by membrane type 1 matrix metalloproteinase stimulates migration of breast carcinoma cells on vitronectin and

enhances tyrosine phosphorylation of focal adhesion kinase. *J. Biol. Chem.* **277**, 9749–9756.

Destaing, O., Block, M. R., Planus, E. and Albiges-Rizo, C. (2011). Invadosome regulation by adhesion signaling. *Current Opinion in Cell Biology* 1–10.

Diaz, B., Shani, G., PASS, I., Anderson, D., Quintavalle, M. and Courtneidge, S. A. (2009). Tks5-Dependent, Nox-Mediated Generation of Reactive Oxygen Species Is Necessary for Invadopodia Formation. *Science Signaling* **2**, ra53–ra53.

Díaz, B., Yuen, A., Iizuka, S., Higashiyama, S. and Courtneidge, S. A. (2013). Notch increases the shedding of HB-EGF by ADAM12 to potentiate invadopodia formation in hypoxia. *The Journal of Cell Biology* **201**, 279–292.

Donaldson, J. G. (2003). Multiple roles for Arf6: sorting, structuring, and signaling at the plasma membrane. *J. Biol. Chem.* **278**, 41573–41576.

Donaldson, J. G. (2009). Phospholipase D in endocytosis and endosomal recycling pathways. *Biochim Biophys Acta* **1791**, 845–849.

Eckert, M. A., Lwin, T. M., Chang, A. T., Kim, J., Danis, E., Ohno-Machado, L. and Yang, J. (2011). Twist1-induced invadopodia formation promotes tumor metastasis. *Cancer Cell* **19**, 372–386.

Egeblad, M. and Werb, Z. (2002). New functions for the matrix metalloproteinases in cancer progression. *Nat Rev Cancer* **2**, 161–174.

Eyster, C. A., Higginson, J. D., Huebner, R., Porat-Shliom, N., Weigert, R., Wu, W. W., Shen, R.-F. and Donaldson, J. G. (2009). Discovery of New Cargo Proteins that Enter Cells through Clathrin-Independent Endocytosis. *Traffic* **10**, 590–599.

Flick, E.D., Habel, L.A., Chan, K.A., Van Den Eeden, S.K., Quinn, V.P., Haque, R., Orav, E.J., Seeger, J.D., Sadler, M.C., Quesenberry, C.P., Sternfeld, B., Jacobsen, S.J., Whitmer, R.A., Caan, B.J., 2007. Statin use and risk of prostate cancer in the California Men's Health Study cohort. Cancer Epidemiol. Biomarkers

Prev. 16, 2218–2225.

Florek, M., Bauer, N., Janich, P., Wilsch-Braeuninger, M., Fargeas, C. A., Marzesco, A.-M., Ehninger, G., Thiele, C., Huttner, W. B. and Corbeil, D. (2006). Prominin-2 is a cholesterol-binding protein associated with apical and basolateral plasmalemmal protrusions in polarized epithelial cells and released into urine. *Cell Tissue Res* **328**, 31–47.

Frittoli, E., Palamidessi, A., Disanza, A. and Scita, G. (2010). Secretory and endo/exocytic trafficking in invadopodia formation: The MT1-MMP paradigm. *European Journal of Cell Biology* 1–7.

Gaylor, J. L. (2002). Membrane-bound enzymes of cholesterol synthesis from lanosterol. *Biochemical and Biophysical Research Communications* **292**, 1139–1146.

Gelissen, I. C. and Brown, A. J. (2011). Drug targets beyond HMG-CoA reductase: Why venture beyond the statins? *Frontiers in Biology* **6**, 197–205.

Gelissen, I. C., Harris, M., Rye, K.-A., Quinn, C., Brown, A. J., Kockx, M., Cartland, S., Packianathan, M., Kritharides, L. and Jessup, W. (2006). ABCA1 and ABCG1 synergize to mediate cholesterol export to apoA-I. *Arterioscler. Thromb. Vasc. Biol.* **26**, 534–540.

Geybels, M.S., Wright, J.L., Holt, S.K., Kolb, S., Feng, Z., Stanford, J.L., 2013. Statin Use in Relation to Prostate Cancer Outcomes in a Population-based Patient Cohort Study. Prostate 73, 1214–1222.

Giannoni, E., Taddei, M. L. and Chiarugi, P. (2010). Src redox regulation: Again in the front line. *Free Radical Biology and Medicine* **49**, 516–527.

Gimona, M., Buccione, R., Courtneidge, S. A. and Linder, S. (2008). Assembly and biological role of podosomes and invadopodia. *Current Opinion in Cell Biology* **20**,

235–241.

Gligorijevic, B., Wyckoff, J., Yamaguchi, H., Wang, Y., Roussos, E. T. and Condeelis, J. (2012). N-WASP-mediated invadopodium formation is involved in intravasation and lung metastasis of mammary tumors. *Journal of Cell Science* **125**, 724–734.

Goetz, J. G. (2009). Bidirectional control of the inner dynamics of focal adhesions promotes cell migration. *Cell Adh Migr* **3**, 185–190.

Goley, E. D., Rodenbusch, S. E., Martin, A. C. and Welch, M. D. (2004). Critical conformational changes in the Arp2/3 complex are induced by nucleotide and nucleation promoting factor. *Molecular Cell* **16**, 269–279.

Golub, T. and Caroni, P. (2005). PI (4, 5) P2-dependent microdomain assemblies capture microtubules to promote and control leading edge motility. *The Journal of Cell Biology* **169**, 151–165.

Graf, G. A., Yu, L., Li, W.-P., Gerard, R., Tuma, P. L., Cohen, J. C. and Hobbs, H. H. (2003). ABCG5 and ABCG8 are obligate heterodimers for protein trafficking and biliary cholesterol excretion. *J. Biol. Chem.* **278**, 48275–48282.

Grant, B. D. and Donaldson, J. G. (2009). Pathways and mechanisms of endocytic recycling. *Nat Rev Mol Cell Biol* **10**, 597–608.

Grass, G. D., Bratoeva, M. and Toole, B. P. (2012). Regulation of invadopodia formation and activity by CD147. *Journal of Cell Science* **125**, 777–788.

Greeve, I., Hermans-Borgmeyer, I., Brellinger, C., Kasper, D., Gomez-Isla, T., Behl, C., Levkau, B. and Nitsch, R. M. (2000). The human DIMINUTO/DWARF1 homolog seladin-1 confers resistance to Alzheimer's disease-associated neurodegeneration and oxidative stress. *The Journal of Neuroscience* **20**, 7345–7352.

Gulyani, A., Vitriol, E., Allen, R., Wu, J., Gremyachinskiy, D., Lewis, S., Dewar, B.,

Graves, L. M., Kay, B. K., Kuhlman, B., et al. (2011). A biosensor generated via high-throughput screening quantifies cell edge Src dynamics. *Nat Chem Biol* **7**, 437–444.

Hao, M., Lin, S. X., Karylowski, O. J., Wüstner, D., McGraw, T. E. and Maxfield, F. R. (2002). Vesicular and non-vesicular sterol transport in living cells. The endocytic recycling compartment is a major sterol storage organelle. *J. Biol. Chem.* **277**, 609–617.

Hanahan, D. and Weinberg, R. A. (2011). Hallmarks of cancer: the next generation. *Cell* **144**, 646–674.

Hanna, S. C., Krishnan, B., Bailey, S. T., Moschos, S. J., Kuan, P.-F., Shimamura, T., Osborne, L. D., Siegel, M. B., Duncan, L. M., O'Brien, E. T., et al. (2013). HIF1α and HIF2α independently activate SRC to promote melanoma metastases. *J. Clin. Invest.* **123**, 2078–2093.

Hashimoto, S., Onodera, Y., Hashimoto, A., Tanaka, M., Hamaguchi, M., Yamada, A. and Sabe, H. (2004). Requirement for Arf6 in breast cancer invasive activities. *Proc. Natl. Acad. Sci. U.S.A.* **101**, 6647–6652.

Hauck, C. R., Hsia, D. A., Ilic, D. and Schlaepfer, D. D. (2002). v-Src SH3-enhanced interaction with focal adhesion kinase at beta 1 integrin-containing invadopodia promotes cell invasion. *J. Biol. Chem.* **277**, 12487–12490.

Hayes, K. E., Walk, E. L., Ammer, A. G., Kelley, L. C., Martin, K. H. and Weed, S. A. (2012). Ableson kinases negatively regulate invadopodia function and invasion in head and neck squamous cell carcinoma by inhibiting an HB-EGF autocrine loop. *Oncogene*.

Hendriksen, P. J. M., Dits, N. F. J., Kokame, K., Veldhoven, A., van Weerden, W. M., Bangma, C. H., Trapman, J. and Jenster, G. (2006). Evolution of the androgen receptor pathway during progression of prostate cancer. *Cancer Research* **66**, 5012–5020.

Hentosh, P., Yuh, S.H., Elson, C.E., 2001. Sterol-independent regulation of 3-hydroxy-3-methylglutaryl coenzyme A reductase in tumor cells. Molecular ....

Hindler, K., Cleeland, C. S., Rivera, E. and Collard, C. D. (2006). The role of statins in cancer therapy. *Oncologist* **11**, 306–315.

Hiroyama, M. and Exton, J. H. (2005). Localization and regulation of phospholipase D2 by ARF6. *J. Cell. Biochem.* **95**, 149–164.

Holmbeck, K., Bianco, P., Yamada, S. and Birkedal-Hansen, H. (2004). MT1-MMP: a tethered collagenase. *J. Cell. Physiol.* **200**, 11–19.

Honda, A., Nogami, M., Yokozeki, T., Yamazaki, M., Nakamura, H., Watanabe, H., Kawamoto, K., Nakayama, K., Morris, A. J., Frohman, M. A., et al. (1999). Phosphatidylinositol 4-phosphate 5-kinase alpha is a downstream effector of the small G protein ARF6 in membrane ruffle formation. *Cell* **99**, 521–532.

Hoshino, D., Branch, K. M. and Weaver, A. M. (2013). Signaling inputs to invadopodia and podosomes. *Journal of Cell Science* **126**, 2979–2989.

Hoshino, D., Jourquin, J., Emmons, S. W., Miller, T., Goldgof, M., Costello, K., Tyson, D. R., Brown, B., Lu, Y., Prasad, N. K., et al. (2012). Network analysis of the focal adhesion to invadopodia transition identifies a PI3K-PKCα invasive signaling axis. *Science Signaling* **5**, ra66.

Howell, B. W. and Cooper, J. A. (1994). Csk suppression of Src involves movement of Csk to sites of Src activity. *Molecular and Cellular Biology* **14**, 5402–5411.

Hu, J., Mukhopadhyay, A., Truesdell, P., Chander, H., Mukhopadhyay, U. K., Mak, A. S. and Craig, A. W. B. (2011). Cdc42-interacting protein 4 is a Src substrate that regulates invadopodia and invasiveness of breast tumors by promoting MT1-MMP endocytosis. *Journal of Cell Science* **124**, 1739–1751.

Hu, J., La Vecchia, C., de Groh, M., Negri, E., Morrison, H., Mery, L., Canadian Cancer Registries Epidemiology Research Group, 2012. Dietary cholesterol intake and cancer. Annals of Oncology 23, 491–500.

Im, Y. J., Raychaudhuri, S., Prinz, W. A. and Hurley, J. H. (2005). Structural mechanism for sterol sensing and transport by OSBP-related proteins. *Nature* **437**, 154–158.

Ingley, E. (2008). Src family kinases: Regulation of their activities, levels and identification of new pathways. *Biochimica et Biophysica Acta (BBA) - Proteins & Proteomics* **1784**, 56–65.

Ingley, E. (2009). Csk-binding protein can regulate Lyn signals controlling cell morphology. *Int. J. Biochem. Cell Biol.* **41**, 1332–1343.

Itoh, K., Sakakibara, M., Yamasaki, S., Takeuchi, A., Arase, H., Miyazaki, M., Nakajima, N., Okada, M. and Saito, T. (2002). Cutting edge: negative regulation of immune synapse formation by anchoring lipid raft to cytoskeleton through Cbp-EBP50-ERM assembly. *J. Immunol.* **168**, 541–544.

Jacob, A., Jing, J., Lee, J., Schedin, P., Gilbert, S. M., Peden, A. A., Junutula, J. R. and Prekeris, R. (2013). Rab40b regulates MMP2 and MMP9 trafficking during invadopodia formation and breast cancer cell invasion. *Journal of Cell Science*.

Jacobs, E.J., Rodriguez, C., Bain, E.B., Wang, Y., Thun, M.J., Calle, E.E., 2007. Cholesterol-lowering drugs and advanced prostate cancer incidence in a large U.S. cohort. Cancer Epidemiol. Biomarkers Prev. 16, 2213–2217.

Jin, H., Garmy-Susini, B., Avraamides, C. J., Stoletov, K., Klemke, R. L. and Varner, J. A. (2010). A PKA-Csk-pp60Src signaling pathway regulates the switch between endothelial cell invasion and cell-cell adhesion during vascular sprouting. *Blood* **116**, 5773–5783.

Kaiser, H.-J., Lingwood, D., Levental, I., Sampaio, J.L., Kalvodova, L., Rajendran, L., Simons, K., 2009. Order of lipid phases in model and plasma membranes. Proc. Natl. Acad. Sci. U.S.A. 106, 16645–16650.

Kamai, T., Shirataki, H., Nakanishi, K., Furuya, N., Kambara, T., Abe, H., Oyama, T. and Yoshida, K.-I. (2010). Increased Rac1 activity and Pak1 overexpression are associated with lymphovascular invasion and lymph node metastasis of upper urinary tract cancer. *BMC Cancer* **10**, 164.

Kandutsch, A., Chen, H. and Heiniger, H. (1978). Biological activity of some oxygenated sterols. *Science* **201**, 498–501.

Kean, M. J., Williams, K. C., Skalski, M., Myers, D., Burtnik, A., Foster, D. and Coppolino, M. G. (2009). VAMP3, syntaxin-13 and SNAP23 are involved in secretion of matrix metalloproteinases, degradation of the extracellular matrix and cell invasion. *Journal of Cell Science* **122**, 4089–4098.

Kawabuchi, M., Satomi, Y., Takao, T., Shimonishi, Y., Nada, S., Nagai, K., Tarakhovsky, A. and Okada, M. (2000). Transmembrane phosphoprotein Cbp regulates the activities of Src-family tyrosine kinases. *Nature* **404**, 999–1003.

Kelly, T., Mueller, S. C., Yeh, Y. and Chen, W. T. (1994). Invadopodia promote proteolysis of a wide variety of extracellular matrix proteins. *J. Cell. Physiol.* **158**, 299–308.

Klein, A.S., Schaefer, M., Korte, T., Herrmann, A., Tannert, A., 2012. HaCaT keratinocytes exhibit a cholesterol and plasma membrane viscosity gradient during directed migration. Experimental Cell Research 318, 809–818.

Kolch, W. (2005). Coordinating ERK/MAPK signalling through scaffolds and inhibitors. *Nat Rev Mol Cell Biol* **6**, 827–837.

Kwon, H. J., Abi-Mosleh, L., Wang, M. L., Deisenhofer, J., Goldstein, J. L., Brown, M. S. and Infante, R. E. (2009). Structure of N-terminal domain of NPC1 reveals distinct subdomains for binding and transfer of cholesterol. *Cell* **137**, 1213–1224.

Krycer, J.R., Brown, A.J., 2013. Cholesterol accumulation in prostate cancer: A classic observation from a modern perspective. Biochimica et Biophysica Acta (BBA) - Reviews on Cancer 1835, 219–229.

Levental, I., Grzybek, M., Simons, K., 2010. Greasing their way: lipid modifications determine protein association with membrane rafts. Biochemistry 49, 6305–6316.

Li, Q., Mullins, S. R., Sloane, B. F. and Mattingly, R. R. (2008). p21-Activated kinase 1 coordinates aberrant cell survival and pericellular proteolysis in a three-dimensional culture model for premalignant progression of human breast cancer. *Neoplasia* **10**, 314–329.

Li, Y.C., Park, M.J., Ye, S.-K., Kim, C.-W., Kim, Y.-N., 2006. Elevated levels of cholesterol-rich lipid rafts in cancer cells are correlated with apoptosis sensitivity induced by cholesterol-depleting agents. The American Journal of Pathology 168, 1107–18– quiz 1404–5.

Lim, L., Manser, E., Leung, T. and Hall, C. (1996). Regulation of phosphorylation pathways by p21 GTPases. The p21 Ras-related Rho subfamily and its role in phosphorylation signalling pathways. *Eur. J. Biochem.* **242**, 171–185.

Linder, S. (2009). Invadosomes at a glance. *Journal of Cell Science* **122**, 3009–3013.

Linder, S. (2007). The matrix corroded: podosomes and invadopodia in extracellular matrix degradation. *Trends in Cell Biology* **17**, 107–117.

Lingwood, D., Simons, K., 2009. Lipid Rafts As a Membrane-Organizing Principle. Science 327, 46–50.

Lizarraga, F., Poincloux, R., Romao, M., Montagnac, G., Le Dez, G., Bonne, I., Rigaill, G., Raposo, G. and Chavrier, P. (2009). Diaphanous-related formins are required for invadopodia formation and invasion of breast tumor cells. *Cancer Research* **69**, 2792–2800.

Lowry, W. E., Huang, J., Ma, Y.-C., Ali, S., Wang, D., Williams, D. M., Okada, M., Cole, P. A. and Huang, X.-Y. (2002). Csk, a critical link of g protein signals to actin cytoskeletal reorganization. *Developmental Cell* **2**, 733–744

Lu, W., Qu, J.-J., Li, B.-L., Lu, C., Yan, Q., Wu, X.-M., Chen, X.-Y. and Wan, X.-P. (2013). Overexpression of p21-activated kinase 1 promotes endometrial cancer progression. *Oncol. Rep.* **29**, 1547–1555.

Lutjohann, D. (2002). Profile of cholesterol-related sterols in aged amyloid precursor protein transgenic mouse brain. *The Journal of Lipid Research* **43**, 1078–1085.

Maxfield, F. R. and Wüstner, D. (2002). Intracellular cholesterol transport. *J. Clin. Invest.* **110**, 891–898.

Macheda, M. L., Rogers, S. and Best, J. D. (2005). Molecular and cellular regulation of glucose transporter (GLUT) proteins in cancer. *J. Cell. Physiol.* **202**, 654–662.

Mader, C. C., Oser, M., Magalhaes, M. A. O., Bravo-Cordero, J. J., Condeelis, J., Koleske, A. J. and Gil-Henn, H. (2011). An EGFR-Src-Arg-cortactin pathway mediates functional maturation of invadopodia and breast cancer cell invasion. *Cancer Research* **71**, 1730–1741.

Magalhaes, M. A. O., Larson, D. R., Mader, C. C., Bravo-Cordero, J. J., Gil-Henn, H., Oser, M., Chen, X., Koleske, A. J. and Condeelis, J. (2011). Cortactin phosphorylation regulates cell invasion through a pH-dependent pathway. *The Journal of Cell Biology* **195**, 903–920.

Mak, V. C. Y., Lee, L., Siu, M. K. Y., Wong, O. G. W., Lu, X., Ngan, H. Y. S.,

Wong, E. S. Y. and Cheung, A. N. Y. (2013). Downregulation of ASPP2 in choriocarcinoma contributes to increased migratory potential through Src signaling pathway activation. *Carcinogenesis* **34**, 2170–2177.

Martin, A., Brown, F. D., Hodgkin, M. N., Bradwell, A. J., Cook, S. J., Hart, M. and Wakelam, M. J. (1996). Activation of phospholipase D and phosphatidylinositol 4-phosphate 5-kinase in HL60 membranes is mediated by endogenous Arf but not Rho. *J. Biol. Chem.* **271**, 17397–17403.

Monovich, L., Mugrage, B., Quadros, E., Toscano, K., Tommasi, R., LaVoie, S., Liu, E., Du, Z., LaSala, D., Boyar, W., et al. (2007). Optimization of halopemide for phospholipase D2 inhibition. *Bioorg. Med. Chem. Lett.* **17**, 2310–2311.

Moon, H., Hill, M.M., Roberts, M.J., Gardiner, R.A., Brown, A.J., 2014. Statins: protectors or pretenders in prostate cancer? Trends in Endocrinology & Metabolism 25, 188–196.

Morishige, M., Hashimoto, S., Ogawa, E., Toda, Y., Kotani, H., Hirose, M., Wei, S., Hashimoto, A., Yamada, A., Yano, H., et al. (2008). GEP100 links epidermal growth factor receptor signalling to Arf6 activation to induce breast cancer invasion. *Nature Cell Biology* **10**, 85–92.

Matsuoka, H. (2003). Mechanism of Csk-mediated Down-regulation of Src Family Tyrosine Kinases in Epidermal Growth Factor Signaling. *J. Biol. Chem.* **279**, 5975–5983.

Mazzone, M., Baldassarre, M., Beznoussenko, G., Giacchetti, G., Cao, J., Zucker, S., Luini, A. and Buccione, R. (2004). Intracellular processing and activation of membrane type 1 matrix metalloprotease depends on its partitioning into lipid domains. *Journal of Cell Science* **117**, 6275–6287.

Mercier, I., Jasmin, J.-F., Pavlides, S., Minetti, C., Flomenberg, N., Pestell, R. G., Frank, P. G., Sotgia, F. and Lisanti, M. P. (2009). Clinical and translational

implications of the caveolin gene family: lessons from mouse models and human genetic disorders. *Lab. Invest.* **89**, 614–623.

Monovich, L., Mugrage, B., Quadros, E., Toscano, K., Tommasi, R., LaVoie, S., Liu, E., Du, Z., LaSala, D., Boyar, W., et al. (2007). Optimization of halopemide for phospholipase D2 inhibition. *Bioorg. Med. Chem. Lett.* **17**, 2310–2311.

Monsky, W. L., Kelly, T., Lin, C. Y., Yeh, Y., Stetler-Stevenson, W. G., Mueller, S. C. and Chen, W. T. (1993). Binding and localization of M(r) 72,000 matrix metalloproteinase at cell surface invadopodia. *Cancer Research* **53**, 3159–3164.

Monsky, W. L., Lin, C. Y., Aoyama, A., Kelly, T., Akiyama, S. K., Mueller, S. C. and Chen, W. T. (1994). A potential marker protease of invasiveness, seprase, is localized on invadopodia of human malignant melanoma cells. *Cancer Research* **54**, 5702–5710.

Morishige, M., Hashimoto, S., Ogawa, E., Toda, Y., Kotani, H., Hirose, M., Wei, S., Hashimoto, A., Yamada, A., Yano, H., et al. (2008). GEP100 links epidermal growth factor receptor signalling to Arf6 activation to induce breast cancer invasion. *Nature Cell Biology* **10**, 85–92.

Mouritsen, O. G. and Zuckermann, M. J. (2004). What's so special about cholesterol? *Lipids* **39**, 1101–1113.

Möbius, W., van Donselaar, E., Ohno-Iwashita, Y., Shimada, Y., Heijnen, H. F. G., Slot, J. W. and Geuze, H. J. (2003). Recycling compartments and the internal vesicles of multivesicular bodies harbor most of the cholesterol found in the endocytic pathway. *Traffic* **4**, 222–231.

Mueller, S. C., Ghersi, G., Akiyama, S. K., Sang, Q. X., Howard, L., Pineiro-Sanchez, M., Nakahara, H., Yeh, Y. and Chen, W. T. (1999). A novel protease-docking function of integrin at invadopodia. *J. Biol. Chem.* **274**, 24947–24952.

Mueller, S. C., Yeh, Y. and Chen, W. T. (1992). Tyrosine phosphorylation of

membrane proteins mediates cellular invasion by transformed cells. *The Journal of Cell Biology* **119**, 1309–1325.

Nakagawa, T., Tanaka, S., Suzuki, H., Takayanagi, H., Miyazaki, T., Nakamura, K. and Tsuruo, T. (2000). Overexpression of the csk gene suppresses tumor metastasis in vivo. *Int. J. Cancer* **88**, 384–391.

Nakahara, H., Mueller, S. C., Nomizu, M., Yamada, Y., Yeh, Y. and Chen, W. T. (1998). Activation of beta1 integrin signaling stimulates tyrosine phosphorylation of p190RhoGAP and membrane-protrusive activities at invadopodia. *J. Biol. Chem.* **273**, 9–12.

Nakahara, H., Nomizu, M., Akiyama, S. K., Yamada, Y., Yeh, Y. and Chen, W. T. (1996). A mechanism for regulation of melanoma invasion. Ligation of alpha6beta1 integrin by laminin G peptides. *J. Biol. Chem.* **271**, 27221–27224.

Nakahara, H., Otani, T., Sasaki, T., Miura, Y., Takai, Y. and Kogo, M. (2003). Involvement of Cdc42 and Rac small G proteins in invadopodia formation of RPMI7951 cells. *Genes to Cells* **8**, 1019–1027.

Naslavsky, N., Weigert, R. and Donaldson, J. G. (2004). Characterization of a nonclathrin endocytic pathway: membrane cargo and lipid requirements. *Molecular Biology of the Cell* **15**, 3542–3552.

NIPPER, M., MAJD, S., MAYER, M., LEE, J., THEODORAKIS, E., HAIDEKKER, M., 2008. Characterization of changes in the viscosity of lipid membranes with the molecular rotor FCVJ. Biochimica et Biophysica Acta (BBA) - Biomembranes 1778, 1148–1153.

Novak, A., Binnington, B., Ngan, B., Chadwick, K., Fleshner, N., Lingwood, C.A., 2013. Cholesterol masks membrane glycosphingolipid tumor-associated antigens to reduce their immunodetection in human cancer biopsies. Glycobiology 23, 1230–1239.

Oh, H.Y., Leem, J., Yoon, S.J., Yoon, S., Hong, S.J., 2010. Lipid raft cholesterol and genistein inhibit the cell viability of prostate cancer cells via the partial contribution of EGFR-Akt/p70S6k pathway and down-regulation of androgen receptor. Biochemical and Biophysical Research Communications 393, 319–324.

Ohvo-Rekilä, H., Ramstedt, B., Leppimäki, P. and Slotte, J. P. (2002). Cholesterol interactions with phospholipids in membranes. *Progress in Lipid Research* **41**, 66–97.

Oikawa, T., Itoh, T. and Takenawa, T. (2008). Sequential signals toward podosome formation in NIH-src cells. *The Journal of Cell Biology* **182**, 157–169.

Okada, M. (2012). Regulation of the SRC family kinases by Csk. *Int. J. Biol. Sci.* **8**, 1385–1397.

Oneyama, C., Hikita, T., Enya, K., Dobenecker, M.-W., Saito, K., Nada, S., Tarakhovsky, A. and Okada, M. (2008). The lipid raft-anchored adaptor protein Cbp controls the oncogenic potential of c-Src. *Molecular Cell* **30**, 426–436.

Oneyama, C., Iino, T., Saito, K., Suzuki, K., Ogawa, A. and Okada, M. (2009). Transforming Potential of Src Family Kinases Is Limited by the Cholesterol-Enriched Membrane Microdomain. *Molecular and Cellular Biology* **29**, 6462–6472.

Oser, M., Yamaguchi, H., Mader, C. C., Bravo-Cordero, J. J., Arias, M., Chen, X., Desmarais, V., van Rheenen, J., Koleske, A. J. and Condeelis, J. (2009). Cortactin regulates cofilin and N-WASp activities to control the stages of invadopodium assembly and maturation. *The Journal of Cell Biology* **186**, 571–587.

Otáhal, P., Pata, S., Angelisová, P., Hořejší, V. and Brdička, T. (2011). The effects of membrane compartmentalization of csk on TCR signaling. *BBA - Molecular Cell Research* **1813**, 367–376.

Parton, R. G., Hanzal-Bayer, M. and Hancock, J. F. (2006). Biogenesis of caveolae: a structural model for caveolin-induced domain formation. *Journal of Cell Science* **119**, 787–796.

Pelton, K., Freeman, M.R., Solomon, K.R., 2012. Cholesterol and prostate cancer. Curr Opin Pharmacol 12, 751–759.

Pichot, C. S., Arvanitis, C., Hartig, S. M., Jensen, S. A., Bechill, J., Marzouk, S., Yu, J., Frost, J. A. and Corey, S. J. (2010). Cdc42-Interacting Protein 4 Promotes Breast Cancer Cell Invasion and Formation of Invadopodia through Activation of N-WASp. *Cancer Research* **70**, 8347–8356.

Pignatelli, J., Tumbarello, D. A., Schmidt, R. P. and Turner, C. E. (2012). Hic-5 promotes invadopodia formation and invasion during TGF- -induced epithelial-mesenchymal transition. *The Journal of Cell Biology* **197**, 421–437.

Poincloux, R., Lizarraga, F. and Chavrier, P. (2009). Matrix invasion by tumour cells: a focus on MT1-MMP trafficking to invadopodia. *Journal of Cell Science* **122**, 3015–3024.

Radhakrishna, H. and Donaldson, J. G. (1997). ADP-ribosylation factor 6 regulates a novel plasma membrane recycling pathway. *The Journal of Cell Biology* **139**, 49–61.

Rengifo-Cam, W., Konishi, A., Morishita, N., Matsuoka, H., Yamori, T., Nada, S. and Okada, M. (2013). Csk defines the ability of integrin-mediated cell adhesion and migration in human colon cancer cells: implication for a potential role in cancer metastasis. *Oncogene* **23**, 289–297.

Ricono, J. M., Huang, M., Barnes, L. A., Lau, S. K., Weis, S. M., Schlaepfer, D. D., Hanks, S. K. and Cheresh, D. A. (2009). Specific cross-talk between epidermal growth factor receptor and integrin alphavbeta5 promotes carcinoma cell invasion and metastasis. *Cancer Research* **69**, 1383–1391.

Remacle, A., Murphy, G. and Roghi, C. (2003). Membrane type I-matrix metalloproteinase (MT1-MMP) is internalised by two different pathways and is recycled to the cell surface. *Journal of Cell Science* **116**, 3905–3916.

Resh, M. D. (1999). Fatty acylation of proteins: new insights into membrane targeting of myristoylated and palmitoylated proteins. *Biochim Biophys Acta* **1451**, 1–16.

Roh-Johnson, M., Bravo-Cordero, J. J., Patsialou, A., Sharma, V. P., Guo, P., Liu, H., Hodgson, L. and Condeelis, J. (2013). Macrophage contact induces RhoA GTPase signaling to trigger tumor cell intravasation. *Oncogene*.

Rohatgi, R., Ho, H. Y. and Kirschner, M. W. (2000). Mechanism of N-WASP activation by CDC42 and phosphatidylinositol 4, 5-bisphosphate. *The Journal of Cell Biology* **150**, 1299–1310.

Rohatgi, R., Ma, L., Miki, H., Lopez, M., Kirchhausen, T., Takenawa, T. and Kirschner, M. W. (1999). The interaction between N-WASP and the Arp2/3 complex links Cdc42-dependent signals to actin assembly. *Cell* **97**, 221–231.

Rowe, R. G. and Weiss, S. J. (2009). Navigating ECM barriers at the invasive front: the cancer cell-stroma interface. *Annu. Rev. Cell Dev. Biol.* **25**, 567–595.

Rozelle, A. L., Machesky, L. M., Yamamoto, M., Driessens, M., Insall, R. H., Roth, M. G., Luby-Phelps, K., Marriott, G., Hall, A. and Yin, H. L. (2000). Phosphatidylinositol 4, 5-bisphosphate induces actin-based movement of raft-enriched vesicles through WASP-Arp2/3. *Curr. Biol.* **10**, 311–320.

Rust, S., Rosier, M., Funke, H., Real, J., Amoura, Z., Piette, J. C., Deleuze, J. F., Brewer, H. B., Duverger, N., Denèfle, P., et al. (1999). Tangier disease is caused by mutations in the gene encoding ATP-binding cassette transporter 1. *Nat. Genet.* **22**, 352–355.

Sabe, H., Hashimoto, S., Morishige, M., Ogawa, E., Hashimoto, A., Nam, J.-M., Miura, K., Yano, H. and Onodera, Y. (2009). The EGFR-GEP100-Arf6-AMAP1

signaling pathway specific to breast cancer invasion and metastasis. *Traffic* **10**, 982–993.

Sabeh, F., Ota, I., Holmbeck, K., Birkedal-Hansen, H., Soloway, P., Balbin, M., Lopez-Otin, C., Shapiro, S., Inada, M., Krane, S., et al. (2004). Tumor cell traffic through the extracellular matrix is controlled by the membrane-anchored collagenase MT1-MMP. *The Journal of Cell Biology* **167**, 769–781.

Sakurai-Yageta, M., Recchi, C., Le Dez, G., Sibarita, J.-B., Daviet, L., Camonis, J., D'Souza-Schorey, C. and Chavrier, P. (2008). The interaction of IQGAP1 with the exocyst complex is required for tumor cell invasion downstream of Cdc42 and RhoA. *The Journal of Cell Biology* **181**, 985–998.

Sánchez-Wandelmer, J., Dávalos, A., Herrera, E., Giera, M., Cano, S., la Peña, de, G., Lasunción, M. A. and Busto, R. (2009). Inhibition of cholesterol biosynthesis disrupts lipid raft/caveolae and affects insulin receptor activation in 3T3-L1 preadipocytes. *BBA - Biomembranes* **1788**, 1731–1739.

Schweitzer, J. K., Sedgwick, A. E. and D'Souza-Schorey, C. (2011). ARF6-mediated endocytic recycling impacts cell movement, cell division and lipid homeostasis. *Seminars in Cell and Developmental Biology* **22**, 39–47.

Singer, S. J. and Nicolson, G. L. (1972). The fluid mosaic model of the structure of cell membranes. *Science* **175**, 720–731.

Sato, H., Kinoshita, T., Takino, T., Nakayama, K. and Seiki, M. (1996). Activation of a recombinant membrane type 1-matrix metalloproteinase (MT1-MMP) by furin and its interaction with tissue inhibitor of metalloproteinases (TIMP)-2. *FEBS Lett.* **393**, 101–104.

Schmidt, A. and Hall, A. (2002). Guanine nucleotide exchange factors for Rho GTPases: turning on the switch. *Genes Dev.* **16**, 1587–1609.

Schnabl, M., Daum, G. and Pichler, H. (2005). Multiple lipid transport pathways to

the plasma membrane in yeast. *Biochim Biophys Acta* **1687**, 130–140.

Schoumacher, M., Goldman, R. D., Louvard, D. and Vignjevic, D. M. (2010). Actin, microtubules, and vimentin intermediate filaments cooperate for elongation of invadopodia. *The Journal of Cell Biology* **189**, 541–556.

Schweitzer, J. K., Sedgwick, A. E. and D'Souza-Schorey, C. (2011). ARF6-mediated endocytic recycling impacts cell movement, cell division and lipid homeostasis. *Seminars in Cell and Developmental Biology* **22**, 39–47.

SEALS, D., AZUCENAJR, E., PASS, I., TESFAY, L., GORDON, R., WOODROW, M., RESAU, J. and COURTNEIDGE, S. (2005). The adaptor protein Tks5/Fish is required for podosome formation and function, and for the protease-driven invasion of cancer cells. *Cancer Cell* 7, 155–165.

Seiki, M. and Yana, I. (2003). Roles of pericellular proteolysis by membrane type-1 matrix metalloproteinase in cancer invasion and angiogenesis. *Cancer Science* **94**, 569–574.

Sharpe, L. J. and Brown, A. J. (2013). Controlling Cholesterol Synthesis beyond 3-Hydroxy-3-methylglutaryl-CoA Reductase (HMGCR). *Journal of Biological Chemistry* **288**, 18707–18715.

Shields, D. J., Murphy, E. A., Desgrosellier, J. S., Mielgo, A., Lau, S. K. M., Barnes, L. A., Lesperance, J., Huang, M., Schmedt, C., Tarin, D., et al. (2011). Oncogenic Ras/Src cooperativity in pancreatic neoplasia. *Oncogene* **30**, 2123–2134.

Simons, K. and Ikonen, E. (1997). Functional rafts in cell membranes. *Nature* **387**, 569–572.

Simons, K., Sampaio, J.L., 2011. Membrane Organization and Lipid Rafts. Cold Spring Harbor Perspectives in Biology 3, a004697–a004697.

Simons, K., Vaz, W.L.C., 2004. Model systems, lipid rafts, and cell membranes. Annu.

Rev. Biophys. Biomol. Struct. 33, 269–295.

Sibony-Benyamini, H. and Gil-Henn, H. (2012). Invadopodia: the leading force. *European Journal of Cell Biology* **91**, 896–901.

Smart, E. J., Ying, Y. S., Donzell, W. C. and Anderson, R. G. (1996). A role for caveolin in transport of cholesterol from endoplasmic reticulum to plasma membrane. *J. Biol. Chem.* **271**, 29427–29435.

Smith-Pearson, P. S., Greuber, E. K., Yogalingam, G. and Pendergast, A. M. (2010). Abl Kinases Are Required for Invadopodia Formation and Chemokine-induced Invasion. *J. Biol. Chem.* **285**, 40201–40211.

Solomon, K. R. and Freeman, M. R. (2008). Do the cholesterol-lowering properties of statins affect cancer risk? *Trends Endocrinol. Metab.* **19**, 113–121.

Solomon, K.R., Freeman, M.R., 2011. The complex interplay between cholesterol and prostate malignancy. Urol. Clin. North Am. 38, 243–259.

Staubach, S., Hanisch, F.-G., 2011. Lipid rafts: signaling and sorting platforms of cells and their roles in cancer. Expert Rev Proteomics 8, 263–277.

Steffen, A., Le Dez, G., Poincloux, R., Recchi, C., Nassoy, P., Rottner, K., Galli, T. and Chavrier, P. (2008). MT1-MMP-dependent invasion is regulated by TI-VAMP/VAMP7. *Curr. Biol.* **18**, 926–931.

Stylli, S. S., Kaye, A. H. and Lock, P. (2008). Invadopodia: At the cutting edge of tumour invasion. *Journal of Clinical Neuroscience* **15**, 725–737.

Stylli, S. S., Stacey, T. T. I., Verhagen, A. M., Xu, S. S., Pass, I., Courtneidge, S. A. and Lock, P. (2009). Nck adaptor proteins link Tks5 to invadopodia actin regulation and ECM degradation. *Journal of Cell Science* **122**, 2727–2740.

Su, W., Yeku, O., Olepu, S., Genna, A., Park, J.-S., Ren, H., Du, G., Gelb, M. H.,

Morris, A. J. and Frohman, M. A. (2009). 5-Fluoro-2-indolyl des-chlorohalopemide (FIPI), a phospholipase D pharmacological inhibitor that alters cell spreading and inhibits chemotaxis. *Mol. Pharmacol.* **75**, 437–446.

Svec, A. (2008). Phosphoprotein associated with glycosphingolipid-enriched microdomains/Csk-binding protein: a protein that matters. *Pathol. Res. Pract.* **204**, 785–792.

Tague, S. E., Muralidharan, V. and D'Souza-Schorey, C. (2004). ADP-ribosylation factor 6 regulates tumor cell invasion through the activation of the MEK/ERK signaling pathway. *Proc. Natl. Acad. Sci. U.S.A.* **101**, 9671–9676.

Takeuchi, S. (2000). Transmembrane Phosphoprotein Cbp Positively Regulates the Activity of the Carboxyl-terminal Src Kinase, Csk. *Journal of Biological Chemistry* **275**, 29183–29186.

Thomas, S. M. and Brugge, J. S. (1997). Cellular functions regulated by Src family kinases. *Annu. Rev. Cell Dev. Biol.* **13**, 513–609.

Tobe, K., Sabe, H., Yamamoto, T., Yamauchi, T., Asai, S., Kaburagi, Y., Tamemoto, H., Ueki, K., Kimura, H., Akanuma, Y., et al. (1996). Csk enhances insulin-stimulated dephosphorylation of focal adhesion proteins. *Molecular and Cellular Biology* **16**, 4765–4772.

Tontonoz, P. and Mangelsdorf, D. J. (2003). Liver X receptor signaling pathways in cardiovascular disease. *Mol. Endocrinol.* **17**, 985–993.

Uittenbogaard, A. and Smart, E. J. (2000). Palmitoylation of caveolin-1 is required for cholesterol binding, chaperone complex formation, and rapid transport of cholesterol to caveolae. *J. Biol. Chem.* **275**, 25595–25599.

Urbani, L. and Simoni, R. D. (1990). Cholesterol and vesicular stomatitis virus G protein take separate routes from the endoplasmic reticulum to the plasma membrane. *J. Biol. Chem.* **265**, 1919–1923.

Vainio, S. (2005). Significance of Sterol Structural Specificity: DESMOSTEROL CANNOT REPLACE CHOLESTEROL IN LIPID RAFTS. *J. Biol. Chem.* **281**, 348–355.

Valacchi, G., Sticozzi, C., Lim, Y. and Pecorelli, A. (2011). Scavenger receptor class B type I: a multifunctional receptor. *Ann. N. Y. Acad. Sci.* **1229**, E1–7.

Vang, T., Torgersen, K. M., Sundvold, V., Saxena, M., Levy, F. O., Skålhegg, B. S., Hansson, V., Mustelin, T. and Taskén, K. (2001). Activation of the COOH-terminal Src kinase (Csk) by cAMP-dependent protein kinase inhibits signaling through the T cell receptor. *J. Exp. Med.* **193**, 497–507.

Webb, B. A., Zhou, S., Eves, R., Shen, L., Jia, L. and Mak, A. S. (2006). Phosphorylation of cortactin by p21-activated kinase. *Arch. Biochem. Biophys.* **456**, 183–193.

Williams, T. M. (2004). Caveolin-1 in oncogenic transformation, cancer, and metastasis. *AJP: Cell Physiology* **288**, C494–C506.

Williams, T. M. and Lisanti, M. P. (2004). The Caveolin genes: from cell biology to medicine. *Ann. Med.* **36**, 584–595.

Wyckoff, J. B., Pinner, S. E., Gschmeissner, S., Condeelis, J. S. and Sahai, E. (2006). ROCK- and Myosin-Dependent Matrix Deformation Enables Protease-Independent Tumor-Cell Invasion In Vivo. *Current Biology* **16**, 1515–1523.

Yamaguchi, H. (2012). Pathological roles of invadopodia in cancer invasion and metastasis. *European Journal of Cell Biology* **91**, 902–907.

Yamaguchi, H. and Oikawa, T. (2010). Membrane lipids in invadopodia and podosomes: key structures for cancer invasion and metastasis. *Oncotarget* **1**, 320–328.

Yamaguchi, H., Lorenz, M., Kempiak, S., Sarmiento, C., Coniglio, S., Symons, M., Segall, J., Eddy, R., Miki, H., Takenawa, T., et al. (2005). Molecular

mechanisms of invadopodium formation: the role of the N-WASP-Arp2/3 complex pathway and cofilin. *The Journal of Cell Biology* **168**, 441–452.

Yamaguchi, H., Takeo, Y., Yoshida, S., Kouchi, Z., Nakamura, Y. and Fukami, K. (2009). Lipid Rafts and Caveolin-1 Are Required for Invadopodia Formation and Extracellular Matrix Degradation by Human Breast Cancer Cells. *Cancer Research* **69**, 8594–8602.

Yamaguchi, H., Yoshida, S., Muroi, E., Kawamura, M., Kouchi, Z., Nakamura, Y., Sakai, R. and Fukami, K. (2010). Phosphatidylinositol 4,5-bisphosphate and PIP5-kinase Iα are required for invadopodia formation in human breast cancer cells. *Cancer Science* **101**, 1632–1638.

Yamaguchi, H., Yoshida, S., Muroi, E., Yoshida, N., Kawamura, M., Kouchi, Z., Nakamura, Y., Sakai, R. and Fukami, K. (2011). Phosphoinositide 3-kinase signaling pathway mediated by p110 regulates invadopodia formation. *The Journal of Cell Biology* **193**, 1275–1288.

Yamamoto, H., Sutoh, M., Hatakeyama, S., Hashimoto, Y., Yoneyama, T., Koie, T., Saitoh, H., Yamaya, K., Funyu, T., Nakamura, T., et al. (2011). Requirement for FBP17 in invadopodia formation by invasive bladder tumor cells. *J. Urol.* **185**, 1930–1938.

Yaqub, S., Abrahamsen, H., Zimmerman, B., Kholod, N., Torgersen, K. M., Mustelin, T., Herberg, F. W., Taskén, K. and Vang, T. (2003). Activation of C-terminal Src kinase (Csk) by phosphorylation at serine-364 depends on the Csk-Src homology 3 domain. *Biochem. J.* **372**, 271–278.

Yvan-Charvet, L., Ranalletta, M., Wang, N., Han, S., Terasaka, N., Li, R., Welch, C. and Tall, A. R. (2007). Combined deficiency of ABCA1 and ABCG1 promotes foam cell accumulation and accelerates atherosclerosis in mice. *J. Clin. Invest.* **117**, 3900–3908.

Zarubica, A., Plazzo, A.P., Stöckl, M., Trombik, T., Hamon, Y., Müller, P.,

Pomorski, T., Herrmann, A., Chimini, G., 2009. Functional implications of the influence of ABCA1 on lipid microenvironment at the plasma membrane: a biophysical study. The FASEB Journal 23, 1775–1785.

Zeisig, R., Koklič, T., Wiesner, B., Fichtner, I., Sentjurč, M., 2007. Increase in fluidity in the membrane of MT3 breast cancer cells correlates with enhanced cell adhesion in vitro and increased lung metastasis in NOD/SCID mice. Arch. Biochem. Biophys. 459, 98–106.

Zerenturk, E. J., Kristiana, I., Gill, S. and Brown, A. J. (2011). The endogenous regulator 24(S),25-epoxycholesterol inhibits cholesterol synthesis at DHCR24 (Seladin-1). *Biochim Biophys Acta*

Zerial, M. and McBride, H. (2001). Rab proteins as membrane organizers. *Nat Rev Mol Cell Biol* **2**, 107–117.

Zhou, K., Wang, Y., Gorski, J. L., Nomura, N., Collard, J. and Bokoch, G. M. (1998). Guanine nucleotide exchange factors regulate specificity of downstream signaling from Rac and Cdc42. *J. Biol. Chem.* **273**, 16782–16786.

Zhuang, L., Kim, J., Adam, R.M., Solomon, K.R., Freeman, M.R., 2005. Cholesterol targeting alters lipid raft composition and cell survival in prostate cancer cells and xenografts. J. Clin. Invest. 115, 959–968.